AD-A114 799   GARRETT PNEUMATIC SYSTEMS DIV PHOENIX AZ   F/G 9/5
               DESIGN GUIDE FOR LAMINAR FLOW FLUIDIC AMPLIFIERS AND SENSORS.(U)
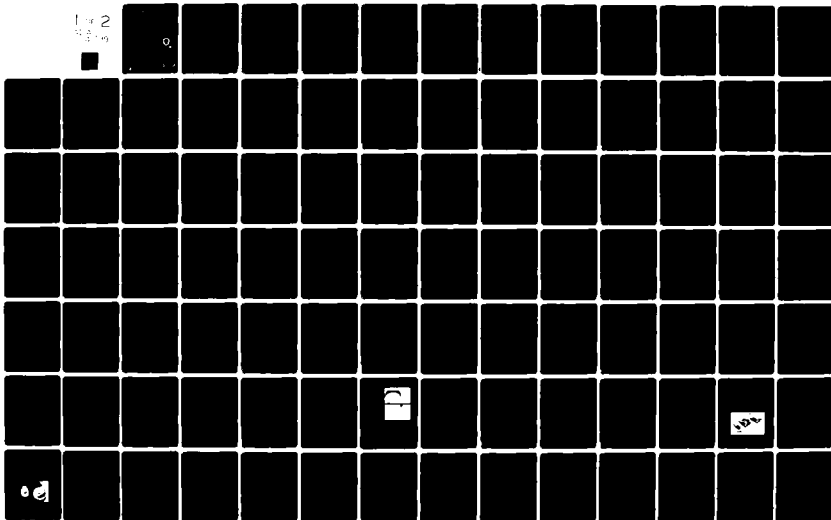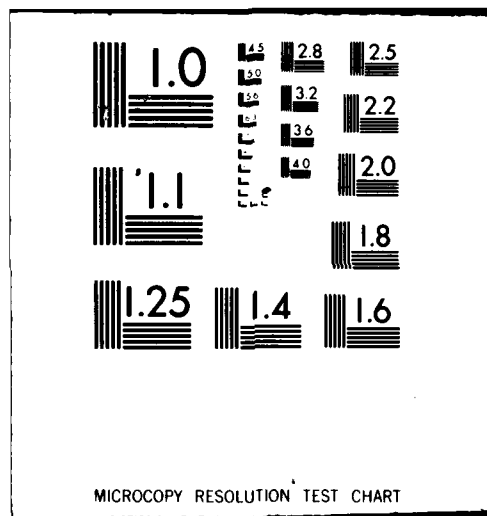   APR 82   M F CYCON, D J SCHAFFER   N00019-78-6-0288
UNCLASSIFIED   41-3228A   HDL-CR-82-288-1   NL

1 OF 2

MICROCOPY RESOLUTION TEST CHART

NATIONAL BUREAU

HDL-CR-82-288-1
APRIL 27, 1982

by M. F. Cycon, Jr.
   D. J. Schaffer

Prepared by
Garrett Pneumatic Systems Division
of The Garrett Corporation
111 South 34th Street
Phoenix, AZ 85010

Under Contract
N00019-78-G-0288

U.S. Army Electronics Research
and Development Command

Harry Diamond Laboratories

Adelphi, MD   20783

DTIC

MAY 24 1982

A

82 05 24 121

SECURITY CLASSIFICATION OF THIS PAGE *(When Data Entered)*

REPORT DOCUMENTATION PAGE		READ INSTRUCTIONS BEFORE COMPLETING FORM
1. REPORT NUMBER HDL-CR-82-288-1	**2. GOVT ACCESSION NO.** AD-A114 749	**3. RECIPIENT'S CATALOG NUMBER**
4. TITLE *(and Subtitle)* Design Guide For Laminar Flow Fluidic Amplifiers and Sensors		**5. TYPE OF REPORT & PERIOD COVERED** Contractor Report 10-80 to 10-81
		6. PERFORMING ORG. REPORT NUMBER 41-3228A
7. AUTHOR(s) M. F. Cycon, Jr. D. J. Schaffer		**8. CONTRACT OR GRANT NUMBER(s)**
9. PERFORMING ORGANIZATION NAME AND ADDRESS Garrett Pneumatic Systems Division 111 South 34th Street Phoenix, AZ 85010		**10. PROGRAM ELEMENT, PROJECT, TASK AREA & WORK UNIT NUMBERS** PRON: 1FOR0012011FA9 DA Project: 1L162120AH25 Program Element: 62120A
11. CONTROLLING OFFICE NAME AND ADDRESS Naval Air Systems Command Washington, DC 20361		**12. REPORT DATE** April 27, 1982
		13. NUMBER OF PAGES 147
14. MONITORING AGENCY NAME & ADDRESS*(If different from Controlling Office)* Harry Diamond Laboratories 2800 Powder Mill Road Adelphi, MD 20783		**15. SECURITY CLASS.** *(of this report)* UNCLASSIFIED
		15a. DECLASSIFICATION/DOWNGRADING SCHEDULE

16. DISTRIBUTION STATEMENT *(of this Report)*

Approved for public release; distribution unlimited

17. DISTRIBUTION STATEMENT *(of the abstract entered in Block 20, if different from Report)*

18. SUPPLEMENTARY NOTES

HDL Project 304034
DRCMS Code: 612120H250011

19. KEY WORDS *(Continue on reverse side if necessary and identify by block number)*

Laminar
Fluidics
Amplifier
Sensor

20. ABSTRACT *(Continue on reverse side if necessary and identify by block number)*

This final report provides technical information on the design, performance, and fabrication of laminar amplifiers and sensors. Standard amplifier designs and formats are presented which allow the user to select amplifier characteristics most suitable for each specific application. Various methods for fabrication of elements are described and information relating to the effects of fabrication inaccuracies are presented in this report. The

DD FORM 1473 EDITION OF 1 NOV 65 IS OBSOLETE

1 SECURITY CLASSIFICATION OF THIS PAGE *(When Data Entered)*

laminar jet angular rate sensor is described and the advantages of applying laminar fluidics to the vast field of sensors is shown. Several circuit arrangements and the performance achieved with these circuits are presented. Charts and other reference material are also included.

DTIC
COPY
INSPECTED
2

Accession For

NTIS QRA&I	☑
DTIC TAB	☐
Unannounced	☐
Justification	

By
Distribution/
Availability Codes
A- and/or
Dist Special

A

FOREWORD

Fluidic technology concepts were developed at the Diamond Ordnance Fuze Laboratory (now Harry Diamond Laboratories) in the late 1950's, with the information disseminated in a press release in early 1960. The jet deflection proportional amplifier was the basic analog element. Although researchers reported on other types of analog devices, the jet or beam deflection amplifier served as the cornerstone for analog fluidics throughout the 1960's and early 1970's. Amplifier operation was in the turbulent regime and while investigators attempted to analyze basic element performance and also circuit operation, the technology remained an art rather than a science. The limitations of fluidic amplification were severe. The units had low dynamic range and low gain since amplifier noise precluded multiple staging.

The research staff of the Harry Diamond Laboratories realized these limitations and in the early 1970's began their investigations of operating amplifiers in the laminar regime. They eventually succeeded in developing a laminar proportional amplifier design. The improvements in amplifier characteristics were tremendous; however, equally important was the fact that analytical techniques could be applied to amplifier and circuit analysis yielding significantly higher correlation with experimental test results. In addition, since laminar flow amplifiers follow the law of Reynolds number scaling, it is possible to scale amplifiers with respect to either size or fluid. Laminar devices offer the possibility of more accurate sensors, comparators, logic, and computational circuits and, in general, elevate fluidics to a viable technology, making a science of what initially had been an art form.

To document the design and methods of applying laminar amplifiers, Garrett Pneumatic Systems Division (GPSD), Phoenix, Arizona, prepared this design guide for the Army's Harry Diamond Laboratories under Navy Contract N00019-78-G-0288, Task 7830 (WY24) during the period from October 1980 to October 1981. Technical monitoring was provided by Messrs. J. Joyce and T. Drzewiecki of the Harry Diamond Laboratories. This guide provides technical information on the design, performance, and fabrication of laminar amplifiers and sensors. The guide includes selected references and an extensive bibliography so that the user may refer to the original paper on any specific topic. In addition, Garrett has incorporated into this document its own experience and developments in the field of fluidics.

Standard amplifier designs and formats have been established, and the purpose of this design guide is not only to familiarize the user with these standards and methods of assembly, but also to permit selection of the amplifier characteristics most suitable for each specific application. Procedures established for staging amplifiers should significantly reduce the time an engineer will spend in a laboratory attempting to achieve optimum performance of a specific circuit design. The various methods for fabrication of elements are described and information relating to the effects of fabrication inaccuracies are shown. These data are of particular importance for those who may wish to experiment with their own production facilities. The Laminar Jet Angular Rate Sensor is described in great detail, not only because of its own tremendous usefulness, but also to show the advantages of applying laminar fluidics to the vast field of sensors. Several circuit arrangements and the performance achieved with these circuits are described. Charts and other reference material constituting a body of design data to assist the fluidics design engineer are also included.

4

It is hoped that this design guide will be a useful addition to the body of fluidics knowledge and will be instrumental in encouraging engineers to apply fluidic technology to the solution of their problems. To quote J. M. Kirshner, formerly Chief of the Fluidic Systems Research Branch at HDL, "Fluidics is now a viable technology with a theoretical base that allows logical design of components and circuits."

CONTENTS

APPENDICES

FIGURES

FIGURES

FIGURES

TABLES

1. BACKGROUND

1.1 Development of Fluid Amplifiers

For many years before the formal introduction of fluidics as a technology, researchers were attempting to achieve some measure of control by directing fluid jets. The Coanda effect had been described early in the century and there were many attempts to utilize this phenomenom. Finally, Bowles, Horton, and Warren, working at the Diamond Ordnance Fuze Laboratory (now Harry Diamond Laboratories), succeeded in developing proportional and bistable amplifiers having sufficient gain and other useful characteristics to encourage the application of fluidics to sensors and controllers. It is not the purpose of this design guide to describe the many forms of amplifiers introduced during the early 1960's. The primary objective of this report is to trace the development of the jet deflection proportional amplifier from its early applications wherein operation was in the turbulent regime to the present laminar flow amplifier and a few of its applications.

1.1.1 Early Applications

The possibility of using rugged, low cost fluidic amplifiers to replace expensive and often delicate mechanical sensing devices was a significant factor in the rapid growth of fluidic technology soon after the disclosures of Bowles, Horton, and Warren. Numerous applications were avidly pursued by research groups in almost every major organization in the country. Through much trial and error, some measure of success was eventually achieved and fluidics began to appear in industrial, commercial, and aerospace equipment.

In the aerospace industry, the fluidic applications initially developed ranged from simple proportional controllers

11

used in aircraft environmental control systems to complex analog computers for controlling advanced jet engines. The turbulent flow jet deflection amplifier was the principal active fluidic component in the majority of the applications investigated. These devices were designed to operate with available power sources such as jet engine compressor bleed air, solid propellant gas generators, and aircraft hydraulic systems. Maximum supply pressure requirements depended on the specific application. Generally, pneumatic controls using engine bleed air required a supply pressure of 70 to 140 kPa above ambient. Amplifiers operated on solid propellant gas generators were generally used in reaction control systems requiring a supply pressure between 3.5 and 20 MPa. Hydrofluidic applications also required a supply pressure in the range of 2 to 20 MPa.

Although turbulent flow jet deflection amplifiers have useful characteristics, their low gain and low dynamic range severely limit the number of applications wherein fluidics could achieve the desired level of performance. It was quickly learned that successful applications were those requiring a minimum number of active fluidic components. As an example, consider the fluidic control currently in production and shown schematically in figure 1. The control circuit senses the difference between valve downstream pressure and cabin pressure and modulates a butterfly valve to maintain the downstream pressure at a specific level above the cabin pressure. The accuracy required is only about ±20 percent of the desired set point. This is achieved with three turbulent flow proportional amplifiers to provide a forward gain of about 70. The butterfly valve is operated with a large diaphragm actuator and has a response requirement of less than 1 Hz. Because of this low bandwidth, fluidic circuit noise is well-attenuated and the controller sensitivity is primarily determined by friction and hysteresis in the actuator. Although the control requirements in this application are not stringent, it was found that

NOTE: SOLENOID ENGAGED
FOR AUTOMATIC
CONTROL-DISENGAGED
FOR MANUAL CONTROL
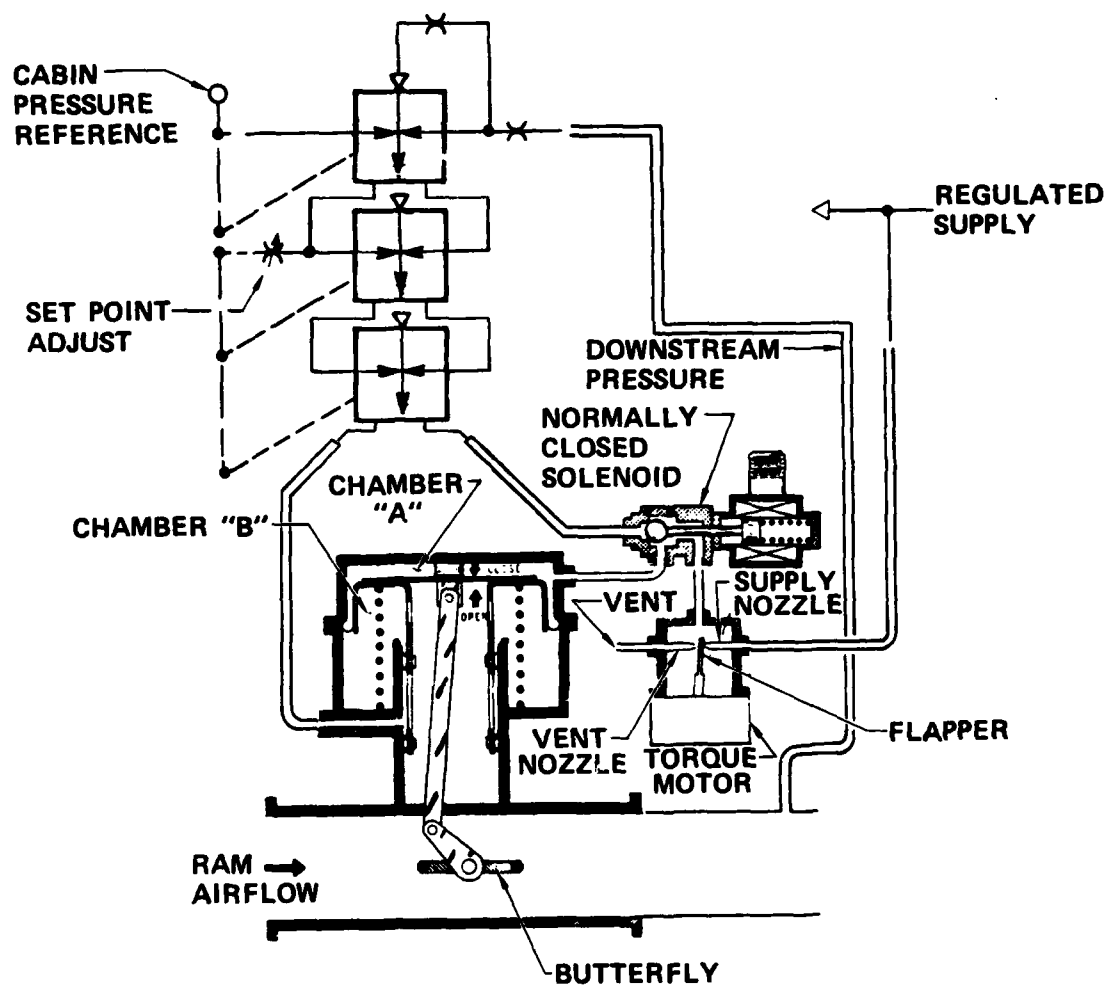
Figure 1. Fluidic differential pressure regulator,
schematic diagram.

13

fluidics offered substantial benefits over an alternative approach using conventional pneumatic servo components.

Experience gained with simple proportional fluidic controllers using turbulent flow amplifiers indicated that the characteristics of these devices would restrict the development of more complex circuits. As noted before, the major deficiencies of turbulent flow amplifiers were their low gain and low signal-to-noise ratio. Staging amplifiers to obtain pressure gains of more than 200 to 300 proved impractical because of the rapid decrease in dynamic range associated with the amplification of noise generated by each stage.

It was recognized early that significant improvements in dynamic range could be achieved by designing amplifiers to operate in the laminar flow regime. In the early 1970's, laminar flow proportional amplifiers were designed which could provide blocked load pressure gains between 8 and 20, a dynamic range of 5000, and bandwidths of over 600 Hz using power jet widths of 0.5 mm.[1] Equally important was the fact that analytical models were developed which gave excellent agreement with both static and dynamic performance predictions. With these devices, laminar flow gain blocks with gains in excess of 1000, a dynamic range over 400, and a bandwidth greater than 100 Hz were shown to be feasible.[2,3]

---

[1] F.M. Manion and T.M. Drzewiecki, "Analytical Design of Laminar Proportional Amplifiers," Proceedings of HDL Fluidic State-of-the-Art Symposium, I, Harry Diamond Laboratories (October 1974).

[2] G. Mon, "Flueric Laminar Gain Blocks and an Operational Amplifier Scaler," Harry Diamond Laboratories HDL-TR-1730 (December 1975).

[3] F.M. Manion and G. Mon, "Fluerics 33: Design and Staging of Laminar Proportional Amplifiers," Harry Diamond Laboratories HDL-TR-1608 (September 1972).

1.1.2 Applications Requiring Laminar Fluidics

When fluidic technology was first introduced, many people visualized fluid amplifiers as a potential replacement for conventional control valves with moving parts as used in fluid power systems. Turbulent flow amplifiers could be made to operate at very high pressures and flow rates and only a small amount of power was required to switch or modulate the fluid stream. Power gain, efficiency, and pressure recovery were the primary parameters of interest.

Other researchers recognized the computational capacity of fluidics and its ability to perform functions such as sensing, logic, and dynamic compensation. This led to numerous fluidic control concepts covering a variety of applications traditionally the domain of electronic, mechanical, and hydro-mechanical controls.

Positive results with simple controls encouraged more complex configurations. As complexity increased, the demand for amplifiers and sensors with lower signal thresholds, improved gain, and reduced power consumption also increased. Laminar flow fluidic devices offer the desired performance characteristics and consequently are rapidly becoming the primary element in advanced fluidic control systems.

Perhaps the strongest force behind the increasing use of laminar fluidic devices has been new developments in fluidic sensors that operate in the laminar regime. Of significant importance is the laminar jet angular rate sensor (LJARS). This sensor, which is described in detail in section 6, produces a differential output signal that is proportional to the applied angular rate. A typical medium range LJARS operating on air has a sensitivity on the order of 0.05 Pa/deg/s. If this sensor is used in a stabilization system application, the maximum rate input could

be as low as 1 deg/s. Since the output signal is only 0.05 Pa at this rate, a gain of 10^5 would be required to increase the output signal to 5 kPa. This would be high enough to interface with power actuating devices or a low range off-the-shelf pressure transducer. Depending on the application, more or less gain could be required.

Clearly this requirement could not be achieved with turbulent flow amplifiers because of the poor signal-to-noise ratio and limitations on staging. Using laminar flow devices, gains in excess of 10^6 have been demonstrated while maintaining an acceptable dynamic range and bandwidth.[4]

1.2 Laminar Flow Device Characteristics

The important characteristics of a laminar proportional amplifier (LPA) are its gain, input/output resistance, null offset, dynamic range, and bandwidth. These properties can be adequately described both mathematically and by experiment. This design guide emphasizes the experimental approach and, where applicable, presents design guidelines and simplified formulas for calculating selected properties. Specific references where more detailed analysis can be found are also noted.

Geometric changes in an LPA design can affect all of the major operating characteristics. Several different geometries are compared in section 2. The characteristic of null offset is most sensitive to the accuracy used during manufacturing. This characteristic is important where either high gain or high accuracy are required. Null offset is defined in section 2 and discussed in sections 5 and 6. Techniques to minimize null offset are also presented in section 4.

---

[4]C.L. Abbott, "Final Report: A Study of Fluidic Gun Stabilization Systems for Combat Vehicles," AiResearch Manufacturing Company of Arizona Report 41-2304 or HDL-CR-80-100-1 (April 1980).

One of the most important parameters related to LPA performance is the Reynolds number, N_R. Gain, dynamic range, and bandwidth are interrelated characteristics with a strong dependence on the operating Reynolds number. Reynolds number is also the parameter used to scale the size of an LPA or to establish the supply requirements for a given design operating with different fluids. Because of its importance, the following section discusses this parameter, reviews the various forms that have been used to calculate Reynolds number, and discusses its relationship to gain, dynamic range, and bandwidth.

1.2.1 Reynolds Number

The Reynolds number, N_R, is a dimensionless characteristic which appears often in fluid flow problems. In its general form, Reynolds number is defined as*

$$N_R = \frac{\rho U L}{\mu}, \tag{1}$$

where

ρ = fluid density, kg/m^3,

U = characteristic velocity, m/s,

L = characteristic dimension, m, and

μ = fluid viscosity, kg/m-s.

Since kinematic viscosity, ν, is defined as μ/ρ [m^2/s], Reynolds number is also given by

$$N_R = \frac{U L}{\nu}. \tag{2}$$

Evaluating the Reynolds number for laminar fluidic devices, therefore, requires establishing a characteristic velocity and a characteristic dimension. The characteristic velocity is derived from the Bernoulli equation for incompressible flow between two points on a streamline. The first point

---

*Technical abbreviations used throughout this report are summarized in Appendix A.

17

is taken in the supply plenum upstream of the nozzle where the velocity is assumed to be zero and the static pressure is P_s. The second point is taken at the supply nozzle exit where the static pressure is equal to the vent pressure, P_v, and the ideal exit velocity is U. The Bernoulli equation gives

$$P_s = P_v + \frac{1}{2} \rho U^2 \qquad (3)$$

or

$$U = (2 \ (P_s - P_v)/\rho)^{1/2}. \qquad (4)$$

Since $P_s - P_v$ is the gauge supply pressure (P_{sv}), the equation for velocity reduces to

$$U = (2 \ P_{sv}/\rho)^{1/2}. \qquad (5)$$

Substituting equation 5 into equation 2 gives

$$N_R = \frac{L \ (2P_{sv}/\rho)^{1/2}}{\nu}. \qquad (6)$$

To complete the expression for Reynolds number requires selection of a characteristic dimension. Several different dimensions have been used; the most frequently used is the power jet width, b_s. This gives

$$N_R = \frac{b_s (2 \ P_{sv}/\rho)^{1/2}}{\nu}. \qquad (7)$$

An alternative form is obtained if N_R is multiplied by aspect ratio, σ, which is the ratio of nozzle depth, h, to width, b_s. This gives

$$\sigma N_R = (\frac{h}{b_s}) \ N_R \qquad (8)$$

$$= \frac{h (2P_{sv}/\rho)^{1/2}}{\nu}.$$

It is noted that σN_R is the Reynolds number based on the nozzle depth.

Equation 7 is the basic form of the Reynolds number and appears often in mathematical expressions for parameters such as gain, supply channel resistance, and output resistance of an LPA[1]. This expression does not accurately predict the upper or lower limits for LPA operation in general; however, it does correlate all Reynolds number dependent properties for a given design. For example, the gain of a given LPA design and aspect ratio is the same for different fluids or for the same fluid at different temperatures, provided that the Reynolds number calculated with equation 7 is maintained at the same value.

Considerable experimental evidence is available to confirm that a Reynolds number based on channel depth (equation 8) adequately defines the upper and lower limits of operation of all laminar proportional amplifiers.[5] These limits are given by

$$500 \leq \sigma N_R \leq 1400. \tag{9}$$

The upper limit is well defined since it marks the transition from laminar-to-turbulent flow. To ensure laminar flow, it is recommended that a slightly lower value, $\sigma N_R = 1000$, be used as a safe upper limit. As σN_R is reduced, shear losses associated with the top and bottom plates cause the power jet to spread, which reduces the amplifier gain. Figure 2 shows the blocked and self-staged gain for a typical LPA as a function σN_R.[2] These curves are valid for aspect ratios greater than 0.3.

---

[1]F.M. Manion and T.M. Drzewiecki, "Analytical Design of Laminar Proportional Amplifiers," Proceedings of HDL Fluidic State-of-the-Art Symposium, I, Harry Diamond Laboratories (October 1974).

[2]G. Mon, "Flueric Laminar Gain Blocks and an Operational Amplifier Scaler," Harry Diamond Laboratories HDL-TR-1730 (December 1975).

[5]T. M. Drzewiecki, F. M. Manion, "Fluerics 40: LJARS, The Laminar Jet Angular Rate Sensor," Harry Diamond Laboratories HDL-TM-79-7 (December 1979).

At lower aspect ratios, the shear losses become more significant even at the higher values of σN_R. The lower limit of σN_R is somewhat arbitrary and will usually depend on the magnitude of the loss of gain that can be tolerated. As indicated in figure 2, both the blocked and self-staged gains at $\sigma N_R = 400$ are significantly lower than their corresponding values at $\sigma N_R = 1000$. Thus, in most cases it is desirable to maintain $500 \leq \sigma N_R \leq 1000$.
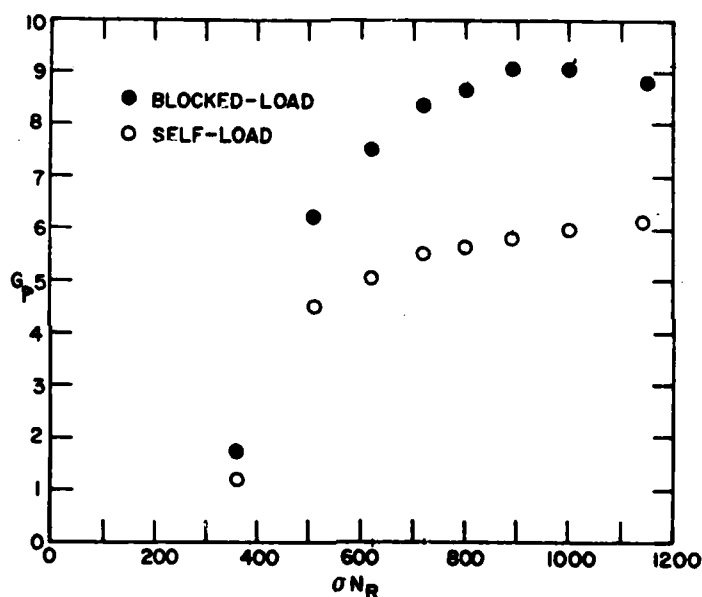
Figure 2.   Typical laminar proportional
amplifier pressure gain
versus σN_R.

Another factor in establishing the desired range of Reynolds number is the relationship between Reynolds number and bandwidth. The bandwidth of an LPA has a strong dependence on the transport time or the time it takes a fluid disturbance to travel the distance from the power jet to the splitter. A disturbance travels at half the average jet velocity so that this

delay time (T_d) is the ratio of the distance x_{sp} to half the average velocity, $U_{avg}/2$:

$$T_d = 2 \frac{x_{sp}}{U_{avg}}. \tag{10}$$

The lower the velocity, the larger the delay time, and consequently the lower the bandwidth (as determined by the accumulated phase lag corresponding to the transport delay T_d). The velocity at the nozzle exit, U_e, is related to the ideal Bernoulli velocity (equation 5) as follows:

$$U_e = c_d U, \tag{11}$$

where

c_d = discharge coefficient.

Although the average value of velocity between the nozzle exit and splitter is slightly less than U_e, as a first approximation,

$$U_{avg} = U_e = c_d U. \tag{12}$$

The discharge coefficient, which is always less than unity, accounts for boundary layer effects which reduce the actual velocity from the ideal value. Using equation 12 together with equation 2 and letting $L = b_s$ gives

$$U_{avg} = \frac{c_d \nu N_R}{b_s}. \tag{13}$$

Substituting equation 13 into equation 10 yields

$$T_d = 2 \, \frac{x_{sp} \, b_s}{c_d \, \nu \, N_R}. \tag{14}$$

Thus, the lower the Reynolds number, the larger the delay time and the lower the bandwidth. For maximum LPA bandwidth, the highest possible value of N_R should be used.

Another characteristic of an LPA which is dependent on the Reynolds number is the dynamic range. Dynamic range is the ratio of the maximum available output signal to the minimum detectable change in output. Since laminar flow has a very low noise spectrum, the measurement of minimum detectable output is usually limited to the threshold of the measuring instrument. Maximum available output, however, increases as the Reynolds number increases. Therefore, if two identical amplifiers are operated in the laminar regime ($\sigma N_R < 1000$), the amplifier with the higher value of N_R will have the larger dynamic range, assuming identical fluid properties.

The average velocity at which the supply flow leaves the nozzle is also used to calculate the flow rate requirements of an LPA. The volumetric flow rate is given by

$$Q = U_{avg} \, b_s h. \tag{15}$$

where

$$Q = \text{volumetric flow, } m^3/s.$$

Substituting equation 13 into equation 15 yields

$$Q = c_d \, \nu \, hN_R. \tag{16}$$

An alternative form of equation 16 is obtained by substituting equation 7 into equation 16:

$$Q = c_d b_s h \; (2 \; P_{sv}/\rho)^{1/2}. \tag{17}$$

The discharge coefficient which appears in the above equations can be obtained experimentally by measuring the amplifier flow rate and calculating c_d using either equation 16 or 17.

Extensive testing at HDL of numerous LPA power jet geometries[6] has shown that the discharge coefficient is a function of the operating Reynolds number, the nozzle width and depth, and the length of the straight channel section ahead of the nozzle exit. These parameters can be grouped to form a modified Reynolds number, N_R', which is defined as follows:

$$N_R' = \frac{N_R}{(1 + X_{th}) \; (1 + \frac{1}{\sigma})^2} \; , \tag{18}$$

where

$$X_{th} = x_{th}/b_s$$

and

x_{th} = length of the nozzle straight section.

Figure 3 presents a plot of the discharge coefficient, c_d, as a function of N_R'. This curve is based on experimental data for a variety of power jet geometries and has proven to be sufficiently accurate for most engineering calculations. This curve yields the following empirical expression from which c_d can be calculated:

$$N_R' = 2.667 \; (e^{6.6c_d^2} -1)/c_d. \tag{18a}$$

---

[6]T.M. Drzewiecki, "Fluerics 37: A General Planar Nozzle Discharge Coefficient Representation," Harry Diamond Laboratories HDL-TM-74-5 (August 1974).
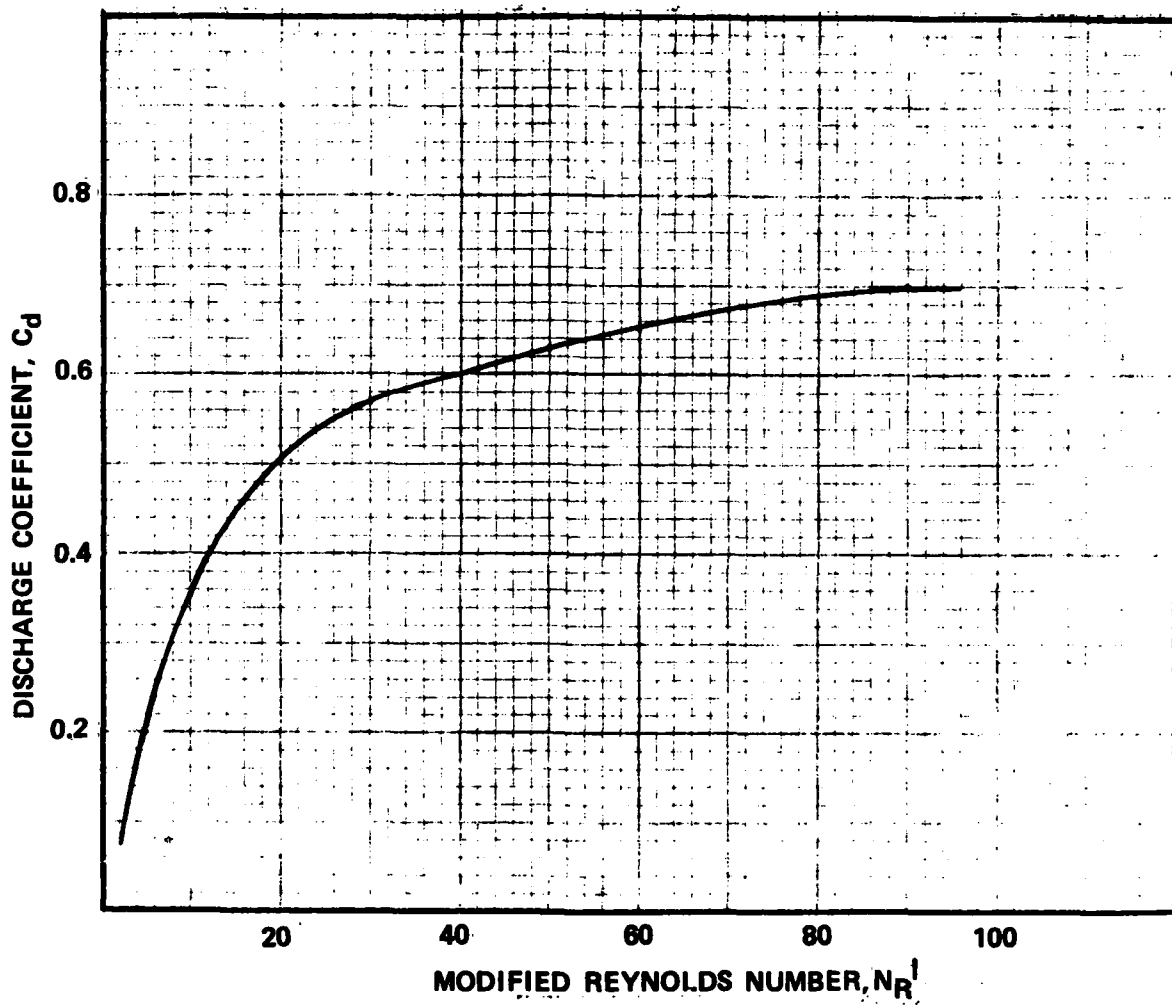
Figure 3. Discharge coefficient versus
modified Reynolds number.

24

2.   TYPICAL LAMINAR PROPORTIONAL AMPLIFIERS

The performance of an LPA is quite sensitive to the geometric design of the amplifier. Although most turbulent flow amplifier designs can be operated in the laminar regime, their performance is not optimum. Over the past 10 years, HDL has used both analytical and experimental techniques to optimize LPA geometry. This section discusses the LPA geometry developed by HDL, reviews the manner in which selected geometric parameters influence performance, and summarizes available data on several different geometries.

2.1 Geometry

Figure 4 presents the plan-view of a typical HDL LPA design and gives the nomenclature for the critical physical dimensions. All critical features are normalized with respect to the nozzle width, b_s. The nozzle depth is h and the ratio h/b_s is called the aspect ratio, σ. In addition to the physical dimensions, certain operating conditions must be defined. These are the supply pressure, P_{sv}, the control bias pressure level, P_B, and the vent pressure, P_v.

The supply pressure is the static pressure in the supply duct and is related to the operating Reynolds number as given by equation 7. The control bias pressure level is defined as the average pressure in the two input control ducts and is expressed as a percentage of the supply pressure, P_{sv},

$$P_B = \frac{P_{C1} + P_{C2}}{2 \, P_{sv}} \times 100. \tag{19}$$

25
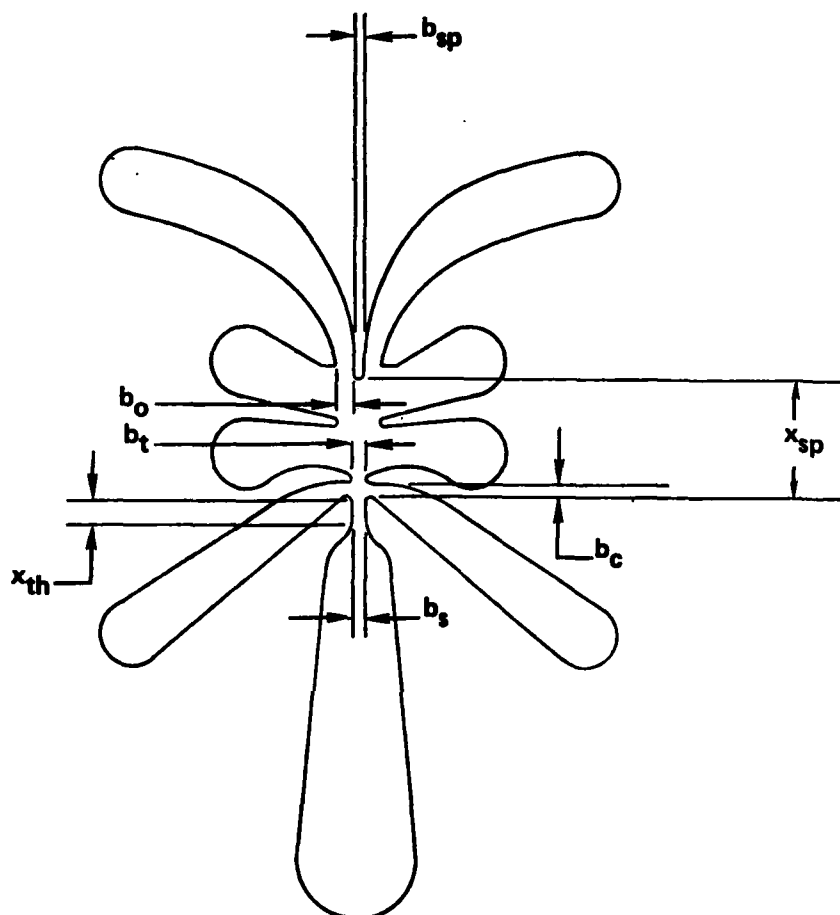
b_s = NOZZLE WIDTH

B_t = DISTANCE BETWEEN DOWNSTREAM CONTROL EDGES = b_t/b_s

B_c = CONTROL WIDTH = b_c/b_s

B_{sp} = SPLITTER WIDTH = b_{sp}/b_s

B_o = RECEIVER WIDTH = b_o/b_s

X_{sp} = NOZZLE-TO-SPLITTER DISTANCE = x_{sp}/b_s

X_{th} = NOZZLE STRAIGHT CHANNEL LENGTH = x_{th}/b_s

Figure 4. Typical LPA geometry and nomenclature.

Vent pressure is defined as the static pressure in the upper and lower vent regions. Normally these are manifolded together to ensure equal vent pressure. The supply pressure is always expressed as the pressure above vent pressure, P_v. The vent pressure can be changed by restricting the vent flow. For gaseous operated amplifiers, the vent pressure is at or above the local ambient pressure and for liquid operated amplifiers the vent pressure is at or above the return line pressure.

The normal procedure is to operate all amplifiers, sensors, and other components in a circuit at a constant vent pressure so that vent pressure effects can be neglected. For a given amplifier geometry, with constant loading, therefore, only supply pressure and control bias level affect the performance.

Supply pressure is related to the operating Reynolds number. Section 1.2.1 shows that LPA gain is related to N_R or, for constant fluid properties, to the supply pressure, P_{sv}. Control bias pressure affects the gain and stability. High positive bias pressures generally cause a decrease in gain. As bias pressure is reduced, the gain will tend to increase. Operation with negative bias pressure (i.e., a pressure level below vent) can lead to instability. Normal staging of amplifiers for pressure gain usually results in bias pressures on the order of 3 to 15 percent, while self-staging of amplifiers produces bias pressures of up to 30 percent.

The extent to which bias pressure affects gain is related to the control width, B_c. Increasing control width tends to increase the gain since more area is available for the input pressure to act on the power jet. The increased area, however, decreases the input resistance so that the advantage is lost when the amplifier is staged. It also increases the sensitivity of the gain to control bias pressure and affects the

output saturation characteristics. The distance between the downstream control edges, B_t, must be increased to adjust for the increased control length; this also reduces gain and input resistance.

The length of the straight section of the nozzle, X_{th}, affects the supply channel resistance and the velocity profile at the nozzle exit. A very long approach length rounds the exit velocity profile and is more sensitive to viscosity than a short approach. To minimize temperature sensitivity, a short approach length is generally recommended.

The nozzle-to-splitter distance, X_{sp}, affects gain and bandwidth. Amplifier gain tends to increase with X_{sp} up to the point where the jet begins to slow and spread out as it moves downstream. The jet transport time also increases with increasing X_{sp}; this reduces amplifier bandwidth.

The size of the receiver width, B_o, is a tradeoff between gain and output resistance. A narrow receiver gives more gain than a wide receiver; however, it also has higher resistance. This is important when amplifiers are staged, especially if the input resistance of the next stage is low. Ideally, the input-to-output resistance ratio of an amplifier should be greater than unity.

The width of the splitter, B_{sp}, affects the gain. Ideally, the splitter should be as small as possible to achieve maximum gain. The splitter position relative to the jet center-line, however, affects the null offset (output pressure differential at zero differential input). A narrow splitter, although preferred for gain characteristics, is fragile and is easily bent during fabrication or handling. For this reason, the splitter is made sufficiently wide to preclude accidental damage.

Although the above parameters have the most influence on overall performance, many other factors can also affect operation. Amplifier symmetry about the jet centerline, for example, influences the null offset. Sidewalls should be smooth and free of burrs, particularly in the supply, control, and output channels. All radii in the interaction region should be smooth and continuous, with no mismatch at the point of tangency with other features.

Table 1 presents data on the critical parameters for several different LPA designs.[3,7] Static and dynamic performance for a few of these designs is discussed in the following section.

2.2 Performance

The use of laminar proportional amplifiers in sensing and control system applications requires information on LPA performance characteristics. The important static characteristics are input/output resistance, null offset, and gain. The dynamic characteristic of interest is the small signal frequency response to establish control system bandwidth. Complete and extensive mathematical modeling of the LPA describing both the

---

[3]F.M. Manion and G. Mon, "Fluerics 33: Design and Staging of Laminar Proportional Amplifiers," Harry Diamond Laboratories HDL-TR-1608 (September 1971).

[7]T. M. Drzewiecki, "A High-Order, Lumped-Parameter, Jet-Dynamic Model for the Frequency Response of Laminar Proportional Amplifiers," 20th Anniversary of Fluidics Symposium," ASME WAM (October 1980).

TABLE 1. CRITICAL DIMENSIONS AND SILHOUETTES
OF SELECTED LPA DESIGNS

HDL Model number	b_s mm	X_{sp}	X_{th}	B_c	B_t	B_o	B_{sp}
2-2B	0.5	8	4.0	4.0	2.0	1.5	0.25
2.3.1.004A	0.5	8	2.0	1.0	1.25	1.5	0.25
3.1.1.8	0.5	8	1.0	1.0	1.125	1.25	0.5

Silhouette	Garrett part number							
a	3169921	0.76	8	1.0	1.0	1.10	1.30	0.5
b	3155350	0.50	8	1.0	1.0	1.13	1.25	0.5
c	3155337	0.38	8	1.25	1.0	1.125	1.31	0.5
d	3155324	0.25	8	1.25	1.0	1.125	1.31	0.5

a   b   c   d
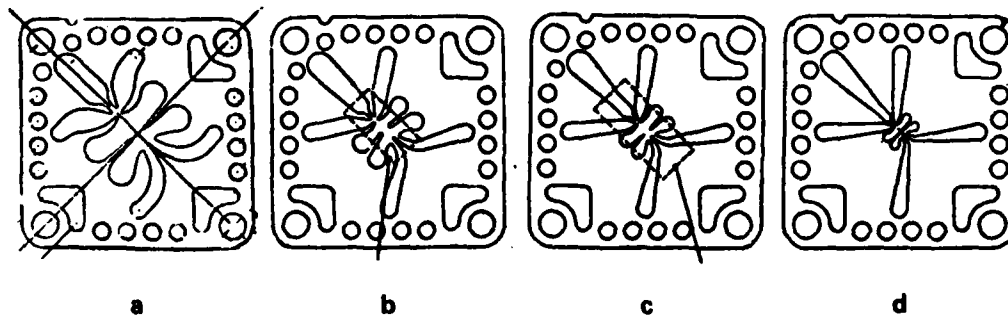
static and dynamic characteristics has been published[1,7] and several computer programs have also been developed.[8,9,10]. The following paragraphs discuss test procedures to determine the LPA characteristics and present test data for a typical LPA design. These test procedures are applicable for both gaseous and liquid powered devices.

2.2.1 Input, Output, and Supply Characteristics

The small-signal resistance (R) of a flow restriction (nozzle, orifice, flow channel, etc.) is defined as the slope of the P-Q (pressure-flow) curve for the restriction

$$R = \frac{\Delta P}{\Delta Q},$$ (20)

where

R = resistance, kg/m^4s^2,

ΔP = change in pressure, kg/m-s^2, and

ΔQ = change in flow, m^3/s.

---

[1]F.M. Manion and T.M. Drzewiecki, "Analytical Design of Laminar Proportional Amplifiers," Proceedings of HDL Fluidic State-of-the-Art Symposium, I, Harry Diamond Laboratories (October 1974).

[7]T. M. Drzewiecki, "A High-Order, Lumped-Parameter, Jet-Dynamic Model for the Frequency Response of Laminar Proportional Amplifiers," 20th Anniversary of Fluidics Symposium," ASME WAM (October 1980).

[8]T. M. Drzewiecki, "Fluerics 38: A Computer-Aided Design Analysis for the Static and Dynamic Port Characteristics of Laminar Proportional Amplifiers," Harry Diamond Laboratories HDL-TR-1758 (June 1976).

[9]J. S. Roundy, "Computer Programs for Laminar Proportional Amplifiers," AiResearch Manufacturing Company of Arizona, Phoenix, AZ, Report 42-0017 (June 1977).

[10]T. M. Drzewiecki, D. N. Wormley, F. M. Manion, "Computer-Aided Design Procedure for Laminar Fluidic Systems," J. Dyn. Syst. Meas. Control, 97, Series G (December 1975).

If the P-Q characteristic is linear, then the resistance is constant; however, if it is nonlinear, the resistance is different at different operating points. The supply nozzle of an LPA, for example, has a nonlinear P-Q characteristic. The operating nominal supply resistance, R_s, is usually defined as the ratio of the pressure drop (at the operating point) to the total supply flow:

$$R_s = \frac{P_s - P_v}{Q_s} = \frac{P_{sv}}{Q_s}.$$ (21)

By using equations 7 and 16, it can be shown that

$$R_s = \frac{\mu\ N_R}{2\ b_s^3\ c_d}.$$ (22)

Supply resistance is often used to normalize other characteristic resistances. It is noted that R_s is dependent on both geometry (b_s, σ) and fluid properties (μ).

Two other resistances of interest are the input and output resistance. The input resistance depends on the control channel resistance and the resistance at the jet boundary. Two operating conditions are of primary interest. In the first case, both control pressures are changed equally so that the jet remains centered. The resulting resistance is called the centered jet resistance, R_c. For the second case, one control pressure is increased (or decreased) while the opposite control pressure is decreased (or increased) by an equal amount. This is referred to as the deflected jet resistance, R_d. The centered jet and deflected jet resistance are obtained from the slopes of the applicable P-Q curve at the operating point of interest.

Figure 5a shows the test setup for measuring the centered jet resistance. Since the flow meter measures the total flow into both control ports, only one-half of the measured value is used to calculate the centered jet resistance. By modifying the test setup as shown in figure 5b, the single-sided P-Q characteristic can also be determined. The centered jet and single-sided P-Q curves can then be used to calculate the deflected jet resistance. The procedure shown in figure 6 is as follows:

1. Choose a bias pressure, P_B, at which R_d is desired.

2. Locate this point on the centered jet characteristics.

3. Go to the point on the single-sided characteristic corresponding to 2 x P_B. This point is still at bias = P_B since

$$P_B = \frac{P_{C1} + P_{C2}}{2} = \frac{2P_B + 0}{2} = P_B.$$

4. Draw a straight line through these two points. The inverse slope of this line is R_d.

The output resistance, R_o, is due to the output channel resistance. This can be measured using the test setup shown in figure 7. The two outputs are connected together so that only one-half of the measured flow is used in calculating output resistance. In making both input and output resistance measurements, the amplifier is operated at the desired Reynolds number which should be specified in reporting the calculated resistance values. More detailed information on measuring amplifier characteristics can be found in reference 11.

---

[11]Fluerics Testing Procedures, Department of Defense MIL-STD-1361 (1971).
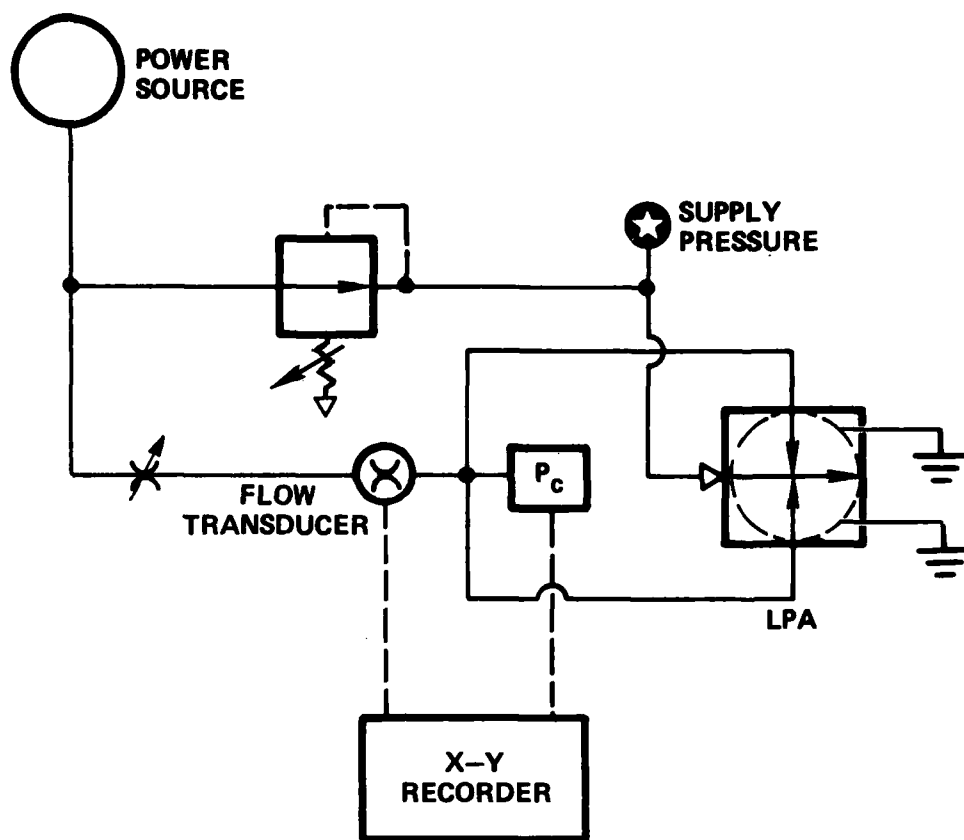
(a.) CENTERED JET RESISTANCE TEST
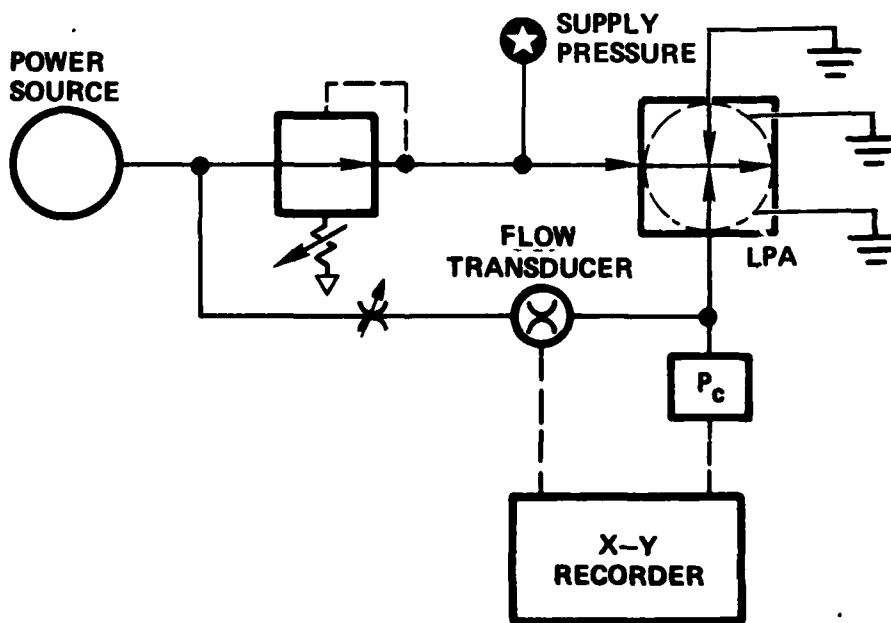
(b.) SINGLE-SIDED DEFLECTED JET RESISTANCE

Figure 5.   Test setup for input resistance measurement.

34
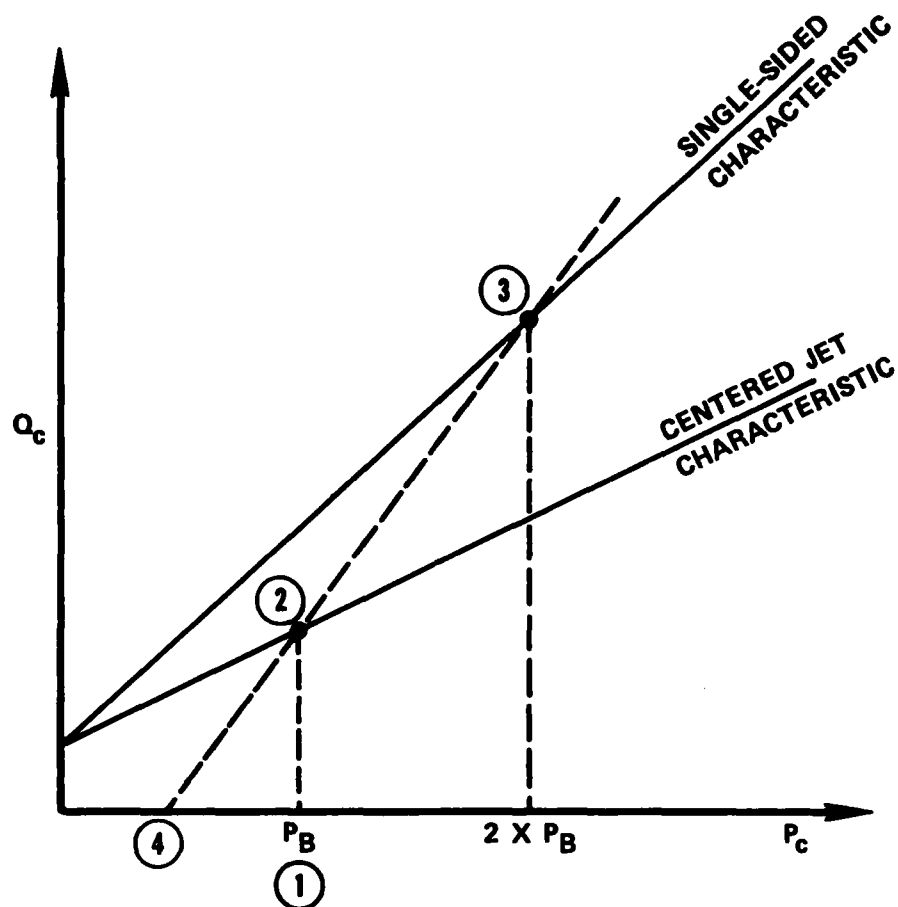
Figure 6.   Graphical method for calculating
deflected jet resistance.
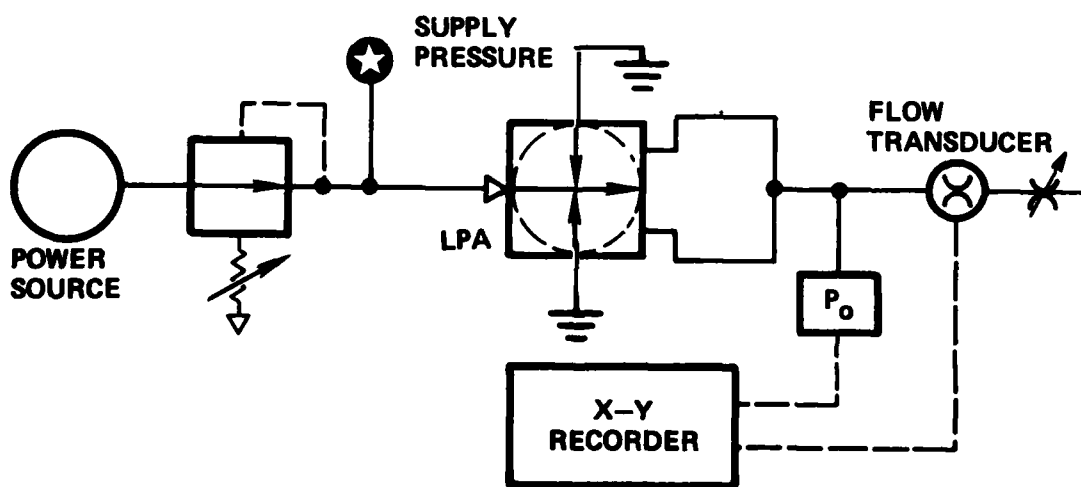
Figure 7.   Test setup for output resistance measurement.

35

Figure 8 shows typical P-Q curves for an LPA. If two amplifiers are staged, the point at which the output P-Q curve of the first (driving) amplifier intersects the centered jet P-Q curve of the second (load) amplifier is the staged operating point. The operating bias pressure corresponds to the pressure at the point of intersection and it is at this point that the deflected jet and output resistance should be calculated.
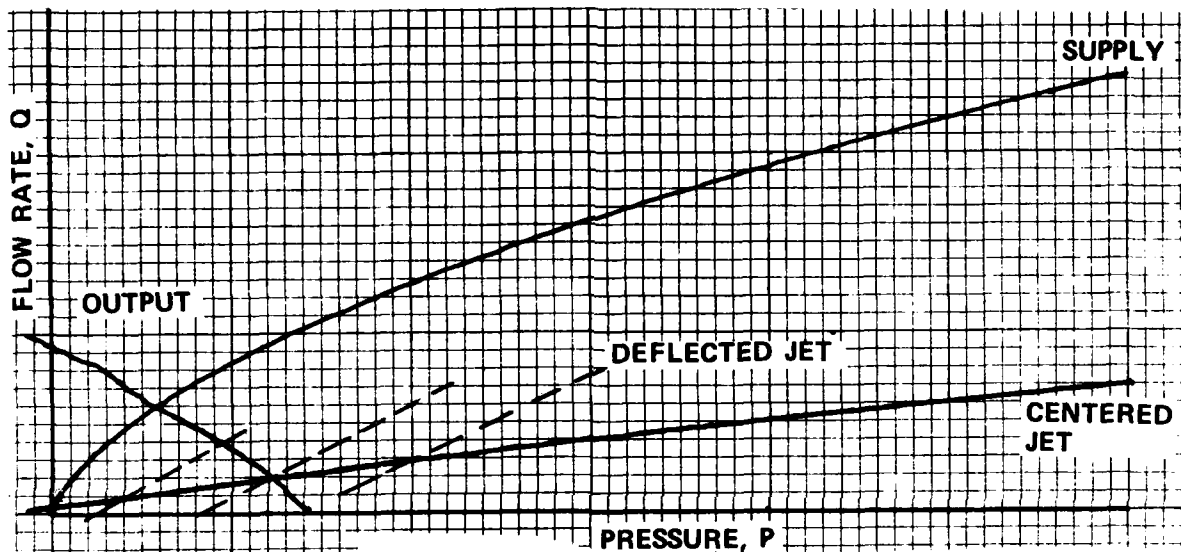
Figure 8. Typical P-Q characteristics of laminar proportional amplifiers.

As defined above, deflected jet resistance corresponds to the condition encountered when two amplifiers are staged. Alternate conditions which would yield different control port characteristics are applications where one control port is held at constant pressure, constant flow, or at a pressure determined by the P-Q characteristics of an input resistive network. For these cases, the deflected jet resistance of the opposite control port would yield a P-Q curve with a different slope. Phillippi[12] compares theoretical and experimental results for several different cases.

---

[12] R. M. Phillippi and T. M. Drzewiecki, "Fluerics 41: Single-Sided Port Characteristics of Laminar Proportional Amplifiers for Arbitrary Input Loading," Harry Diamond Laboratories HDL-TR-1901 (February 1980).

2.2.2 Null Offset

The null offset of an LPA is defined as the differential output pressure with zero differential control pressure. It is usually expressed as a percentage of the operating supply pressure

$$\text{NULL OFFSET} = \frac{\Delta P_o}{P_{sv}} \times 100. \tag{23}$$

Ideally, a perfect LPA should have zero null offset. Manufacturing inaccuracies, however, yield some degree of geometric asymmetry which results in a misalignment of the jet with the receiver ports, an adverse pressure field which deflects the jet away from the receivers, and/or mismatched output areas which result in different recovered pressures for an ostensibly centered jet.

The null offset characteristic is measured using the test setup shown in figure 9a. To eliminate input/output impedance mismatch, the control ports are cross-coupled or shunted and referenced to the vent pressure level and the outputs are connected to a differential pressure transducer (blocked load conditions). The supply pressure is increased from zero up to the point where the transition to turbulent flow is evidenced by an abrupt increase in output pressure fluctuation. The null offset is usually reported as the maximum observed value prior to transition to turbulent flow. Figure 9b shows a typical LPA null offset characteristic.

2.2.3 Gain

Steady-state pressure gain (G_p) is defined as the ratio of the change in output pressure (ΔP_o) to the change in control pressure (ΔP_c):

$$G_p = \frac{\Delta P_o}{\Delta P_c}. \tag{23}$$

37
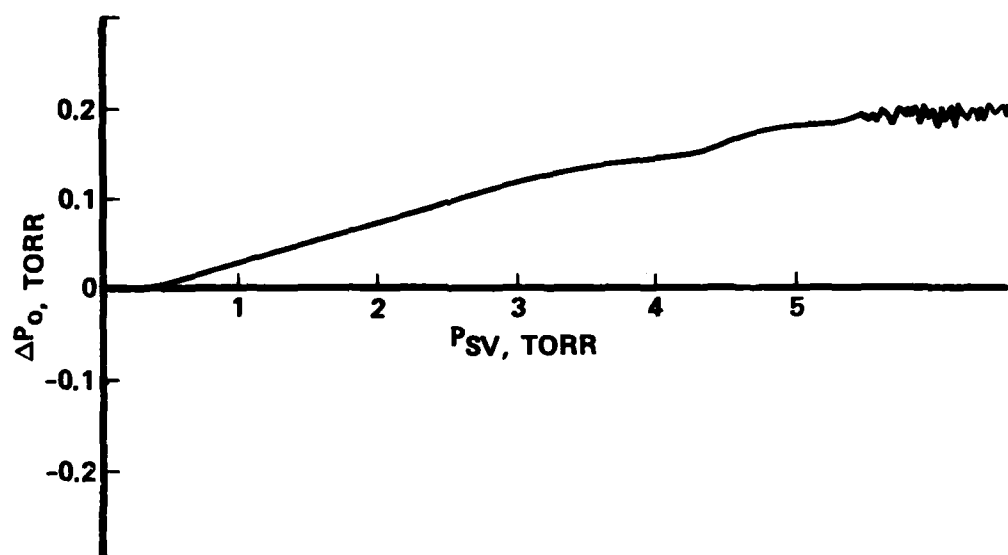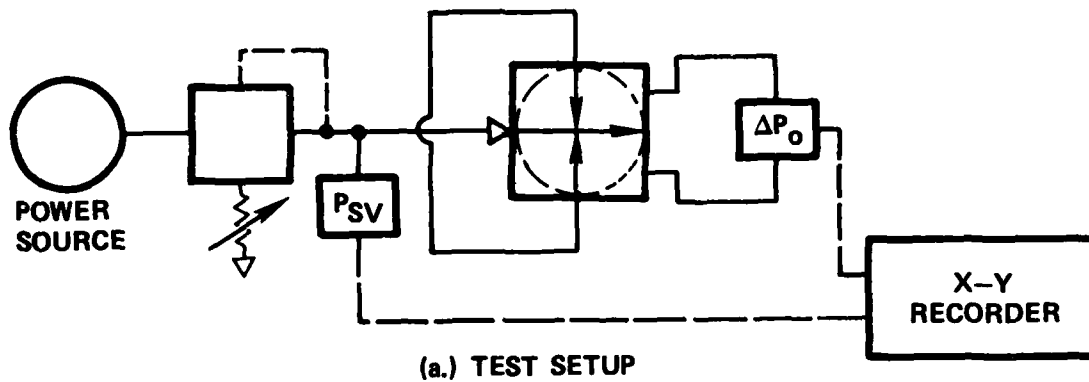
(a.) TEST SETUP

(b) TYPICAL NULL OFFSET DATA

Figure 9.   Test setup for null offset measurement.

The gain is a function of amplifier geometry, bias pressure level, the operating Reynolds number, and the load conditions. Maximum gain is achieved when the amplifier is block loaded (infinite resistance load). When the amplifier is connected to a load which has resistance R_L, the gain is given by

$$G_P = \frac{G_{po}}{(1 + R_O/R_L)},$$ (24)

where

G_{po} = blocked load gain,

R_O = amplifier output resistance, and

R_L = load resistance.

If the load is another amplifier, the load resistance is the deflected jet input resistance of the load amplifier.

For a typical HDL LPA design, the gain increases as σN_R increases. Maximum gain is usually obtained in the range $1000 < \sigma N_R < 1400$. This was shown in figure 2. If the Reynolds number is held constant, increasing the aspect ratio also results in an increase in gain since this corresponds to an increase in σN_R. The normal range for σ is given by $0.3 < \sigma < 3$. For aspect ratios below 0.3, the amplifier gain decreases because of boundary layer effects. Although an increase in gain can be obtained with aspect ratios above 3, the supply pressure becomes too low to work with since the supply pressure has to be decreased to maintain $\sigma N_R < 1400$. High aspect ratios also reduce the input resistance.

Self-staged gain is the best figure of merit for an LPA. A wide control width amplifier such as HDL Model 2-2B has a blocked load gain of about 20; however, because of its low input resistance, the self-staged gain is only about 2. Narrow control

39

width amplifiers have blocked load gains of about 10; however, the self-staged gain is about 5.5. When amplifiers are staged to form high-gain gain blocks, it is desirable for the input-to-output resistance ratio to be greater than one. Self-staging three identical narrow control amplifiers (such as HDL Model 3.1.1.8) would yield a gain of over 125 with an input-to-output resistance ratio between 1 and 2.

As mentioned before, increasing the bias pressure causes a decrease in gain. The sensitivity to bias pressure depends on the control width, B_c. Amplifiers such as HDL Model 2-2B, which has wide controls, have the most gain sensitivity to bias pressure. Amplifiers such as HDL Model 2.3.1.004A and 3.1.1.8, which have narrow controls, exhibit less gain sensitivity. This is illustrated in figure 10.

2.2.4 Low-Frequency Dynamics

The previous discussion addressed steady-state characteristics of the LPA; dynamically only the relationship between jet transport time and phase lag were mentioned in section 1.2.1. The dynamics of an LPA are more complex than this. Control and output channels, for example, have impedance given by

$$Z = R_c + j\omega L_c. \tag{25}$$

The frequency-dependent component of the channel impedance has been assumed to be purely inductive. The fluid compliance may be negligible, even in high-frequency gaseous applications, if it is small compared with the compliance (capacitance) associated with the volume swept out by the deflecting jet. Typically, for small devices ($b_s \leq 0.25$ mm), channel capacitance cannot be neglected. Fluid inductance (inertance) is defined as the product of the fluid density and
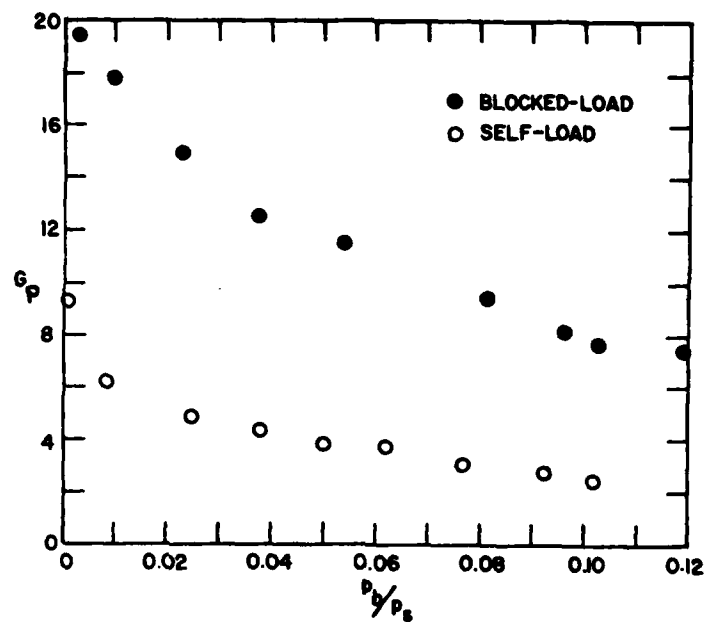
(MODEL 2-2B)
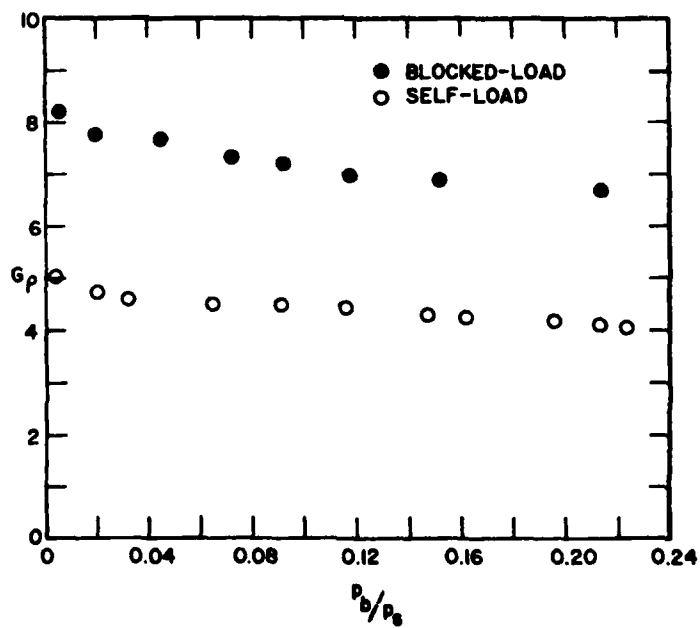
(MODEL 2.3.1.004A)

Figure 10. Effect of bias pressure on gain

41

the channel length divided by the average cross-sectional area of the channel. For the control channel,

$$L_c = \frac{x_c}{\overline{b}_c h},$$ (26)

where

L_c = inductance, kg/m^4,

ρ = fluid density, kg/m^3,

x_c = channel length, m,

$\overline{b}_c$ = average control channel width, m, and

h = channel depth, m.

Manion and Drzewiecki[1] express the pressure gain, G_p, as a second order function of the form

$$G_p = G_{po}/[(A_2/A_0)(j\omega)^2 + (A_1/A_0)j\omega + 1],$$ (27)

where G_{po} is the blocked load gain and the coefficients A_0, A_1, and A_2 are real numbers whose values are determined from amplifier geometry and operating conditions.

The variation of gain and phase angle as a function of frequency is usually presented in a Bode diagram. The magnitude of the gain (absolute value of G_p) may be written as

$$\left| G_p(\omega) \right| = G_{po}A_0/([A_0-A_2(2\pi F)^2]^2 + A_1^2 (2\pi F)^2)^{1/2}.$$ (28)

---

[1]F.M. Manion and T.M. Drzewiecki, "Analytical Design of Laminar Proportional Amplifiers," Proceedings of HDL Fluidic State-of-the-Art Symposium, I, Harry Diamond Laboratories (October 1974).

The phase shift (the ratio of real to imaginary parts of G_p, plus the phase shift due to transport time) is

$$\phi(\omega) = \tan^{-1} [A_1(2\pi F)/(A_0 - A_2(2\pi F)^2)] + 720\, X_{sp}F \qquad (29)$$

where

F = normalized frequency,

$$F = f\, b_s/[c_d(2P_{sv}/\rho)^{1/2}], \qquad (30)$$

f = frequency, Hz, and

$$= \omega/2\pi.$$

Figure 11 presents the theoretical gain and phase of a typical LPA operating on air.[8] For control system analysis, the bandwidth is assumed to be the frequency where the phase shift is 45 degrees. From figure 11, this occurs at a normalized frequency of about 0.007. The bandwidth in Hertz is calculated from equation 30 as follows:

$$f = F[c_d\,(2P_{sv}/\rho)^{1/2}]/b_s, \qquad (31)$$

$$\rho = 1.2059 \text{ kg/m}^3 \text{ at } 22C,$$

$$P_{sv} = 700 \text{ kg/m-s}^2,$$

$$c_d = 0.7,$$

$$b_s = 0.5 \times 10^{-3}\text{m},$$

$$f = 0.007\ [0.7\ (2(700)/1.2059)^{1/2}]/0.5 \times 10^{-3}, \text{ and}$$

$$f = 334 \text{ Hz}.$$

---

[8]T. M. Drzewiecki, "Fluerics 38: A Computer-Aided Design Analysis for the Static and Dynamic Port Characteristics of Laminar Proportional Amplifiers," Harry Diamond Laboratories HDL-TR-1758 (June 1976).
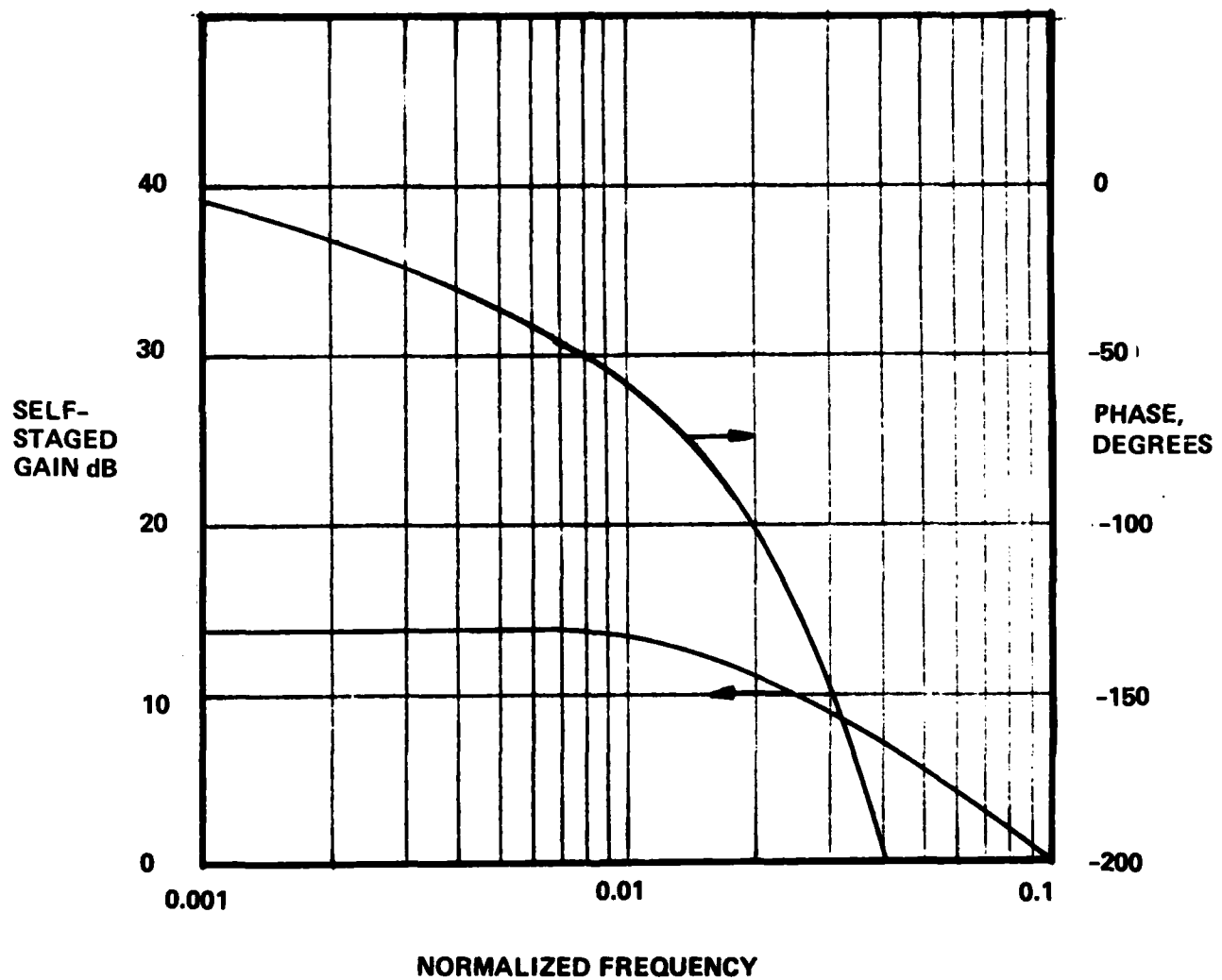
Figure 11.   Gain and phase of a typical LPA
versus normalized frequency.

After the gain and phase data have been normalized, the effects of variations in Reynolds number or aspect ratio on bandwidth can be estimated. For example, if the aspect ratio of the amplifier is increased from 1 to 2 and the Reynolds number is reduced to 600 (σN_R = 1200), then the normalized bandwidth will still correspond to F = 0.007. The supply pressure required for σN_R = 600 is reduced by a factor of four; therefore, the actual bandwidth frequency is reduced by a factor of two. Thus, the bandwidth for this configuration is only 167 Hz. Similarly, the normalized bandwidth will remain at approximately the same value for small variations in the operating Reynolds number. To obtain the bandwidth in Hertz, the supply pressure required for the desired Reynolds number is calculated and substituted into equation 31 with F = 0.007.

The normalized gain and phase characteristics are sensitive to the LPA geometry, which influences the values of the coefficients A_0, A_1, and A_2 in equation 27. Wide controls, such as HDL design 2-2B, increase the jet capacitance effect and this reduces the overall response. The normalized bandwidth for this type of amplifier geometry has a phase lag of 45 degrees at about F = 0.005.

2.2.5 High-Frequency Dynamics

In the above paragraphs, the bandwidth of the LPA was defined as the frequency where the phase lag is 45 degrees. It has also been observed that, at much higher frequencies, the amplitude response exhibits multiple resonances, even though the phase continues to fall off rapidly. These resonant peaks, which are more pronounced for high aspect ratio amplifiers ($\sigma > 2$), permit useful signal amplification at a higher bandwidth. This characteristic is particularly useful in applications such as audio amplification where the emphasis is on amplitude response over a specific bandpass.

45

Drzewiecki[7] has developed a high-order, lumped parameter, jet-dynamic model for LPA's that has good agreement with experimental measurements for the amplitude frequency response and excellent agreement for the phase shift.

The range of interest of frequency response of an LPA generally lies between the characteristics obtained for the case of blocked load and that of self-staged load. For each case, the maximum bandwidth over which useful gain occurs corresponds to $F \simeq 0.1$. Drzewiecki expresses the maximum bandwidth (f_{bw}) using the modified Reynolds number (N_R') substituted into equation 31 as follows,

$$f_{bw} = F \left[\frac{c_d \nu N_R' \ (1 + X_{th}) \ (1 + 1/\sigma)^2}{b_s^2} \right]. \tag{32}$$

The resonant peaks are at maximum amplitude when the modified Reynolds number is high ($N_R' = 120$). Using this value of N_R' and substituting $F = 0.1$, $c_d = 0.7$, and $X_{th} = 1$ gives

$$f_{bw} = \frac{16.8 \ \nu \ (1 + 1/\sigma)^2}{b_s^2}. \tag{33}$$

The supply pressure corresponding to $N_R' = 120$ is given by

$$P_{sv} = \frac{28,800 \nu^2 \ (1 + 1/\sigma)^4}{b_s^2}. \tag{34}$$

---

[7]T. M. Drzewiecki, "A High-Order, Lumped-Parameter, Jet-Dynamic Model for the Frequency Response of Laminar Proportional Amplifiers," 20th Anniversary of Fluidics Symposium," ASME WAM (October 1980).

Using equations 33 and 34, a map for air at 22C is obtained, where $\nu = 1.4864 \times 10^{-5}$ m^2/s and $\rho = 1.2059$ kg/m^3. This is shown in figure 12. This figure shows that current LPA's with nozzle widths of 0.5 mm have sufficient bandwidth to be used in audio amplification. Ultrasonic operation of these devices is feasible, assuming that the small dimensions can be manufactured with sufficient accuracy.
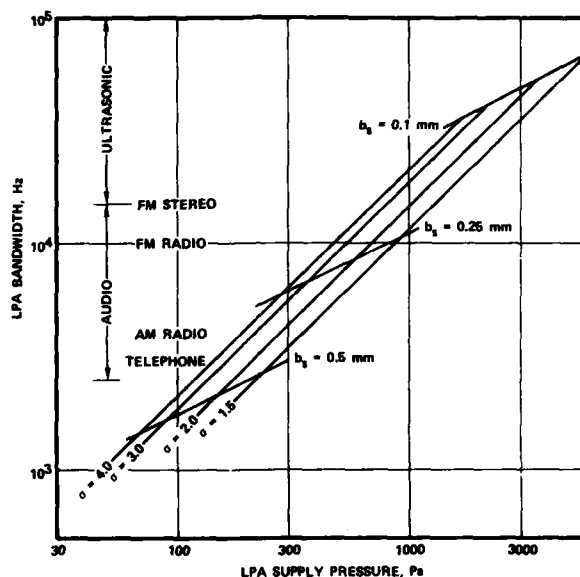
Figure 12.   Engineering guide for the bandwidth of high aspect ratio LPA's.

Experimental evidence shows that maximum bandwidth is obtained with a staged amplifier because the load effectively produces a lead term. The worst case is for a single blocked loaded amplifier where the normalized bandwidth corresponds to $F = 0.01$, or ten times less than given by equation 33. If many amplifiers are staged together in series and the last stage is blocked, care must be taken, when describing the overall bandwidth, to take into account the reduced frequency response of the last stage.

47

3. SCALING LAMINAR PROPORTIONAL AMPLIFIERS

Scaling a fluidic device such as an LPA or laminar flow sensor refers to the changing of size (geometric scaling), operating fluid (kinematic scaling), or both, to obtain either similar or different operating characteristics. For example, scaling is used in water table studies of laminar flow devices in order to visualize the internal flow patterns and to evaluate the effect of geometric parameters on performance.[13] The test model can be made many times larger than the actual size of the final part and performance with a variety of fluids can be simulated. In this case, both geometric and kinematic scaling is used. Another example of scaling is that associated with determining the supply requirements (pressure-flow) when the same device is operated on different fluids and comparable performance is desired. Since the geometry is constant, only kinematic scaling is required. Graphical data for density and viscosity of the most commonly used fluids are presented in Appendix B.

In fluid mechanics, scaling is synonymous with similarity. Geometric similarity requires that the ratios of corresponding lengths between two devices be the same. Kinematic similarity requires that the ratios of corresponding velocities and accelerations are the same at corresponding points in the flow field of the two devices. For geometric and kinematic similarity to exist simultaneously, the dimensionless form of each physical variable must have the same value at corresponding points in the flow fields. Forces acting on corresponding fluid masses must be related by dimensionless ratios dependent on inertia, static pressure, viscosity, gravity, elasticity, heat conduction, and surface tension effects.

---

[13]C. E. Spyropoulos, "Large Scale Modeling of Laminar Fluidic Devices," Harry Diamond Laboratories HDL-TM-73-28 (February 1978).

With laminar flow, many of these forces are considered negligible. Normally, velocities are low enough so that even in gaseous devices the flow can be assumed to be incompressible and thus elasticity (compressibility) forces are neglected. For both liquids and gases, static pressure forces, gravity, heat conduction, and surface tension forces are considered negligible; only viscous and inertial forces dominate. Therefore, to maintain similarity between viscous and inertial forces, it is only necessary to maintain the Reynolds number constant.

In describing the geometry of a typical LPA (section 2), all of the critical dimensions were normalized with respect to the nozzle width, b_s. It can be stated, therefore, that two LPA's are geometrically similar if their normalized dimensions are identical. As an example, consider the HDL Standard LPA which has a supply nozzle width of 0.5 mm and the following normalized dimensions (see figure 4 for definitions):

$$B_c = 1.0$$
$$B_o = 1.25$$
$$B_t = 1.125$$
$$B_{sp} = 0.50$$
$$X_{sp} = 8$$
$$X_{th} = 1.0$$
$$\sigma = 1.0$$

An LPA with a supply nozzle width of 1.0 mm and the same normalized dimensions as the LPA described above is geometrically similar even though it is physically twice the size of the LPA whose supply nozzle is only 0.5 mm wide. The performance of these two amplifiers, operating on the same or different fluids, will be equivalent provided that kinematic similarity exists.

49

Kinematic similarity exists if the operating Reynolds number is the same for each amplifier. It should also be evident that two geometrically identical LPA's operating on different fluids will have equivalent performance if the Reynolds number is the same for both.

The performance parameters of interest are gain, input resistance, output resistance, and bandwidth. Clearly, the requirement to maintain kinematic similarity (equal N_R) is going to result in different values of pressures and flow rates when geometrically similar amplifiers are operated on the same or different fluids. Equivalent performance is defined by the use of nondimensional performance parameters. Pressure data are normalized with respect to the supply-to-vent differential pressure (P_{sv}) and flow data are normalized with respect to the supply flow, Q_s.

Pressure gain was defined in equation 23 as the ratio of output pressure change to input pressure change ($\Delta P_o / \Delta P_c$). Since this is a dimensionless parameter, two geometrically and kinematically similar amplifiers have the same gain for the same equivalent loading (blocked or self-staged). If the differential output and input pressures are normalized with respect to the supply pressure, plotting $\Delta P_o / P_{sv}$ versus $\Delta P_c / P_{sv}$ will yield a single steady-state transfer characteristic valid for all geometric and kinematic similar amplifiers. (Unless stated otherwise, any subsequent reference to similarity in this report will mean both geometric and kinematic similarity).

Input and output resistances are defined as the slopes of the appropriate P-Q curves at the operating point of interest. The P-Q data are normalized with respect to the supply pressure and supply flow. The slope of the normalized curve (P/P_{sv} versus Q/Q_s) gives the normalized input resistance, R_c', and the normalized output resistance, R_o', is defined as follows:

$$R'_C = \frac{R_C}{R_S}, \qquad (35)$$

$$R'_O = \frac{R_O}{R_S}, \qquad (36)$$

where

$$R_S = \frac{P_{sv}}{Q_S}. \qquad (37)$$

Two similar LPA's, therefore, will have the same normalized input and output resistances. Actual input and output resistance (R_C, R_O) could be quite different because of the differences in supply resistance, R_S, for each case.

Normalized bandwidth (phase response) was introduced in section 2 and is given by equation 30. Again, two similar LPA's will have the same normalized frequency response. The actual bandwidth for each will be different because of the differences in physical dimensions or fluid properties. It is noted that amplifiers of the same size operating on fluids of the same kinematic viscosity (e.g., air and MIL-H-5606 hydraulic fluid at a temperature of 30C) have very different operating pressures; however, they will both have the same bandwidth.

Geometric similarity and Reynolds number scaling make it possible to establish a set of simplified engineering guidelines based on the performance of a single LPA operating on air.[14] The guidelines summarized below use convenient working units in place of SI units, and are based on the geometry of the standard LPA design (reference HDL model 3.1.1.8). For this amplifier,

---

[14]T. M. Drzewiecki, "A Fluidic Voice Communication System and Data Link," D. Eng. Thesis, Naval Postgraduate School, Monterey, CA (March 1980).

51

b_s 0.5 mm,

$\sigma = 1.0$,

$X_{th} = 1.0$,

$N_R' = 120$,

$P_{sv} = 4$ mm Hg, and

$Q_s = 0.3$ LPM.

The design guidelines, valid for any geometrically similar amplifier, are as follows:

1. The operating point is $\sigma N_R = 1000$.

2. At the operating point, $c_d = 0.7$.

3. The Reynolds number is

   $$N_R = 1000 \, b_s \, (\text{mm}) \, [P_{sv} \, (\text{mm Hg})]^{1/2}.$$

4. The operating pressure in mm Hg is

   $$P_{sv} = (1/\sigma b_s \, (\text{mm}))^2.$$

5. The operating flow in LPM is

   $$Q_s = 0.3 \, (N_R'/120) \, [b_s \, (\text{mm})/0.5].$$

6. The supply resistance in mm Hg/LPM is

   $$R_s = P_s/Q_s = 13.3 \, (N_R'/120) \, (1/\sigma)^2 \, [(0.5/b_s \, (\text{mm})]^3.$$

7. The input resistance is

   $$R_i = 0.75 R_s.$$

8. The output resistance is

   $$R_o = 0.5 \, R_s.$$

9. The blocked gain is $8 \leq G_{po} \leq 10$.

10. The loaded gain is

$$G_p = G_{po} \, [1/(1 + R_o/R_L)].$$

11. The saturation output signal is twice the pressure recovery, P_R, where $P_R = 0.35 \, P_{sv}$.

4. AMPLIFIER FORMAT AND AMPLIFIER STAGING

Laminar proportional amplifiers and sensors are active (flow consuming) devices that form the building blocks of fluidic control systems. A typical application requires several of these active devices interconnected to perform a specific control function. A packaging design concept is required that can provide a means to interconnect these devices, distribute the supply and vent flow, and accommodate additional components such as flow restrictors and volumes required to accomplish various control functions. The packaging concept is dependent on the component configuration which, in turn, is a function of the method used to fabricate the various control elements. The most convenient configuration is to use a planar element format which has two flat sides. Section 5 discusses various fabrication methods which can be used to produce components in this configuration.

This section presents a planar design format which permits integrated, modular fluidic circuit construction. At present, there is no industry standard for fluidic circuit design, although the format presented herein has been adopted in a slightly modified form for general use by the government. The format presented here has proven to be quite versatile for preliminary research and development and cost effective for production applications. It is recommended that this format be adopted as an industry standard. Also discussed are design procedures for staging LPA's with illustrations of typical circuit assemblies using the proposed standard format.

4.1 Standard Amplifier Format

The standard amplifier format is a planar laminate (with two flat sides) 3.3 cm x 3.3 cm (1.3 in. x 1.3 in.) square. Laminate thicknesses depend on the functional purpose of each laminate and the method of fabrication. For stamped or photo-chemically milled laminates, individual laminate thicknesses are usually between 0.1 mm (0.004 in.) and 0.64 mm (0.025 in.). Each laminate has a functional purpose: it could be an LPA, a vent plate, an exhaust plate, a gasket, or it may have another special function. The individual laminates are arranged in a vertical stack buildup to obtain an integrated circuit assembly. Figure 13 shows the outline of a typical assembly and the plan view of the laminate configuration at several different sections. Each laminate has four bolt holes which are used for alignment and mounting of the stack. If the laminates are not bonded to form a solid structure, a rigid cover plate should be placed on top to evenly distribute the bolt forces and ensure adequate laminate-to-laminate sealing.
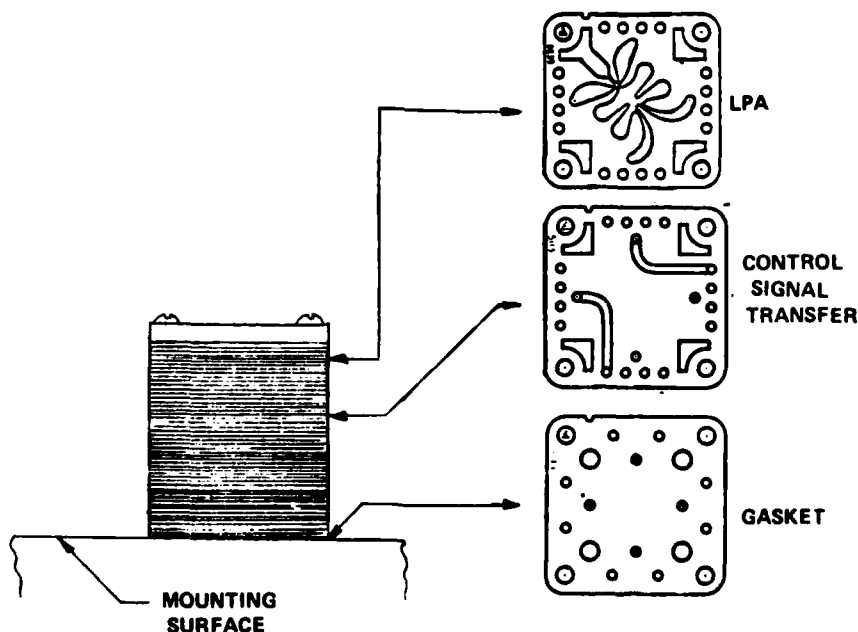
Figure 13. Typical fluidic assembly using the standard amplifier format.

A loosely stacked laminated assembly, when it is securely bolted down, provides adequate performance for laboratory development. With this approach, however, there are always minute leak paths at laminate interfaces which can adversely affect circuit performance. The problem is aggravated if the circuit is exposed to wide variations in temperature since the capillary-like leak paths are very sensitive to temperature changes. One method for eliminating this problem is to bond the final circuit assembly into a single monolithic structure. Stainless-steel laminations can be diffusion bonded by using high temperatures and high surface loading. Garrett uses a modified procedure called assisted diffusion bonding.[15] A low melting point alloy is electro-deposited on each laminate, allowing the final circuit assembly to be bonded at much lower temperatures and pressures than required for pure diffusion bonding. Most of the alloy actually diffuses into the metal during heating. A small amount of residual material remains, however, which fills small voids along the mating joint where insufficient clamping forces exist for complete bonding to occur. Control of this plating thickness, therefore, is critical since excessive plating will plug small passages while insufficient plating will result in an inadequate bond.

Two basic hole patterns are used for all laminates as illustrated in figure 13. Where the stack interfaces with its mounting surface, the configuration has the hole pattern shown in figure 14. All other laminates have the hole pattern shown in figure 15. Fewer holes are used on the bottom plate to allow use of either a gasket seal or an O-ring interface. Holes in the base plate that correspond to the same hole in the upper laminate are identified with the same number or letter. Figure 16 shows the laminate buildup required to transfer information from the base hole pattern to the hole pattern of figure 15. The

---

[15]T. G. Sutton, W. J. Anderson, "Aerospace Fluidic Applications and Circuit Manufacture," AGARD-AG-215 (January 1976).

0.520 (TYP)
(13.2)

0.342 (TYP)
(8.69)

0.170 (TYP)
(4.32)

NO. 6-32 BOLT HOLE
0.148 — 0.154 DIA
(3.76 — 3.91 DIA)
4 PLACES

0.160 DIA (TYP)
(4.06)

0.090 DIA (TYP)
(2.29)

NOTE: ALL DIMENSIONS ARE IN INCHES (mm)
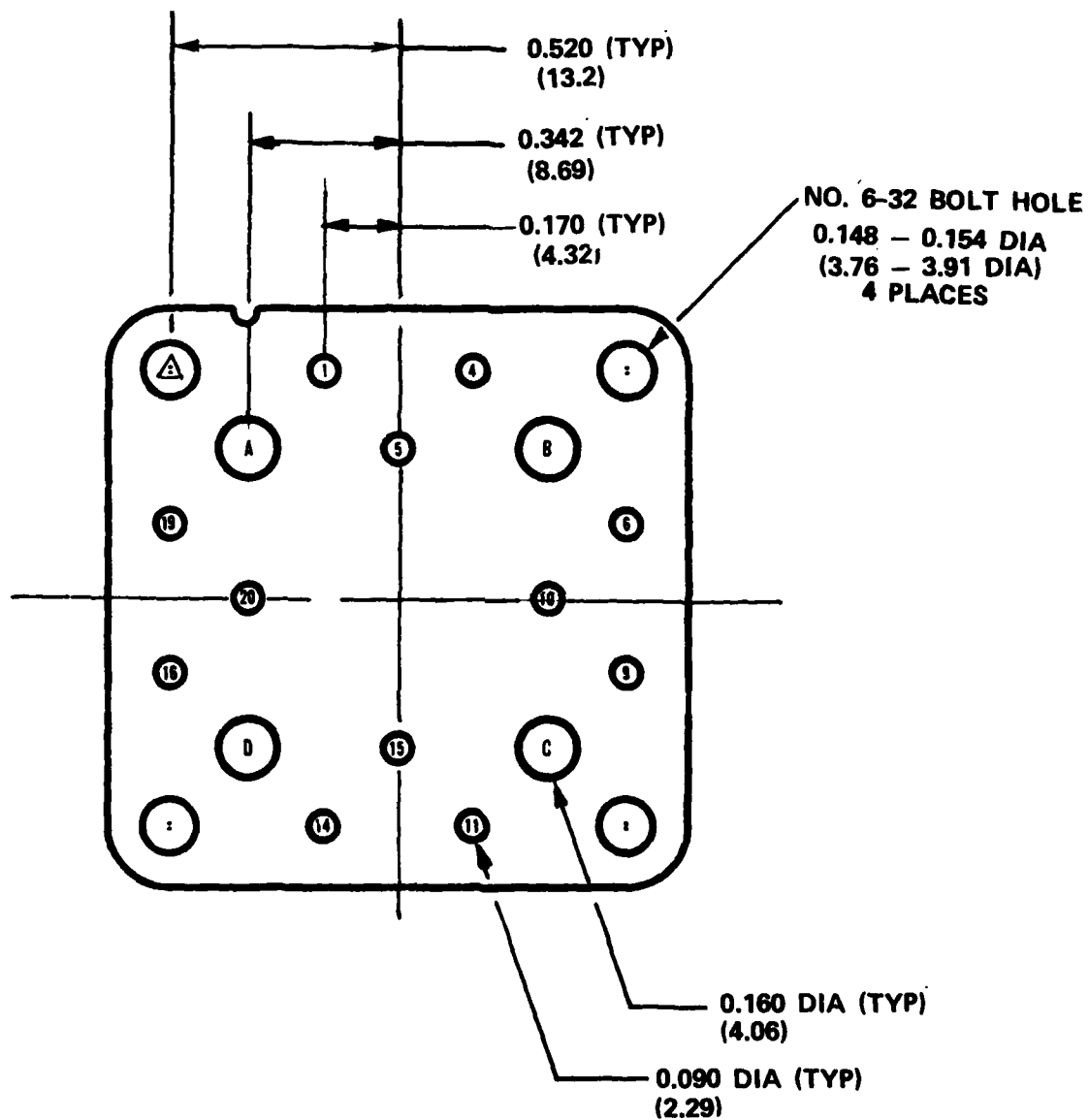
Figure 14. Standard amplifier format hole pattern at mounting surface interface.

0.520 (TYP)
(13.2)

0.210 (TYP)
(5.33)

0.070 (TYP)
(1.78)

NO. 6-32 BOLT HOLE
0.148-0.154 DIA
(3.76-3.91 DIA)
4 PLACES

0.090 DIA (TYP)
(2.29 DIA)

VENT AND SUPPLY HOLE
0.141 DIA (TYP)
(3.58 DIA)
4 PLACES

0.378 (TYP)
(9.60)

0.090 DIA (TYP)
(2.29)

0.434 (TYP)
(11.0)

0.555 (TYP)
(14.1)
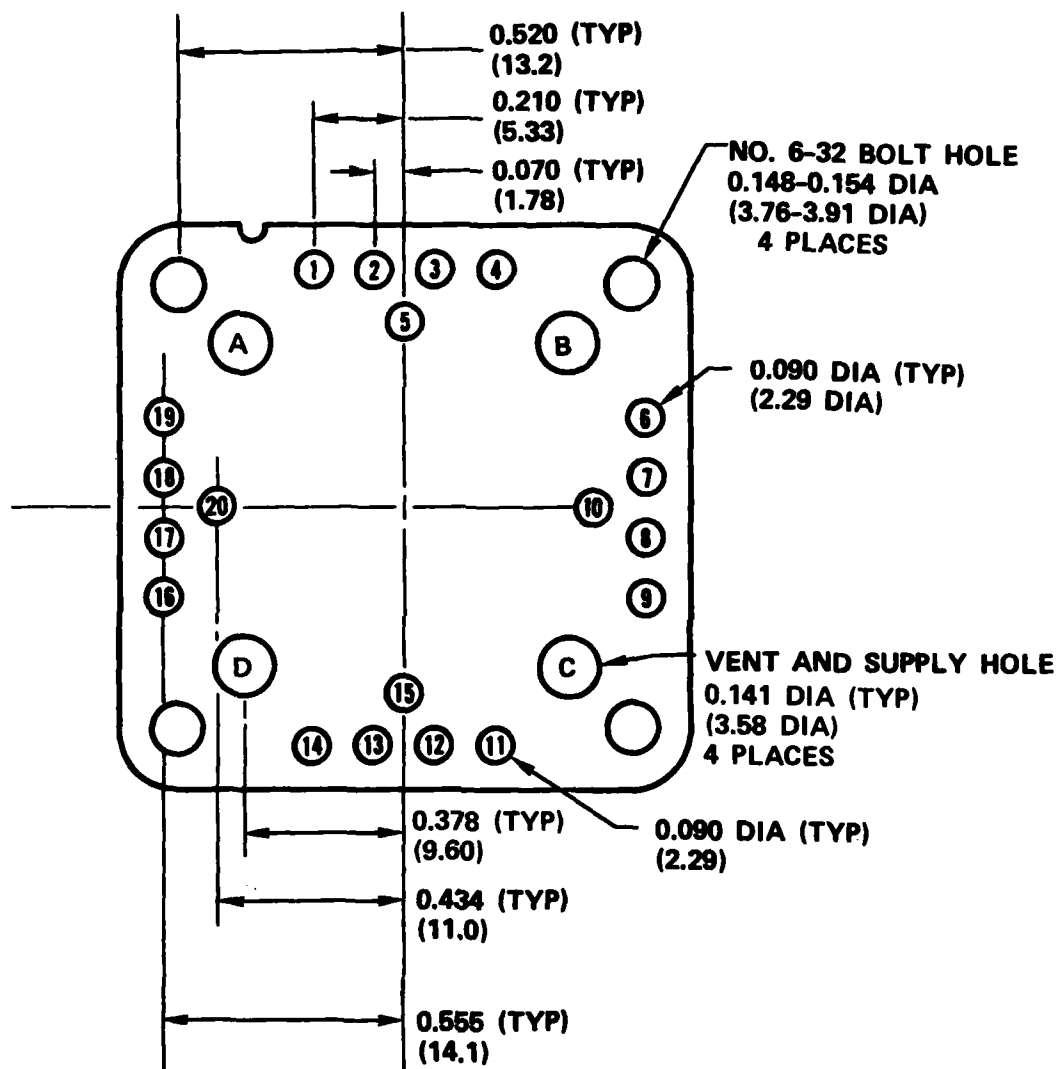
NOTE: ALL DIMENSIONS ARE IN INCHES (mm)

Figure 15. Standard amplifier format hole pattern.

larger openings (labeled A, B, C, and D on figures 14 and 15) are used as supply and vent manifolds. The smaller holes (labeled 1-20 on figure 15) are used to transmit the various fluidic pressure signals.

When this format was originally developed, it was desirable to provide the maximum size supply and vent transfer. This led to selection of the irregularly shaped holes shown on figures 13 and 16. With laminar flow circuits, however, it was found that this geometry can create excessive flow noise; therefore, a round supply/vent transfer is recommended as shown in
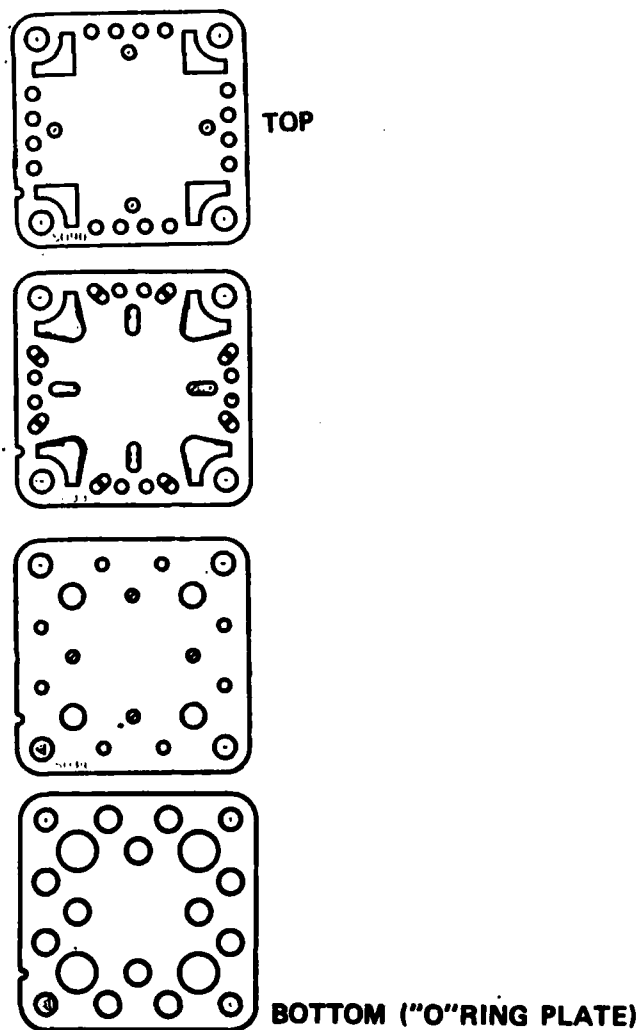
Figure 16.   Stacking sequence to interface with base plate.

figure 15. (In subsequent illustrations, the original design is shown since this corresponds to existing Garrett components. The round hole is preferred and is used in the HDL version of this format.)

Amplifiers are positioned diagonally on the laminates so that the supply nozzle is directly in line with the corner supply hole. This orientation has three advantages. First, it provides for a smooth inlet connection with the supply plenum; second, it allows several different size amplifiers to fit on the same format; and third, it places the highest pressure points where the clamping force is at its maximum. Amplifier control and output channels are connected to the four innermost transfer holes (labeled 5, 10, 15, and 20 on figure 15). The remaining holes can then be used for transferring input and output signals and for monitoring pressures.

Each laminate has a small notch which is used as a reference for orientation. Because of the symmetry of the laminate, there are eight possible orientations. This is demonstrated in figure 17 where the eight different positions are identified with letters A through H. By giving each different laminate design a separate part number, a complete stacking diagram can be developed by calling out the part number and laminate orientation.

Figure 17. Permutations of laminate orientations.

Amplifiers are positioned diagonally on the laminate and since they are symmetrical about the diagonal, there are two ways in which to orient them (e.g., A or F, B or G, C or H, etc.). If seve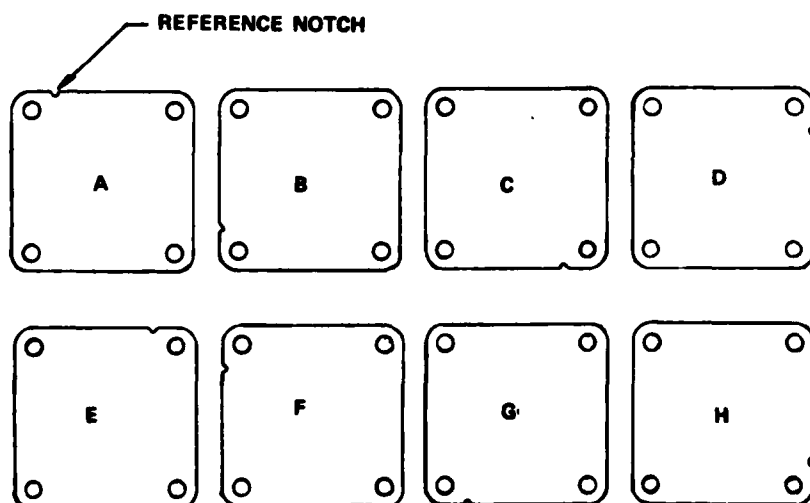ral amplifier laminates are stacked on top of each other to make up a required thickness, alternating their position, such as A-F-A-F, helps to cancel out manufacturing inaccuracies and often results in an improvement in the null offset characteristic of the amplifier. Similarly, when two amplifiers are staged, this technique can be used to reduce the null offset of the staged amplifiers by letting the null offset of one amplifier cancel the null offset of the next amplifier.

Since the amplifier is in a planar format, the laminates positioned immediately above and below it form the upper and lower jet boundary. These adjacent plates are also required to vent the interaction region and collect the vent flow without producing an adverse vent pressure gradient. For gaseous applications, it is often possible to vent the amplifier to ambient through the side of the stack; however, this approach is generally undesirable since the vents may then transmit spurious outside noise. Therefore, for most operations, and especially liquid operation, all vent flow must be collected and returned to a sump. Side venting of individual amplifiers is possible if the entire stack is mounted in a housing that also serves as a collecting manifold. Figure 18 shows two possible stacking arrangements for amplifier venting. Depending on amplifier design and operating conditions, satisfactory operation may be possible with the amplifier vented from only one side; a plain gasket would then be used on the opposite side.

In addition to the amplifier, vent, and exhaust (vent flow) plates, gasket plates are required to block off specific flow passages and transfer plates are required to transfer a signal from one location to another. Special-purpose laminates that are frequently used include flow restriction passages (linear and nonlinear) to create desired pressure drops and laminates with large open areas to create internal volumes.

60
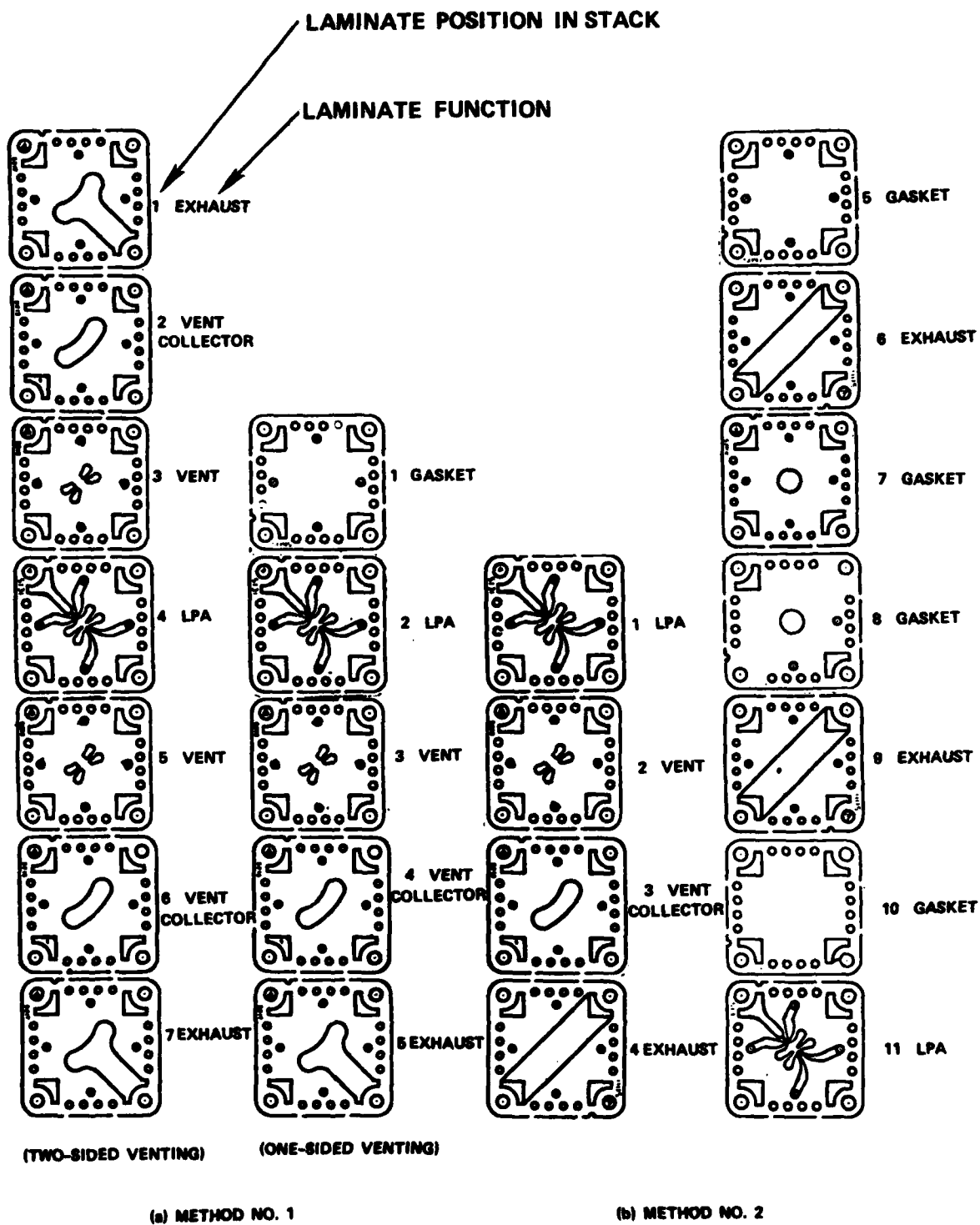
Figure 18. Stacking sequence for amplifier venting.

Figure 19 shows a few of these additional laminate types in the standard format.

RESTRICTIONS   TRANSFERS   GASKETS   MISCELLANEOUS
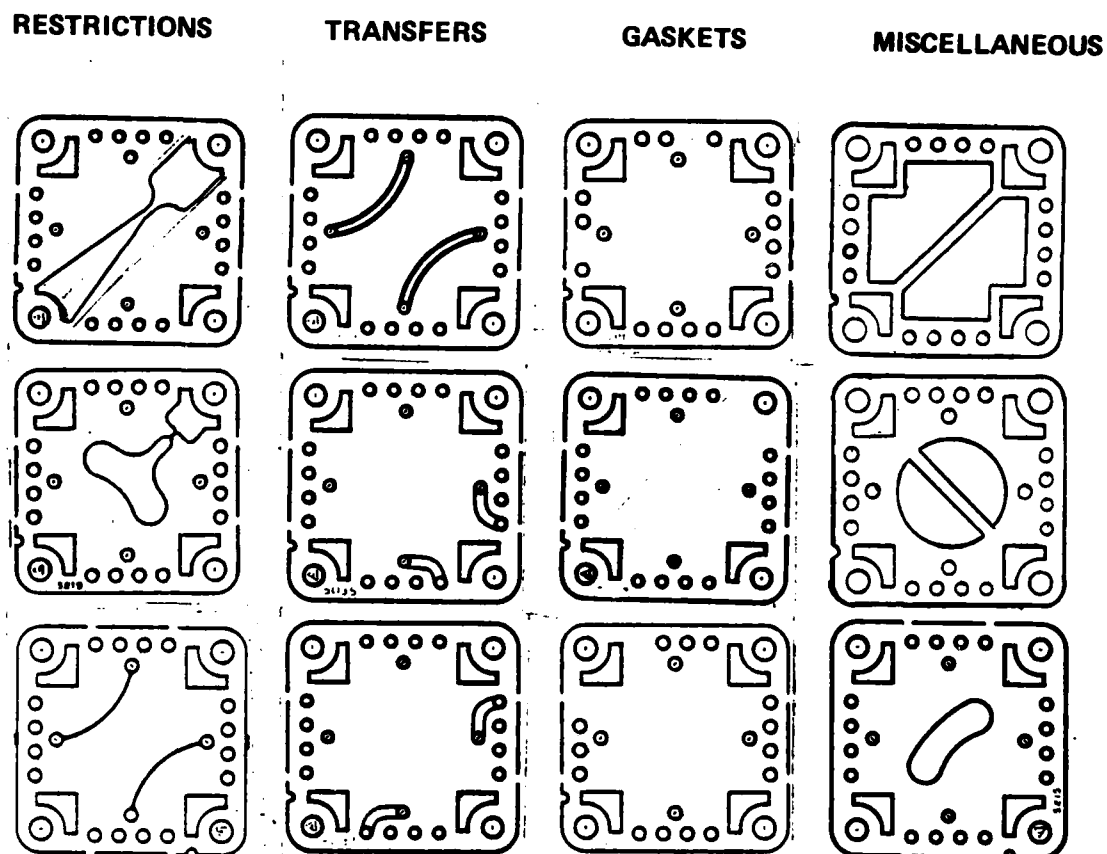
Figure 19.   Typical laminates used with standard
amplifier format.

4.2   Staging Laminar Proportional Amplifiers

Staging is the process of connecting two or more amplifiers in series to obtain an increase in gain. In section 2 it was stated that an LPA has pressure gain; a small change in pressure at the inputs produces a larger change in pressure at the outputs. The pressure gain is at a maximum when

62

flow is delivered at the outputs (blocked load). Pressure gain decreases as flow is withdrawn from the amplifier outputs. If the amplifier outputs are wide open, the pressure gain is essentially zero.

An LPA also has flow gain; a small change in flow at the inputs produces a larger change in flow at the outputs. Flow gain is a maximum when the amplifier outputs are wide open and is zero when the amplifier is operated block-loaded. Since power is defined as the product of pressure and flow, an LPA also has power gain. This can be expressed as the ratio of power output $(P_o Q_o)$ to power input $(P_c Q_c)$ measured at the controls. The power gain is zero when the amplifier is blocked loaded $(Q_o = 0)$ or when it is wide open $(P_o = 0)$. The power gain is a maximum when the product $P_o Q_o$ is a maximum. This occurs at only one particular loading which depends on the P-Q characteristics of the amplifier and load resistances. For linear output and load resistances, the maximum power gain occurs when the load resistance, R_L, is equal to the amplifier output resistance, R_o. In general, for two self-staged LPA's, these two resistances will be almost linear; the load resistance for maximum power gain, therefore, has a value very close to the amplifier output resistance. For self-staged LPA's, $R_d \sim R_o$; hence, the power gain is a maximum.

Of the three gains described above, staging for pressure gain is the most common requirement. The following section discusses pressure gain staging techniques and shows a typical buildup of a three-stage gain block using the standard amplifier format.

4.2.1 Staging for Pressure Gain

There are several methods of staging LPA's to obtain pressure gain. For example, amplifiers can be self-staged by

connecting identical elements all operating at the same supply pressure. This practice is convenient for assembly and manifolding and for maximizing the input/output resistance ratio; however, dynamic range is not optimized. Dynamic range is related to the maximum available output signal which, for laminar proportional amplifiers, increases with an increase in supply pressure. If two identical amplifiers operating at the same supply pressure are staged, the first amplifier will saturate the second amplifier before the first amplifier reaches its own saturation level. Thus, the full dynamic range of the first amplifier is not being used. In some applications, the single-stage amplifier dynamic range is high enough so that a self-staged reduction in dynamic range can be tolerated.

Figure 20 gives the complete stacking diagram for three self-staged amplifiers using the standard amplifier format. The output stage is located at the bottom of the stack; the input stage is located at the top. Control (input) signals are transmitted to the top of the stack where they are then transferred to the input amplifier. The amplifier vent flows are collected using the method shown in figure 18a.

The single amplifier dynamic range can be maintained for a multi-stage cascade by raising the supply pressure of the later stages in the same proportion as the self-staged pressure gain and decreasing the aspect ratio. Higher supply pressure stages may be operated in parallel so that a given stage input and output resistance is about the same as that of the previous stage. For example, when the self-staged gain is five, the next stage supply pressure is increased by a factor of five, and about five elements would be paralleled to maintain the ratio of supply pressure to supply flow at a constant value.
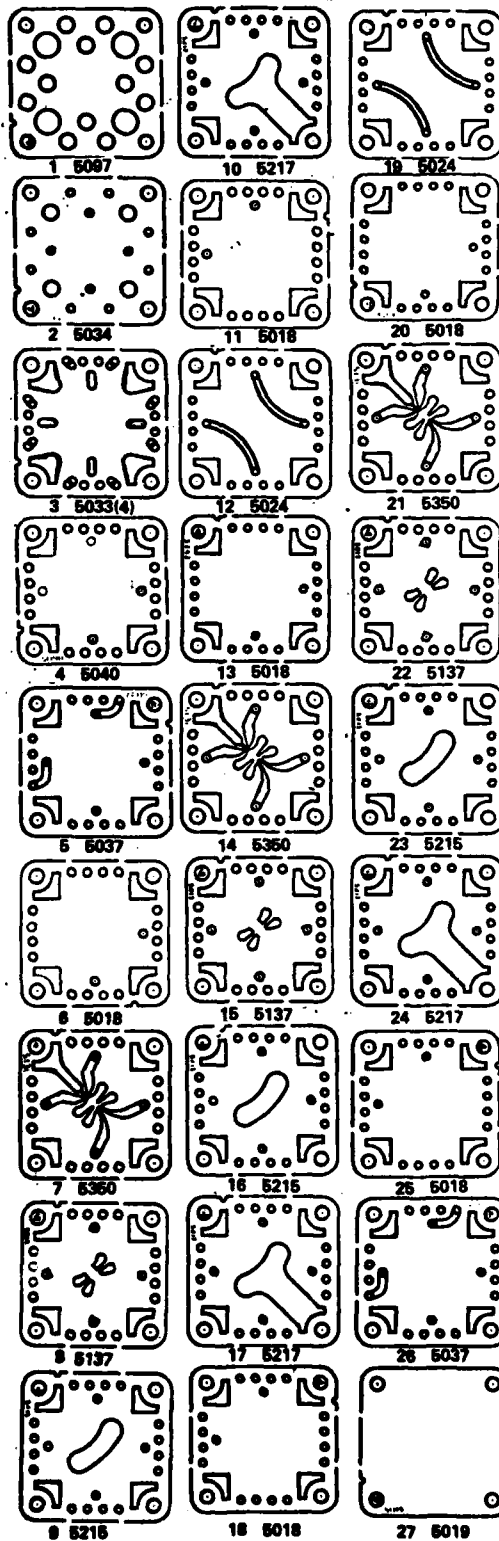
Figure 20. Stacking sequence for three self-staged LPA's

Maximum gain is obtained when an amplifier is operated in a block-loaded manner. Therefore, the staged gain can be increased by increasing the input resistance of the later stages. This can be achieved by reducing the aspect ratio of later stages while also raising the supply pressures. Decreasing the power jet width of the later stages also raises the input resistance and allows each stage to operate at a more favorable aspect ratio. Ideally, the aspect ratio of each stage should be near one to achieve the highest gain. Each stage is sized (power jet width and depth) to operate near $\sigma N_R = 1000$.

As an illustration of this approach, a three-stage gain block operating on air can be considered. The supply pressure required for $\sigma N_R = 1000$ can be calculated using design guideline Number 4 presented in section 3.

$$P_{sv}(\text{mm Hg}) = (1/\sigma b_s (\text{mm}))^2 \qquad (38)$$
$$= (1/h\ (\text{mm}))^2$$

where

$\qquad$ h = nozzle depth.

Table 2 presents the calculated supply pressures for nozzle depths between 0.10 and 1.00 mm and also shows the aspect ratios for four different power jet widths. The aspect ratios within the heavy lines on table 2 correspond to the range of values most frequently used. An aspect ratio of one is usually optimal for highest gain; however, slightly higher and lower values can be used.

The data in table 2 can be used as the starting point in the design of a gain block using staged supply pressure and increasing input resistance. As an example, assume that it is desired to use a first-stage amplifier with $b_s = 0.75$ mm and

TABLE 2. SUPPLY PRESSURE REQUIRED FOR $\sigma N_R = 1000$
(OPERATION ON AIR AT STANDARD TEMPERATURE AND PRESSURE)

h mm	P_{sv} Torr	b_s, mm			
		0.25	0.38	0.50	0.75
		$\sigma = h/b_s$			
0.10	100.0	0.40	0.26	0.20	0.13
0.15	44.4	0.60	0.39	0.30	0.20
0.20	25.0	0.80	0.53	0.40	0.27
0.25	16.0	1.00	0.66	0.50	0.33
0.30	11.1	1.20	0.79	0.60	0.40
0.35	8.2	1.40	0.92	0.70	0.47
0.40	6.3	1.60	1.05	0.80	0.53
0.45	5.0	1.80	1.18	0.90	0.60
0.50	4.0	2.00	1.32	1.00	0.67
0.55	3.3	2.20	1.45	1.10	0.73
0.60	2.8	2.40	1.58	1.20	0.80
0.65	2.4	2.60	1.71	1.30	0.87
0.70	2.0	2.80	1.84	1.40	0.93
0.75	1.8	3.00	1.97	1.50	1.00
0.80	1.6	3.20	2.11	1.60	1.07
0.85	1.4	3.40	2.24	1.70	1.13
0.90	1.2	3.60	2.37	1.80	1.20
0.95	1.1	3.80	2.50	1.90	1.27
1.00	1.0	4.0	2.63	2.00	1.33

$\sigma = 1.2$. A good rule of thumb for maximum dynamic range is that each succeeding stage should be 1/3 as thick as the previous stage. Since the first stage has a depth of 0.90 mm, the second stage should be 0.3 mm and the third stage should be 0.1 mm thick. Referring to table 2, amplifier sizes that give aspect ratios near unity for the required values of h are then selected. Thus, a possible choice is summarized in table 3:

TABLE 3. STAGING EXAMPLE

Stage No.	b_s mm	h mm	σ	P_{sv} Torr
1	0.75	0.90	1.2	1.2
2	0.38	0.30	0.79	11.1
3	0.25	0.10	0.40	100.0

The above configuration is one of several possible arrangements. The optimum configuration can be determined either experimentally or analytically. A simplified computer program for staging LPA's is presented in Appendix C.

Although the above staging technique can achieve more gain than self-staged amplifiers, the disadvantage is that the last stage has a higher output resistance than the input resistance of the first stage. This may be acceptable in some applications; however, for most control system applications, the input-to-output resistance ratio must to be greater than one. The best compromise is a combination of the two methods: staging supply pressures (using different power jet sizes) and using parallel amplifier stages to reduce output resistance.

Figure 21 is a schematic of a three-stage hydraulic gain block developed by MIT[16] that uses the combined method. Two parallel first-stage amplifiers drive three second-stage amplifiers. These, in turn, drive six parallel amplifiers that make up the third stage.
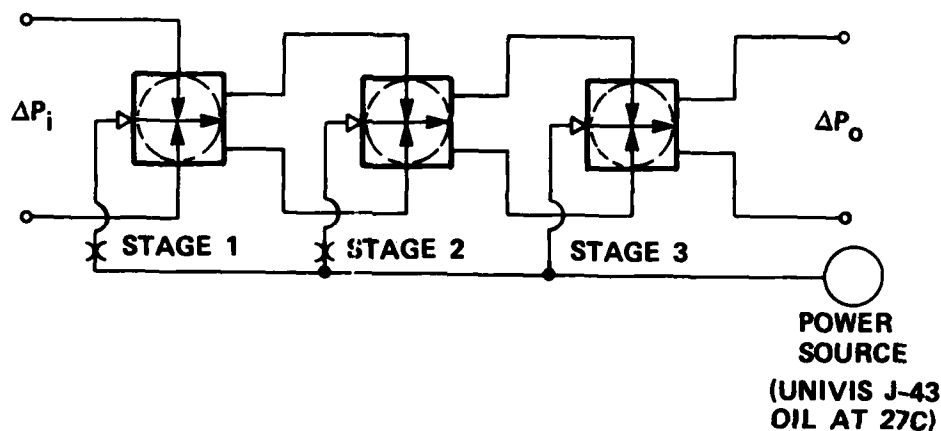
STAGE	b_s (mm)	σ	P_{SV} kPa	NO. OF PARALLEL SECTIONS
1	0.75	0.67	400	2
2	0.50	0.5	1600	3
3	0.375	0.33	6890	6

Figure 21.   Three-stage operation gain block.

---

[16]K. M. Lee, D. N. Wormley, "Fluidic Integrated Component Servovalve Description and Characteristic Performance," Department of Mechanical Engineering, Massachusetts Institute of Technology, Quarterly Report to HDL Contract No. DAAK21-79-C-0158 (May 1981).

Figure 22 presents a complete stacking sequence for this circuit using the standard amplifier format. The circuit is mounted on a manifold block that has ports for supply pressure, control signals, output signals, and return to sump. The output stage operates at the full supply pressure (6890 kPa). However, this pressure is reduced for the first two stages by using low aspect ratio converging/diverging nozzles. This type of restriction is preferred over orifices because they generate much less flow noise.

5.   LAMINAR AMPLIFIER FABRICATION

This section reviews manufacturing methods suitable for fabrication of two-dimensional planar fluidic amplifiers and sensors. Some of these methods have been successfully used to produce turbulent flow amplifiers and sensors and the same techniques can be adapted for fabrication of laminar flow devices. Since laminar flow devices are often used in applications requiring very high gain, the performance obtained is related to the quality of the manufacturing method used to fabricate the various components. One measure of performance, which is directly related to the quality of the fabrication process, is the null offset characteristics of laminar proportional amplifiers and sensors.

Null offset of an LPA is defined in section 2. Figure 23 is a typical LPA null offset characteristic. The null offset curve will shift to the right or left with changes in fluid temperature. However, if the offset is normalized (i.e., $\Delta P_o/P_{sv}$) and plotted as a function of Reynolds number, the data reduces to a single curve.
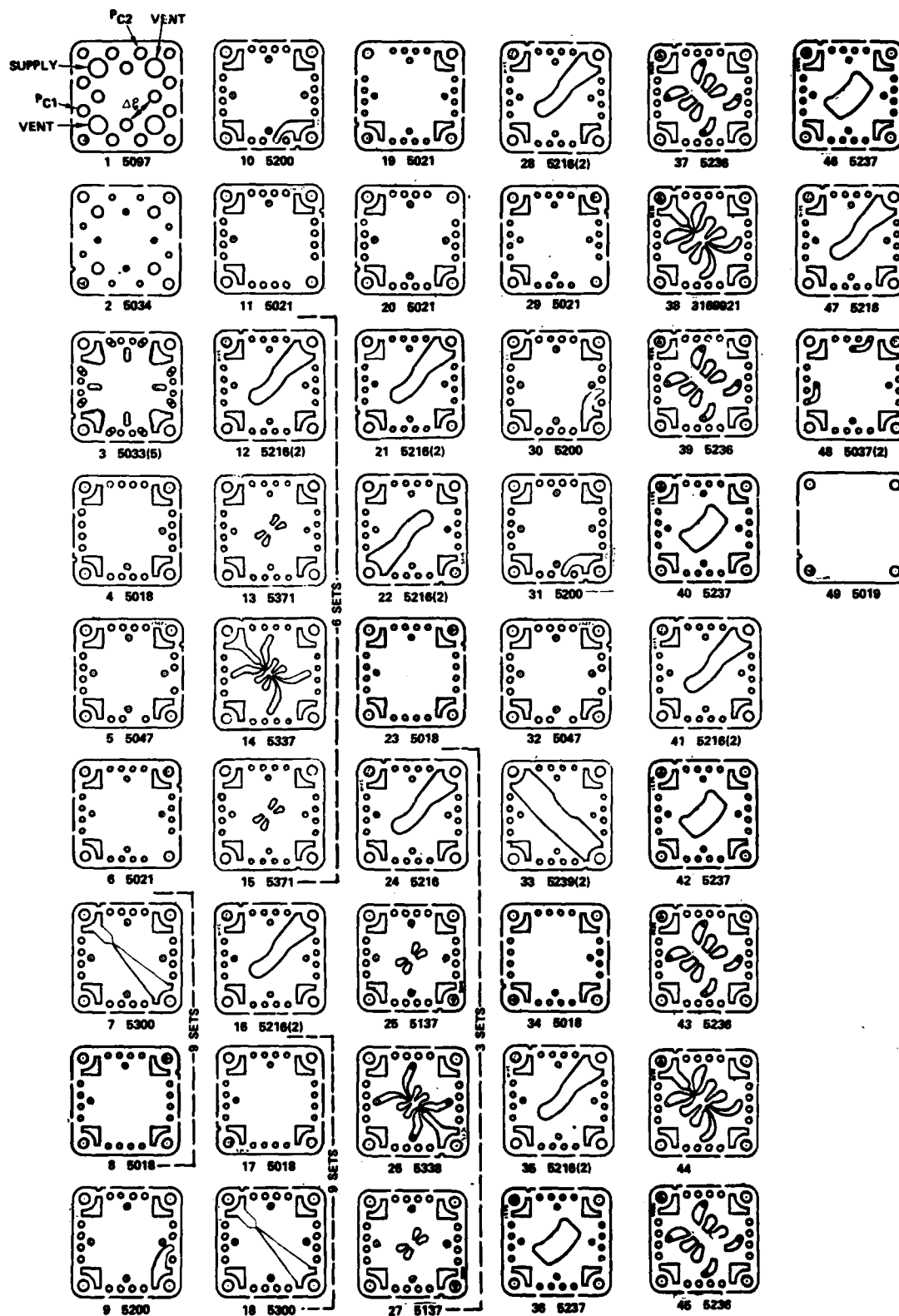
Figure 22. Stacking sequence for three-stage
hydraulic gain block.

71
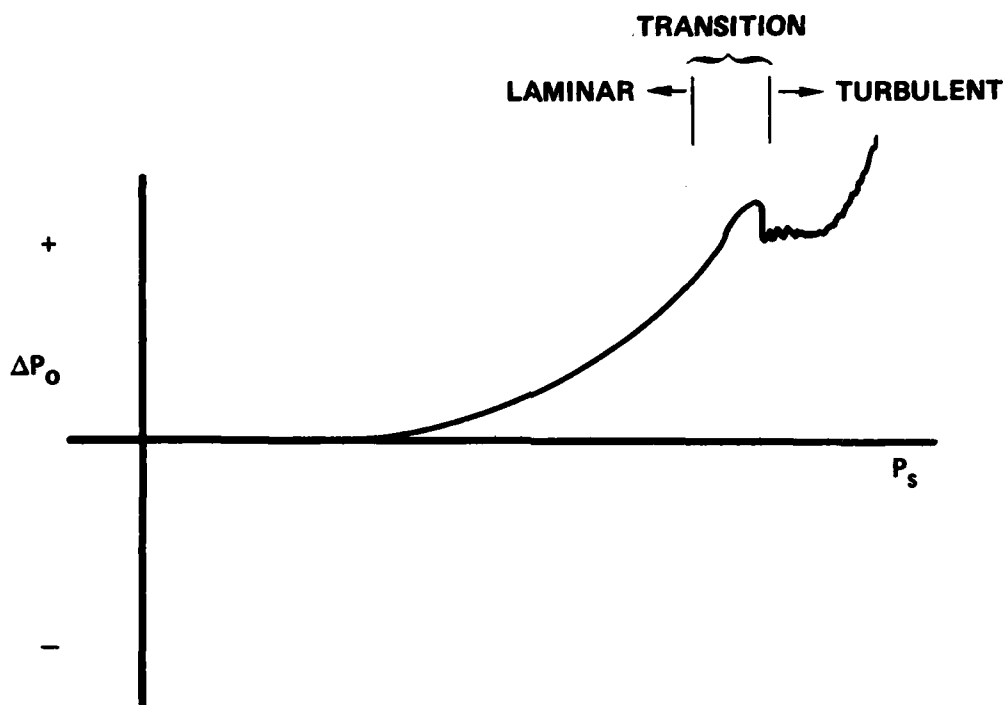
Figure 23.   Typical LPA null offset characteristic.

Null offset has been found to be directly related to the geometric symmetry of the amplifier and, therefore, to the quality of the manufactured component. Nozzle-splitter alignment, parallelism of the nozzle straight section, nozzle exit symmetry, and sidewall condition are a few of the parameters which influence the null offset.

The production methods described in the following paragraphs yield components having varying degrees of dimensional accuracy, overall quality, and cost.   Cost and accuracy are tradeoffs to be considered in light of the application requirements, thus making it difficult to single out any one method above the others.   The need for improved accuracy and low cost in high production applications will continue to stimulate

72

further research into improved fabrication methods. The methods described herein will ultimately be supplemented by new developments.

5.1 Photochemical Milling

Photochemical milling of metal was a well-established process by the time that fluidic researchers entered the field. It has been and still is the most common method of producing fluidic laminates.[15] In this process, the surface of the metal is first coated with a light-sensitive photoresist material that behaves somewhat like photographic paper. The image of the desired feature is printed on a stabilized transparent material (a positive image tool) which is then laid over the coated metal and exposed to light. Subsequent development of the exposed coated metal surface changes the characteristics of the coating. The light exposed areas become resistant to certain acids which are capable of dissolving the metal areas masked by the positive image tool. After chemical milling, the photoresist material is removed with a chemical wash.

Since the photoresist is only a surface preparation, chemical milling results in an undercut producing a nonperpendicular sidewall. To minimize this undesirable characteristic, the foregoing process is applied to both sides of the metal. Since undercutting now occurs from both sides, the process results in a slight ridge at approximately the center of the material. This is illustrated in figure 24.

---

[15]T. G. Sutton, W. J. Anderson, "Aerospace Fluidic Applications and Circuit Manufacture," AGARD-AG-215 (January 1976).

SIDE VIEW
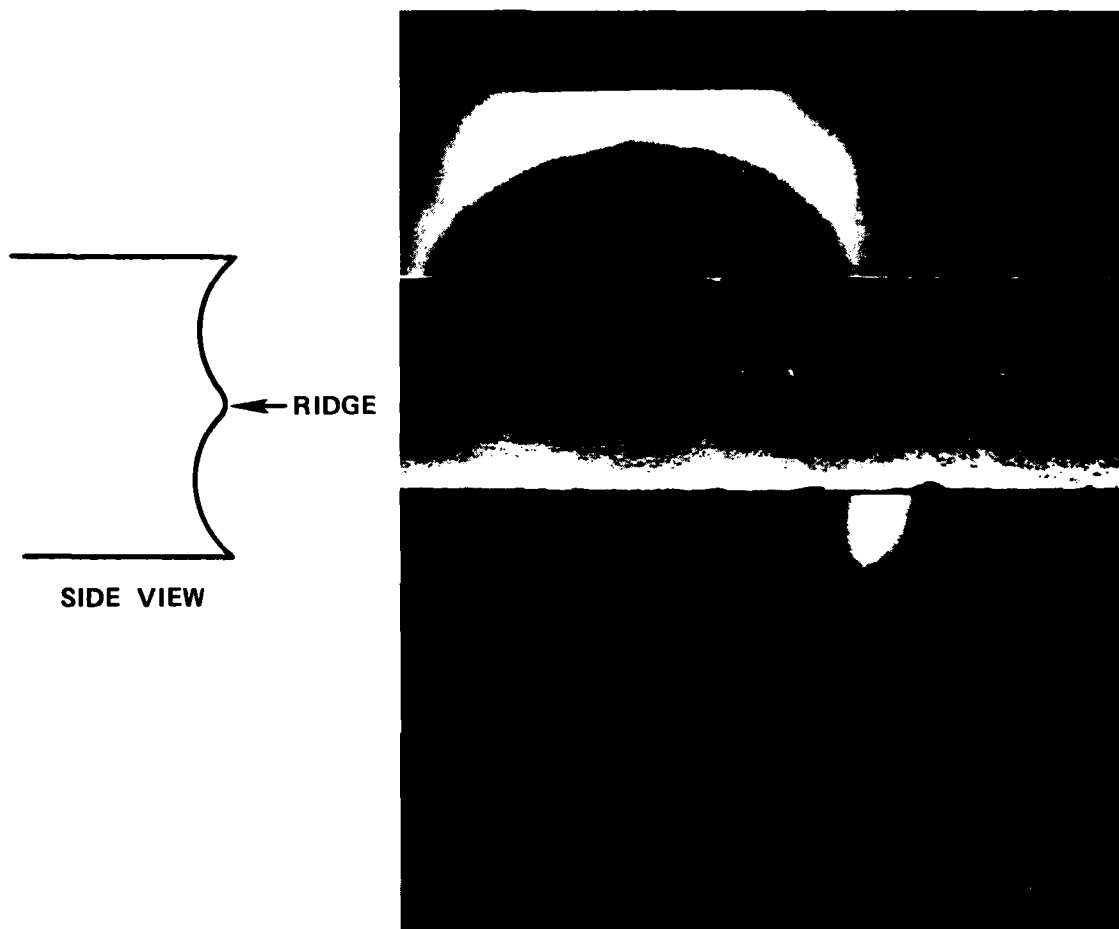
←RIDGE

Figure 24. Sidewall profile of a photochemically milled laminate.

The center ridge can adversely affect critical laminar flow components. The ridge can be minimized by using thin metal sheets (0.15 mm or less) and stacking several finished laminates together to achieve the desired thickness. Noncritical components can be made from thicker sheets (up to 1 mm). A general rule is that the minimum feature dimension (nozzle width, slot width, hole size, etc.) should be no smaller than three times the thickness of the material. Typical milling time for stainless steel material is 0.025 mm per minute.

The accuracy of parts produced with this process depends on several factors. Dimensional accuracy of the positive image tooling and the method used to align and transfer the image onto the coated metal sheets are very critical. Good quality parts can be achieved by using thin stock. Features with a tolerance of 0.025 mm can be achieved with material up to 0.13 mm thick. When several thin laminates are stacked to form a thicker amplifier, however, the stack alignment affects the final performance. Null offsets for stacked, chemically milled LPA's are generally unpredictable and range up to about ±10 percent of the supply pressure.[17,18]

Photochemical milling has also been used to produce fluidic components from non-metals. One type of material which exhibits light sensitivity and can be chemically milled is a special class of ceramics, photoceramics.[19] Unlike the coated metal sheets, the light sensitivity of this material extends through the entire depth so that, when chemically milled, there is no undercut or center ridge. This permits most amplifiers to be milled to the desired thickness, thus eliminating the alignment error associated with stacking several thin plates together.

[17]L. E. Scheer, J. S. Roundy, J. Joyce, "Manufacturing Techniques for Producing High Quality Fluidic Laminates in Production Quantities," 20th Anniversary of Fluidics Symposium, ASME WAM (November 1980).

[18]J. S. Roundy, "Manufacturing Techniques for Producing High Quality Fluidic Laminates at Low Cost," AiResearch Manufacturing Company of Arizona Report 41-2697 (September 1980).

[19]R. W. Van Tilburg, "Area Experience in Moderate Volume Fabrication of Pure Fluid Devices," Proceedings of the Fluid Amplification Symposium, VOL III, pp335-349 (October 1965).

Photoceramic material can be easily diffusion bonded to form integrated circuits. Operating temperatures up to 370C can be tolerated. The major disadvantage is that the material is brittle and will easily fracture under shock or stress loads. Overall, slightly better accuracy can be achieved with photo-ceramics than with chemically milled metal parts. For some applications without severe shock or vibration, this method of fabrication has excellent potential.

Photosensitive plastic materials such as Dycril were also used for a brief period in the early development of fluidic amplifiers. Equipment cost was low and new designs could be quickly evaluated. The primary disadvantage was material insta-bility. An amplifier made and tested one day would have dif-ferent characteristics a few days later. Until significant material improvements are made, this does not appear to be a viable method of fabrication.

5.2 Casting and Injection Molding

The basic process of metal casting and its extension, injection molding of plastics, was used extensively during the early and mid-1960s and, to some extent, is still used today. These methods were primarily used for fabricating large-scale components such as flow diverter and vortex modulating valves. Some work has also been done using silicone rubber molds for casting fluidic amplifiers made of epoxy resins.

In the injection molding process, hot plastic material is forced into a metal die. Several commercial organizations produced and marketed a complete line of fluidic elements based on this technique, each experimenting with different plastic compositions. The most serious disadvantage was warpage and

shrinkage of the material, which degraded the amplifier performance over a period of time.[20] Lack of compatibility with various fluids and a limited usable temperature range are additional drawbacks. Since it is possible to make highly accurate dies, injection molding could be an attractive method for high volume, low cost applications within the limits of available plastic materials. The use of this process will probably increase in the future.

5.3 Electroforming

In the electroforming process, metal is deposited to precisely controlled thickness on special electroconductive tools, a conductive wax being the most frequently used for fabricating fluidic amplifiers. Overall accuracy and repeatability are very good and surface finishes better than 32 rms are obtainable. The process is best suited to manufacturing planar fluidic circuits as opposed to individual elements which can be assembled in a vertical stacking.

At least two companies, one in Great Britain and the other in the United States, have manufactured and marketed fluidic controls using this process.[21,22] The fluidic circuits have been incorporated into production engine controls used on

---

[20]L. S. Cox, "Fabrication Requirements in Fluidics Technology," AGARD-AG-215 (January 1976).

[21]D. C. Cheffy, "Development of a Fluidic Pressure Ratio Control Unit For Vertical Take-off Aircraft Lift Engine," Proceedings of the Fourth Cranfield Fluidics Conference, VOL. 2, Paper L5 (March 1970).

[22]W. Posingies, "Production Suitability of an Electroformed Conductive Wax Process for the Manufacture of Fluidic Systems, Phase II," USSAAMRDL-TR-76-42 (January 1977).

commercial aircraft. The major disadvantages of this process are the time and cost required to make even minor variations or corrections to a given circuit design.

5.4 Electro-Spark Discharge Machining (EDM)

The process of using a specially shaped electrode to "burn" through metal has been available for many years. An electrical arc formed in a small gap between the electrode and metal causes the metal to melt. The molten metal is flushed away with a special solution which also acts as a coolant. The electrode can be machined very accurately and although it never physically contacts the metal, erosion of the electrode does occur at the same time that the metal part is being machined. Consequently, the electrode is made as long as feasible so that the eroded end can be machined off to restore the desired shape.

A recent development in the EDM process is to use a small diameter wire electrode coupled to a numerically controlled machine that can precisely position the part being machined. The wire EDM process is especially suited for producing complex two-dimensional shapes with profile accuracy of 0.005 mm. Using wire diameters as small as 0.08 mm allows machining straight or curved channels as small as 0.10 mm wide. Wire is continually transferred from one spool to another to compensate for wire erosion during the cutting process.

Wire EDM has been used to manufacture LPA's on stainless-steel blanks. This process has demonstrated the ability to produce LPA's with null offsets of three percent or less with good repeatability.

Machines are currently available which can cut a 10-cm thick stack at a linear rate of 2.5 cm/hr. Total cutting time depends on the perimeter of the profile being machined. For a

typical laminate blank thickness of 0.5 mm, 200 parts could be cut with one setup. Because of its accuracy and ability to machine relatively thick material, wire EDM is also used to make dies and punches used to manufacture amplifiers by fine blanking and precision stamping (see paragraphs 5.6 and 5.7).

5.5 Laser Machining

Laser machining is much like wire EDM except that a laser beam rather than a wire does the cutting or burning. The numerically controlled table, in combination with beam size, determines accuracy and wall conditions. The power of the laser beam determines beam size, cutting rate, and material depth. Attempts with pulsed laser beam machining to date have not been satisfactory primarily due to very poor wall surface conditions. However, the potential for this method of machining amplifiers appears to be very good, particularly when continuous laser beams become available and improvements are made in surface heat removal. Setup time should be reduced, burning rate increased, and, of course, wire breakage and vibration are eliminated. Developments in laser machining technology should be watched closely.

5.6 Precision Stamping

From the standpoint of cost and high production rates, stamping has always been viewed as an ideal fabrication method. At least one attempt to stamp amplifiers was made in the mid-1960's; however, proper die accuracy could not be achieved and the laminates produced were unsatisfactory. Conventional stamping has been refined by a process called precision stamping wherein die clearances are held to within 0.013 mm and spring-loaded counterpunches supp·· + the material during cutting to obtain a flatter laminate w: .a a greater portion of the side walls sheared rather than torn. A cross-sectional view of a

precision stamping die is shown in figure 25. Figure 26 shows a precision stamping die for an LPA wherein punches, die cavity, and multiple stations are seen.
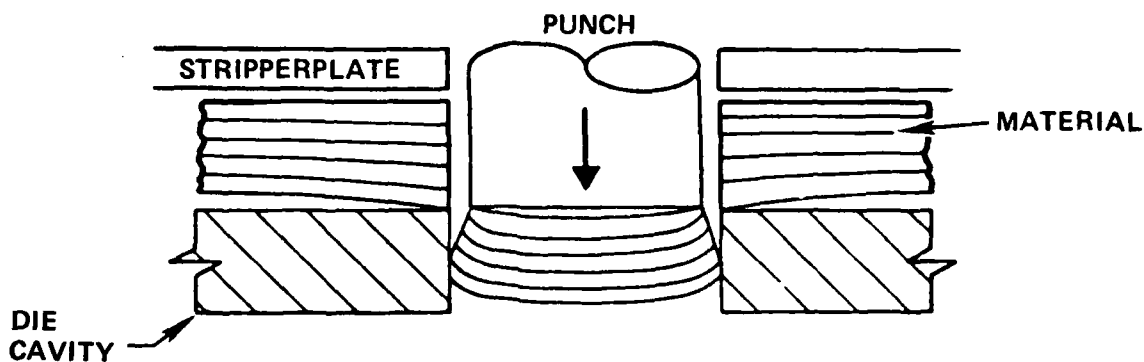

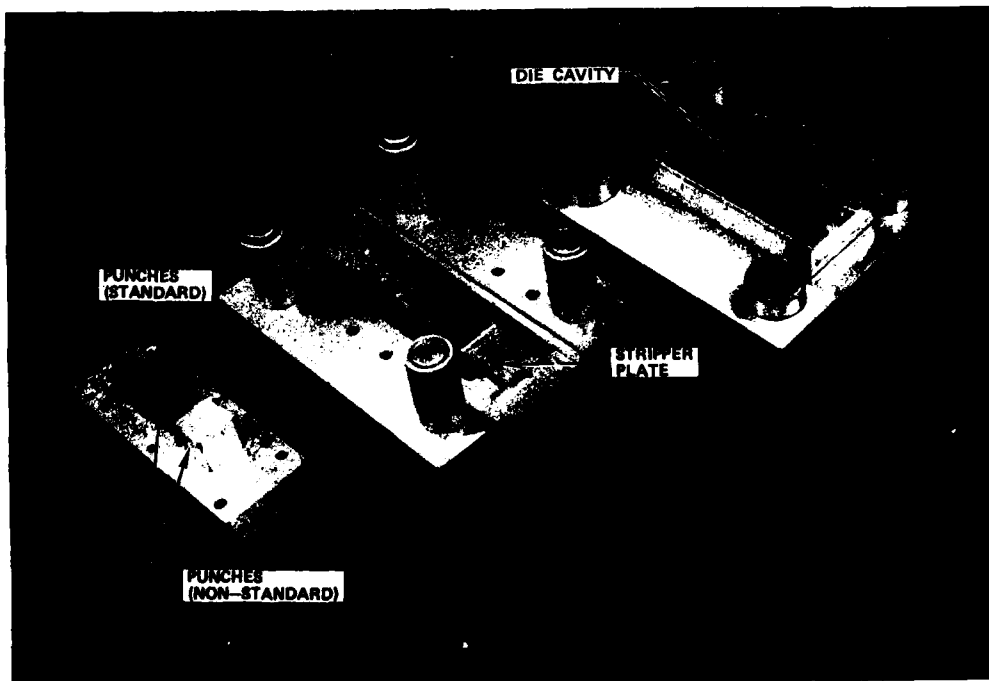Figure 25. Cross-sectional view of precision stamping and die fabricating a part.

Figure 26. Typical precision stamping dies.

One of the advantages of a multiple station die is that different laminates can be fabricated by removing punches or by substituting a new punch and die cavity. In the latter case, die cost is approximately half that of a complete new die set. Highly accurate parts (i.e., parts with minimal null offset) may be obtained by evaluating an initial sampling of amplifiers and then modifying the die as necessary. This modification usually consists of hand-honing or polishing to improve power jet or amplifier receiver symmetry.[17,18] The stamping rate is a function of the material thickness and size of the part. For most fluidic laminates, the production rate will be between 70 and 120 laminates per minute. Problems still encountered are poor surface finishes due to tearing and the inability to stamp either very thin (< 0.2 mm) or moderately thick (> 0.5 mm) parts without excessive deformation.

5.7 Fine Blanking

Fine blanking is similar to precision stamping except that the counter-force that supports the material during blanking is controlled by cam action rather than spring-loaded pads. Blanking die clearances are comparable to or smaller than those of precision stamping dies. For material thickness above 6.35 mm, the blanking die is made with a V-groove to hold the material and prevent it from flowing around the die radius, thus minimizing burr formation. For thin laminates, this V-groove is usually eliminated. A cross-section of this die is shown on figure 27. Figure 28 shows a fine blanking die for an LPA.

---

[17] L. E. Scheer, J. S. Roundy, J. Joyce, "Manufacturing Techniques for Producing High Quality Fluidic Laminates in Production Quantities," 20th Anniversary of Fluidics Symposium, ASME WAM (November 1980).

[18] J. S. Roundy, "Manufacturing Techniques for Producing High Quality Fluidic Laminates at Low Cost," AiResearch Manufacturing Company of Arizona Report 41-2697 (September 1980).
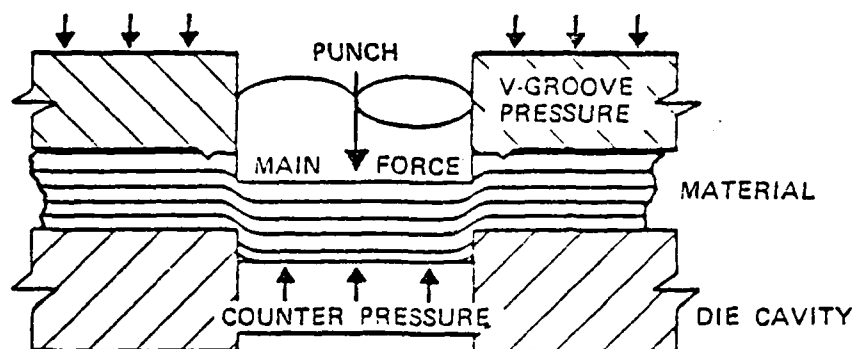
Figure 27. Cross-sectional view of a fine
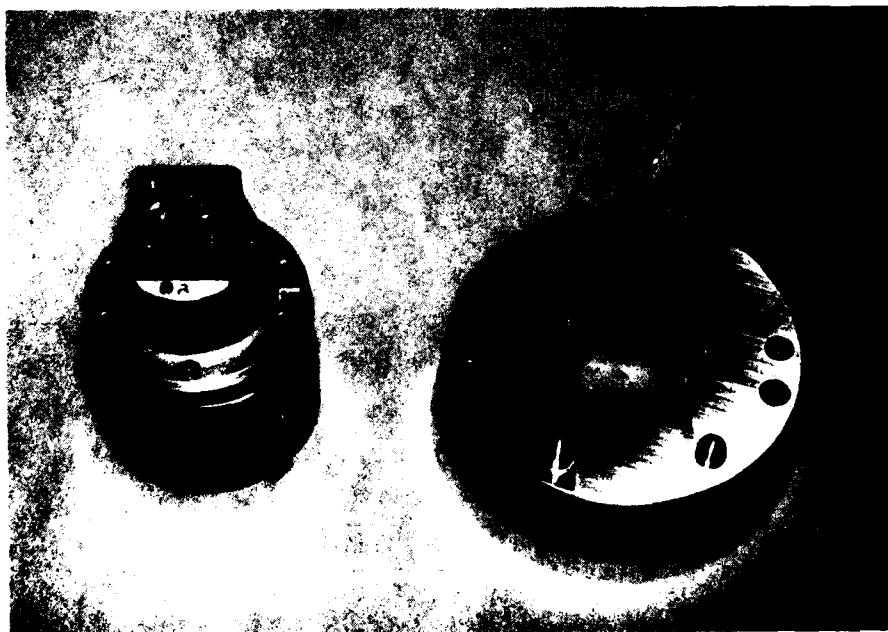blanking die fabricating a part.

Figure 28. Fine blanking die.

One of the advantages of fine blanking is the quality of the sheared walls of the finished part. A comparison of a typical fine blanked and precision stamped part is shown in figure 29
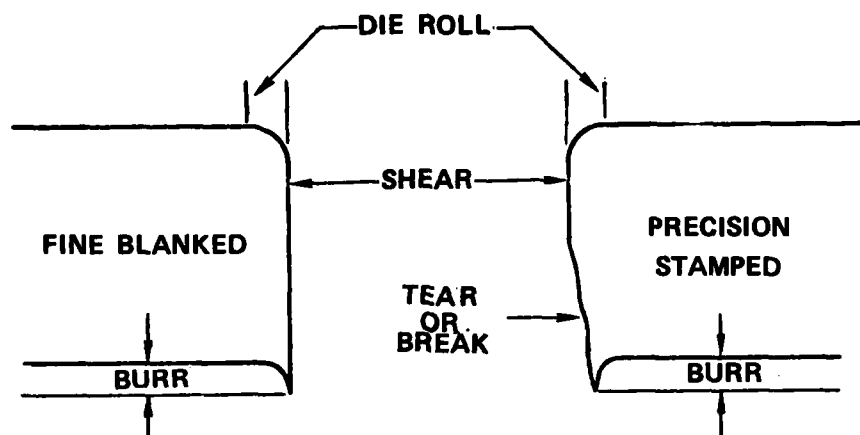
Figure 29. Cross-sectional view of a typical fine blanked and precision stamped part.

The fine blanking die generally consists of a single sta' on; thus, the laminate is fabricated in one stroke instead of the three or four strokes required in a multiple station die. If different amplifier designs are desired from the same set of dies, the fine blanking die could be made in multiple stations for punch and die cavity replacement. However, the cost saving generally does not warrant making a two-station die for punch and die cavity replacement only. As in the case of precision stamping dies, fine blanking dies may be modified after part evaluation by polishing to improve amplifier null offset accuracy. This may be a good reason for multiple station dies. Critical areas of an amplifier may be stamped or blanked at separate stations, thus greatly facilitating die modifications after evaluation of initially produced parts.

The shearing rate during fine blanking is slower than that possible in precision stamping. Production rates are limited to about 30 to 40 laminates per minute. The production rates for both precision stamping and fine blanking assume that parts can be ejected from the machine automatically using an air-blast or equivalent method. Otherwise, especially for thin laminates (0.25 mm or less), parts must to be removed by hand or by some gentle automated process that most likely will reduce the production rates cited herein.

6. THE LAMINAR JET ANGULAR RATE SENSOR

A low cost, rugged angular rate sensor, particularly for missile and combat vehicle stabilization systems, has been sought for many years. Vortex rate sensors have been used with mixed results; pneumatic sensors of this type yielded insufficient gain to be of any use, while hydraulic sensors consumed significant amounts of power and were difficult to compensate for Reynolds number effects.[23]

The idea for the use of an unconfined jet of fluid as an angular rate sensor was presented at least as long ago as 1942.[24] There is no documentation of any fabrication or testing of this concept. However, it is doubtful that success could have been achieved without the amplifying capabilities of laminar fluidics, for even present pressure transducers are insufficiently sensitive to sense the low output of an angular jet rate sensor without prior amplification.

---

[23]A. E. Schmidlin and J. M. Kirshner, "Fludic Sensors - A Survey," AGARD-AG-215 (January 1976).

[24] H. Ziebolz, "Characteristics of Hydraulic and Pneumatic Relays as Energy-Converting Devices," Instruments, 15 (September 1942).

A general discussion of design and performance character-
istics of a laminar jet angular rate sensor follows; however,
specific details related to development and analysis may be
found in reference 5.

6.1 Description

The laminar jet angular rate sensor (LJARS) is a modi-
fied LPA, particularly with respect to an increase in nozzle to
receiver distance. The jet deflection results from the Coriolis
induced curvature in a jet of fluid issuing from a nozzle as the
device is rotated. The most familiar analogy is that of a
garden hose. There is an apparent curvature in the water jet as
the hose nozzle is rotated.

The geometry of a typical LJARS is shown in figure 30.
The jet is received by two identical receiver ports located
symmetrically about the centerline. As a particle of fluid
travels from the rotating nozzle to the receivers, it will fol-
low a straight line in inertial space. The distance that the
receivers move during the particle travel time is determined by
the rate of rotation of the sensor and the velocity of the
particle. At an angular rate of zero, the fluid particles in a
jet will be evenly divided between the two receivers. Assuming
that perfect alignment exists, the resulting differential flow
or pressure between the two output channels will be zero. At an
angular rate other than zero about an axis normal to the plane
of the nozzle and receivers, the jet will be unevenly divided by
the splitter between the receivers. The differential output
signal is a linear function of angular rate.

---

[5]T. M. Drzewiecki, F. M. Manion, "Fluerics 40: LJARS, The
Laminar Jet Angular Rate Sensor," Harry Diamond Laboratories
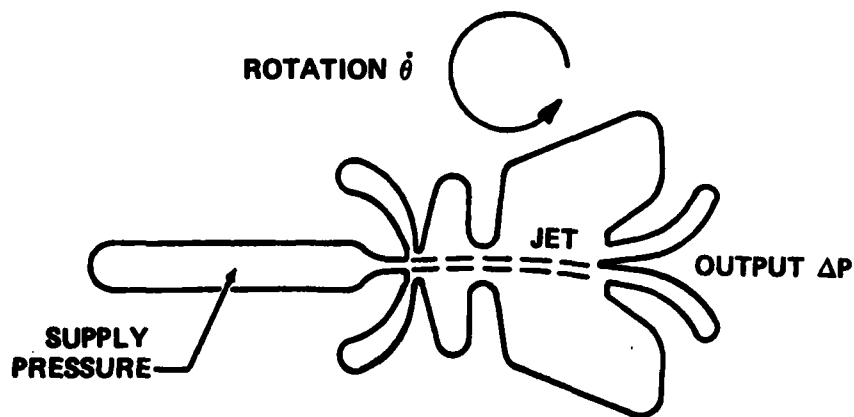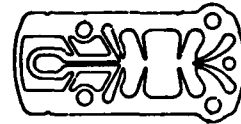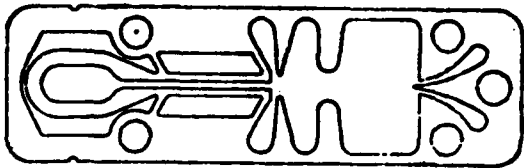HDL-TM-79-7 (December 1979).

Figure 30. Geometry of a typical laminar jet angular rate sensor.

This signal may either be amplified and processed in an all-fluidic system or be amplified and transduced for use in a hybrid system. It is immediately obvious that since the LJARS is a modified proportional amplifier, any amplifier located downstream of the sensor and oriented in the same plane may add to or subtract from the rate signal. As a practical matter, only the first or second stage of amplification has any significant effect; by proper orientation of these stages, the signal may actually be augmented.

6.2 Design Parameters

The physical characteristics of a laminar jet angular rate sensor are similar to those of a laminar proportional amplifier. The geometric parameters critical to the performance of the rate sensor are (see figure 4 for identification)

b_s = nozzle width,

h = nozzle height,

x_{th} = nozzle throat length,

x_{sp} = nozzle to splitter distance, and

b_o = output receiver width.

The effects of these characteristics on performance are interrelated; however, through a considerable amount of development, a range of values can be recommended to achieve satisfactory results from an initially designed sensor. The critical dimensions, normalized with respect to the nozzle width, b_s, are summarized in table 4.

TABLE 4. RECOMMENDED GEOMETRY FOR THE LJARS

Parameter	Recommended Range
$X_{th} = x_{th}/b_s$	1 to 20
$X_{sp} = x_{sp}/b_s$	16 to 20
$B_o = b_o/b_s$	0.7 to 1.7
$\sigma = h/b_s$ (aspect ratio)	1.0 to 3.0

The actual design starts with the bandwidth requirements, or frequency at which the phase shift equals 90 degrees, and also the accuracy (or threshold) necessary for a particular application. These are dependent upon the time it takes for the fluid to traverse the nozzle-to-receiver distance and some compromise must be made between bandwidth and accuracy as shown in figure 31.
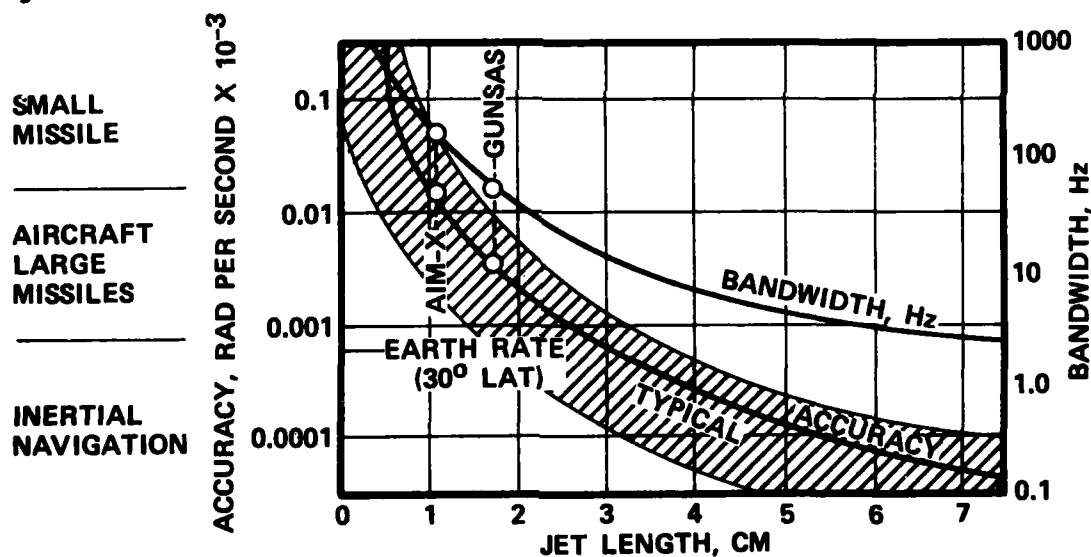

Figure 31. LJARS tradeoff between bandwidth and accuracy for existing industrial state of the art.

Drzewiecki and Manion[5] derived the following equation used to predict bandwidth.

[5]T. M. Drzewiecki, F. M. Manion, "Fluerics 40: LJARS, The Laminar Jet Angular Rate Sensor," Harry Diamond Laboratories HDL-TM-79-7 (December 1979).

$$f = \frac{c_d \, N_R \, \nu}{16 \, X_{sp} b_s^2},$$ (39)

where

f = frequency in Hz at which phase lag is 90 degrees,

c_d = nozzle discharge coefficient,

N_R = Reynolds number = $b_s (2P_{sv}/\rho)^{1/2}/\nu$, and

ν = kinematic viscosity of fluid.

Sensitivity or gain of the sensor is defined as the slope of the output differential pressure versus angular rate curve around zero rate input. The following expression has been derived to estimate sensitivity.[5]

$$S = \frac{\Delta P_o}{\dot{\theta}} = \frac{1}{57.3} \frac{\mu N_R}{c_d} \frac{P_{rec}}{P_{sv}} X_{sp}^2,$$ (40)

where

S = sensitivity, Pa/deg/s,

μ = absolute viscosity of fluid, and

P_{rec} = mean output pressure level (blocked load conditions at zero rate).

The value of P_{rec}/P_{sv} can be measured or calculated from the following[5]

$$P_{rec}/P_{sv} = \frac{c_\theta}{B_o} \left(1 - \frac{8X_{sp}}{c_\theta N_R \sigma^2}\right) \left[1 - \frac{1.1 B_{sp}}{(c_d N_R \frac{B_{sp}}{2})^{1/2}}\right],$$ (41)

where

c_θ = momentum flux discharge coefficient,

= $1.15 \, c_d^2$.

[5] T. M. Drzewiecki, F. M. Manion, "Fluerics 40: LJARS, The Laminar Jet Angular Rate Sensor," Harry Diamond Laboratories HDL-TM-79-7 (December 1979).

Typical frequency response and sensitivity plots for an air-powered rate sensor are shown in figures 32 and 33.
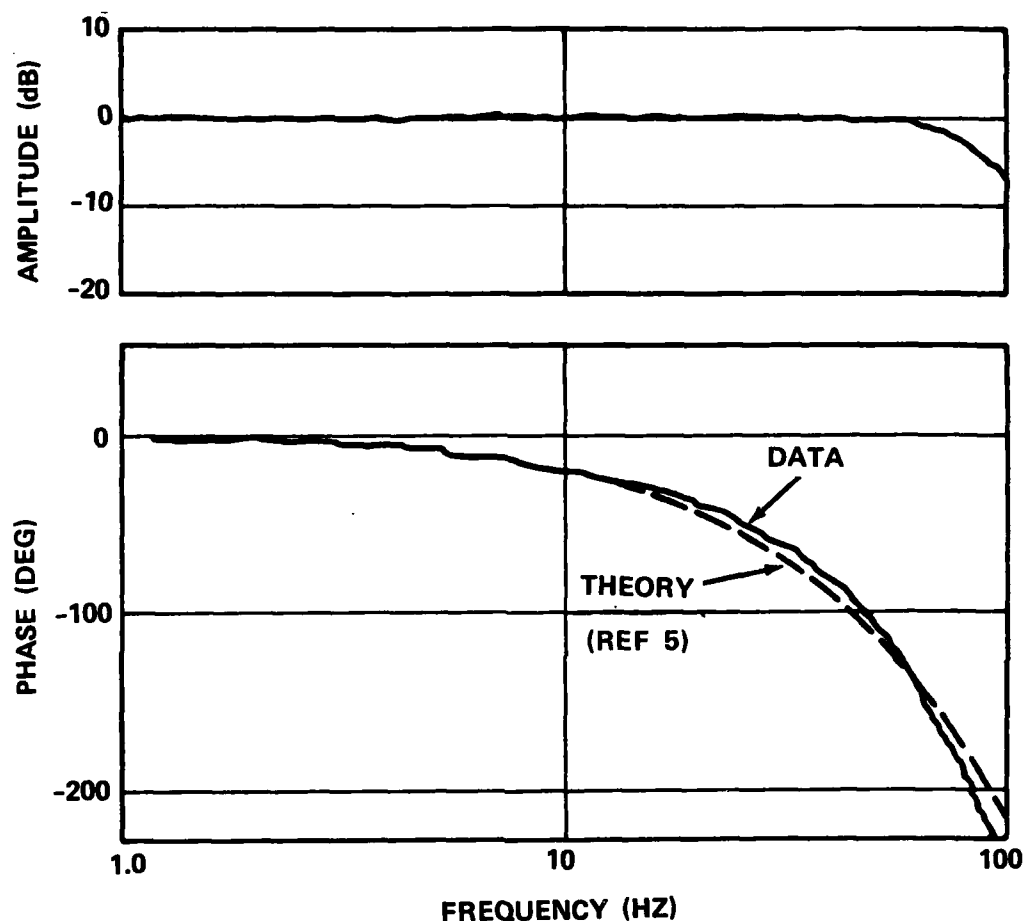
Figure 32.   Typical LJARS frequency response data.

From the foregoing equations, it can be seen that increasing X_{sp} increases the sensitivity or rate gain of the sensor, but reduces the bandwidth.   Also, both sensitivity and bandwidth increase with N_R; however, a limiting factor is the need to maintain laminar flow in the jet.   As with laminar amplifiers, the upper value of N_R satisfies the condition $\sigma N_R \leq 1000$.
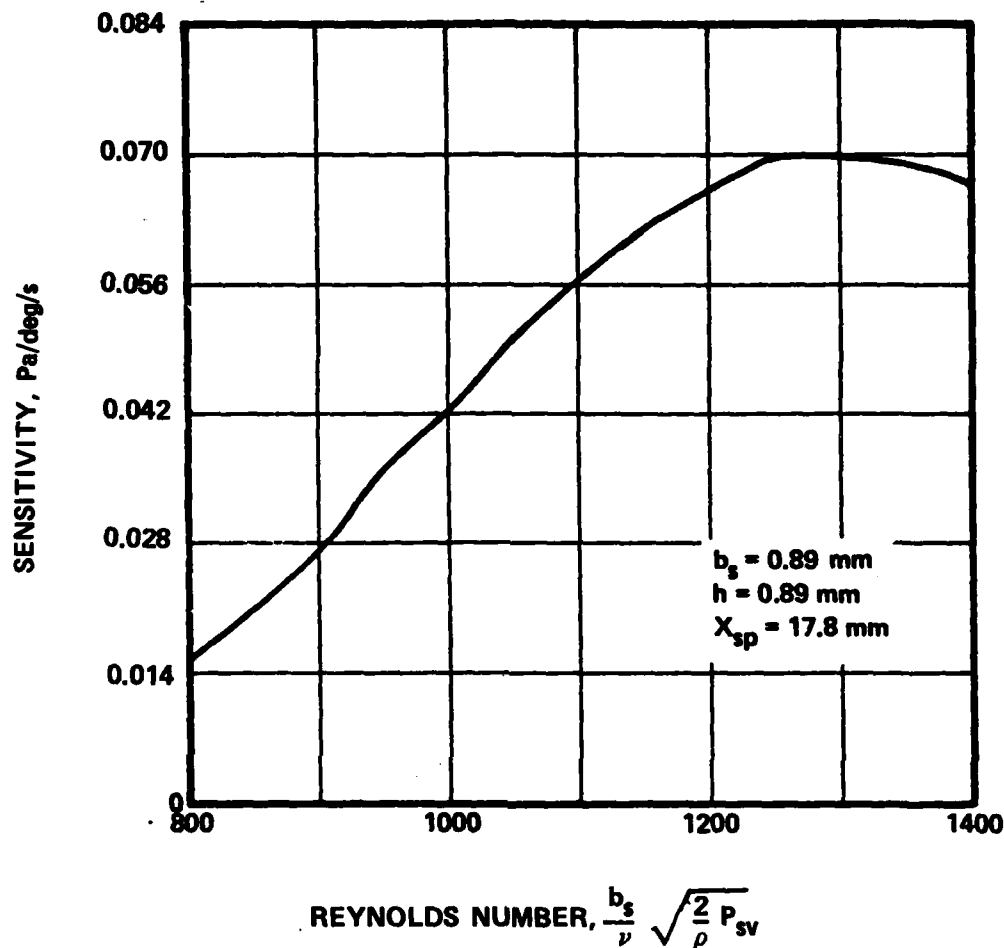
Figure 33. Typical LJARS sensitivity data.

For most rate sensor applications, the sensor bandwidth is the major consideration and should be used to establish the sensor geometry at the minimum allowable value of N_R. At higher values of N_R, therefore, the bandwidth and sensitivity both increase. Normally, a 2:1 change in sensitivity (which establishes the sensor operating range at values of σN_R between 500 and 1000) can be tolerated.

It should be noted that recommended values of X_{th} of up to 20 are considerably higher than the values of 1 to 2 used

91

for LPA's. The purpose of the longer approach length is to guide the flow in the nozzle so that the flow is as straight as possible. This results in a softer jet and may increase the sensor gain and appears to improve the null offset characteristics; this approach, however, results in a considerably higher sensitivity to changes in viscosity and, hence, temperature. Reynolds number control is required to maintain adequate sensor performance as indicated in the following sections. Methods of controlling Reynolds number are described in Appendix D.

6.3 Performance

6.3.1 Null Offset and Drift

The operating principle of the LJARS was described in section 6.1. From this discussion, it is obvious that a sensor error will result in the form of a null offset if there is misalignment between the nozzle and the splitter, or if the jet *does not follow the path determined by the nozzle.* Both of these error sources result from inaccuracies in the manufacturing process.

Splitter/nozzle asymmetry will result in a monotonic increase in offset as the Reynolds number (N_R) of the jet increases. This effect is shown in figure 34. Nozzle exit asymmetry affects the path of the fluid leaving the nozzle which results in a non-monotonic relationship between offset and N_R as shown in figure 35.

$$N_R = \frac{b_s}{\nu} \sqrt{\frac{2}{\rho} P_{sv}}$$
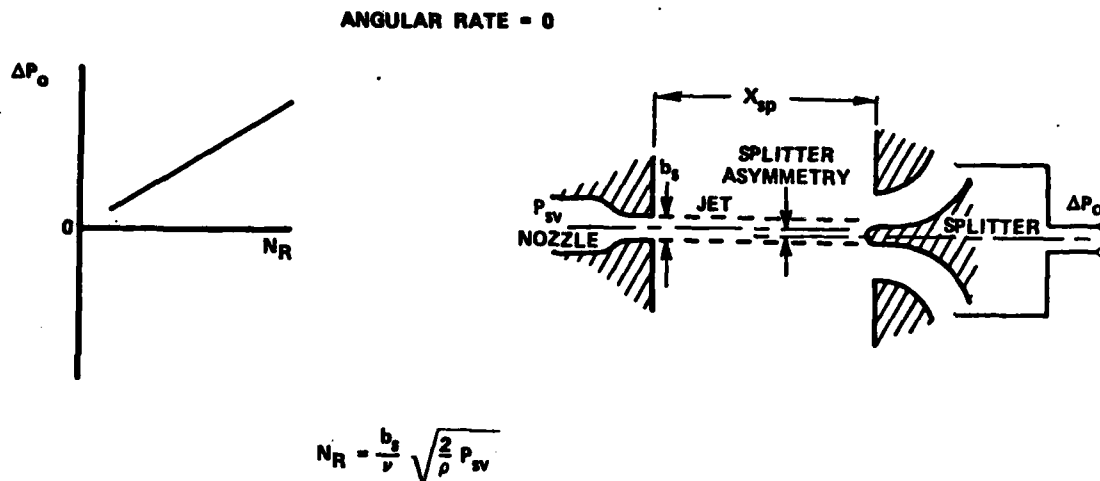
Figure 34. Effect of splitter/nozzle asymmetry on
LJARS null offset.

To minimize the offset of the LJARS output, the var-
iations in both the manufacturing accuracy and the Reynolds num-
ber must be minimized.   Even with the best manufacturing
accuracy achievable at this time, the described asymmetries in
the rate sensor result in null offsets of as much as two percent
of the sensor maximum rate range.

To permit rate sensors to be used in the as-fabricated
condition for applications requiring very low offset, it would
be necessary to have manufacturing methods that yield accuracies
many times better than are now available. Consider for example
a rate sensor driving a gain block with a gain of 10^6. If the
saturated output of the gain block is 20 kPa, then an output
from the LJARS of 2×10^{-5} kPa (0.02 Pa) causes saturation. A
rate sensor operating typically at 50 Pa recovers at saturation
about 20 Pa; however, an output of 0.02 Pa saturates the gain
block. Since 0.02 Pa is only 1/1000 of the rate sensor satura-
tion pressure, a 0.1 percent offset is intolerable. An offset
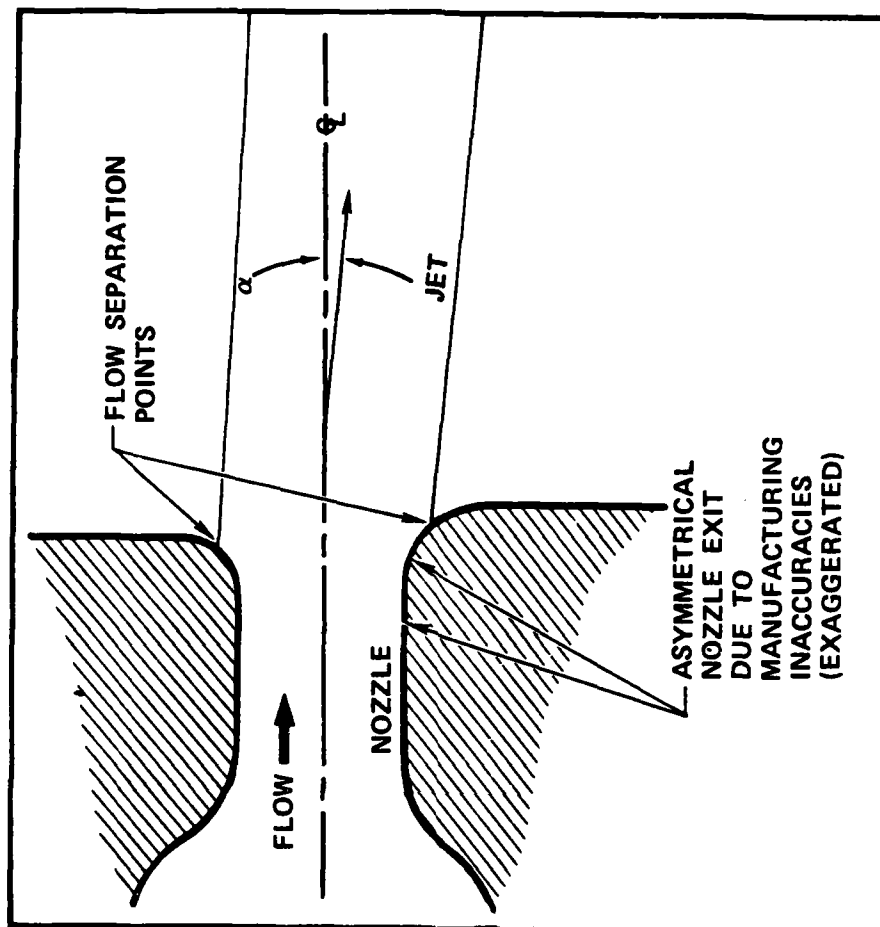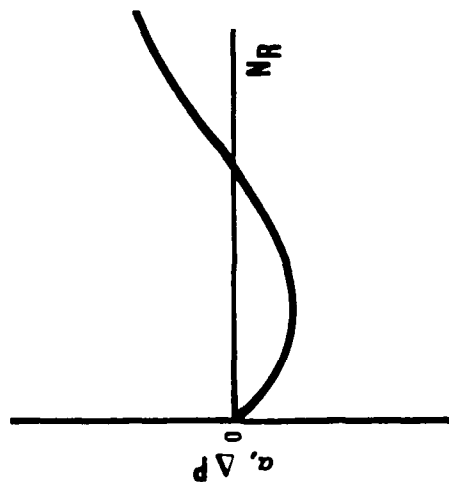
Figure 35. Effect of nozzle exit asymmetry on LJARS null offset.

of no more than 0.01 percent or 200 times less than normal is required. Since the rate sensor nozzle-to-splitter distance (X_{sp}) is 20, this corresponds to a deflection or geometric alignment of less than 0.000015 deg or a displacement of the splitter of 0.0001 b_s relative to the nozzle. For b_s = 0.5 mm, this represents the physically impossible tolerance requirement of 0.05 μm (2×10^{-6} in.).

Some possibilities for obtaining improved dimensional accuracy are described in section 5 of this report. An alternate approach is to design the rate sensor with mechanical adjustments so that nozzle exit and splitter asymmetries can be trimmed after the rate sensor is assembled. The cross section of a rate sensor designed in this manner is shown in figure 36.
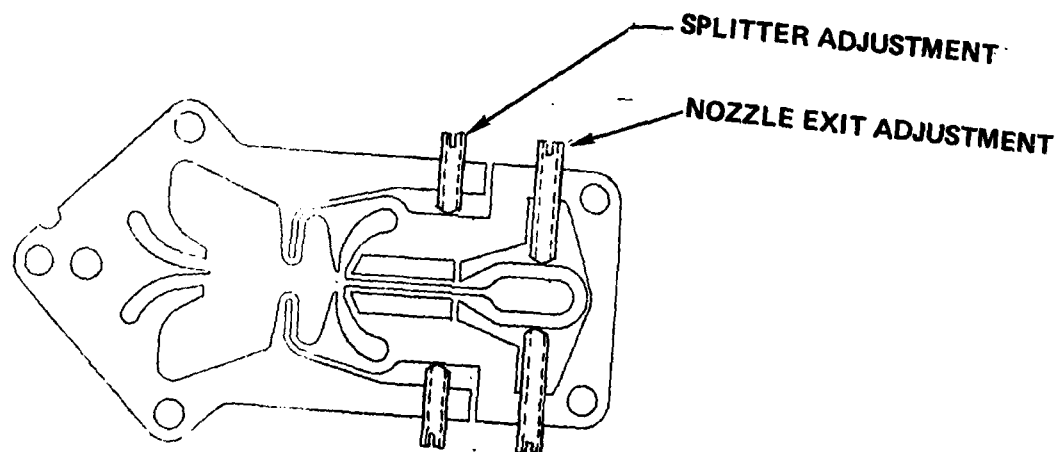
Figure 36. Cross-sectional view of LJARS with mechanical adjustments to reduce null offset.

Nozzle/splitter asymmetry correction is made by bending the rate sensor body between the nozzle and receivers to obtain zero differential pressure output at the mid-point of the
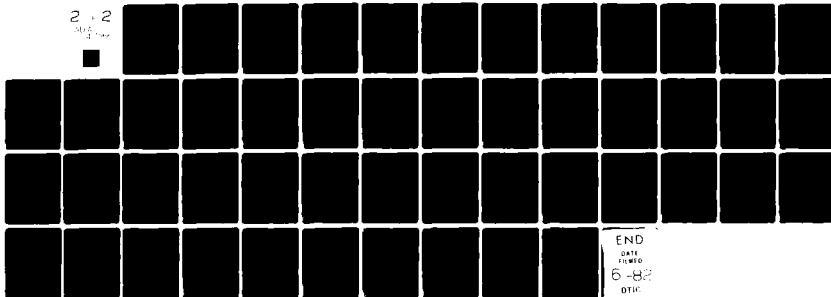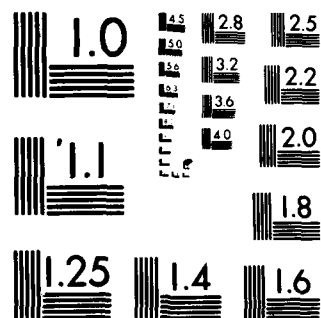
MICROCOPY RESOLUTION TEST CHART

NATIONAL BUREAU OF

desired operating Reynolds number range. Nozzle exit asymmetry is corrected by moving the sides of the nozzle relative to one another along the axis of the jet so that rate sensor output remains zero over as great a range as possible. The performance of this sensor when each of the adjustments has been made is shown on figure 37.
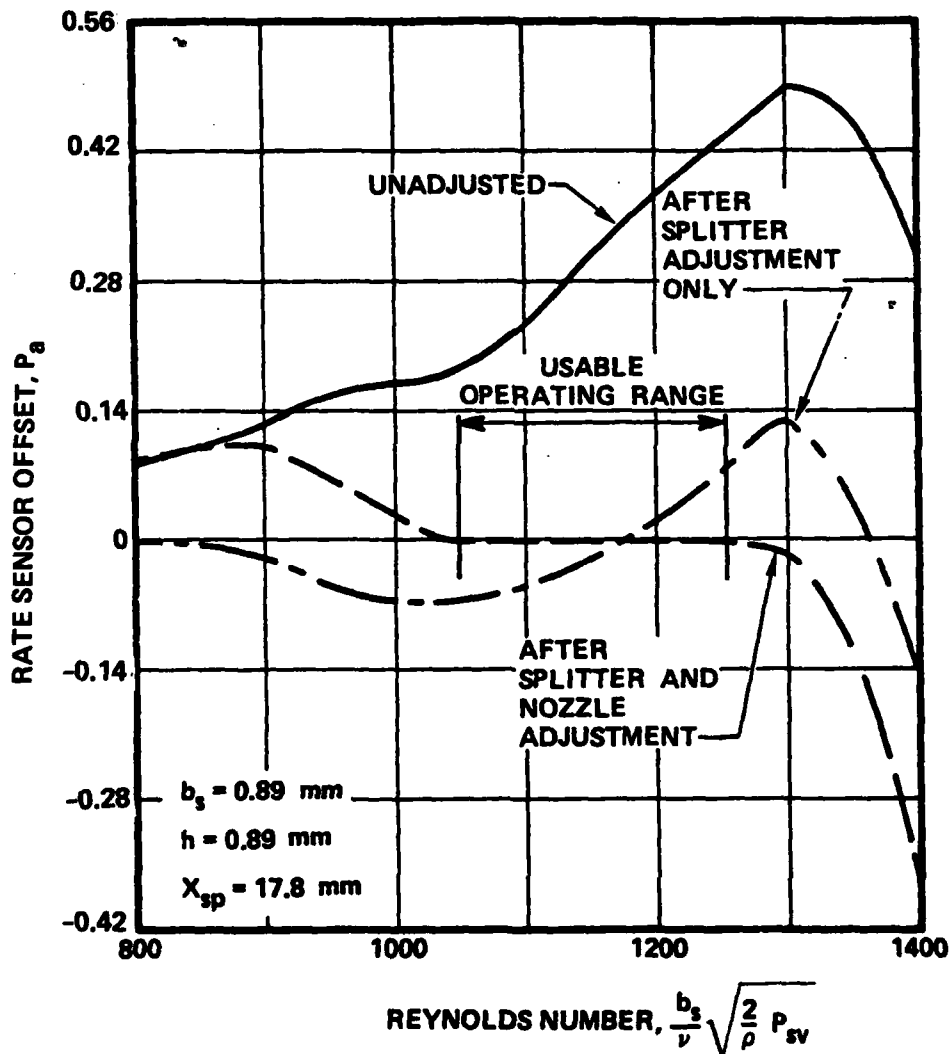
Figure 37.   LJARS null offset before and after mechanical adjustments.

96

The foregoing adjustments result in extremely small dimensional changes which are considerably less than 0.015 mm from the fabricated condition. Induced stresses will cause the material to creep under imposed environmental conditions such as shock, vibration, and temperature transients resulting in null changes with time. Mechanical adjustments, therefore, are only acceptable in applications where null offset is not critical and the operating environment is not severe.

Another method of correcting for nozzle/splitter asymmetry is to use bleed-off restrictors on the rate sensor outputs whereby a small portion of the flow from either receiver channel can be diverted to vent through an adjustable orifice. This method, combined with nozzle exit polishing or tighter control of the Reynolds number operating range, would be more satisfactory for most applications.

Another method to reduce null offset is to use negative feedback. In this approach, a small portion of the rate sensor output is fed back (negative feedback) to the controls through a resistive circuit. Null offset is improved at the expense of a slight loss in gain. Each of these methods produces about an order of magnitude reduction in null offset. Hence, if the sensor offset is two percent, three mutually exclusive methods (e.g., mechanical adjustment, bleed-off, and negative feedback) should reduce the offset to less than 0.002 percent.

Drift in a fluidic rate sensor is defined in the same manner as for a rate gyroscope, which is the integrated error with respect to some period of time. The causes of drift are different, of course. In a perfectly manufactured fluidic sensor operating at a constant Reynolds number, the drift would be zero. Referring to figure 37, it is seen that it may be possible to greatly minimize drift by adjusting the sensor so that

the offset is as close to zero as possible over a range of Reynolds number. Methods of controlling Reynolds number are described in Appendix D.

6.3.2 Dynamic Response

For design engineering, a delay of four times the transport time predicts the frequency for a phase shift of 90 degrees. Since phase shift, ϕ, is defined as the ratio of delay time, T_d, to period of oscillation, then in degrees

$$\phi = 360 \ fT_d, \tag{42}$$

and at $\phi = 90$ deg,

$$f = \frac{1}{4T_d} = \frac{1}{4} \ \frac{c_d (2P_{sv}/\rho)^{1/2}}{4b_s \ X_{sp}} \ . \tag{43}$$

Since

$$N_R = b_s \ (2P_{sv}/\rho)^{1/2} / \nu , \tag{44}$$

the frequency response is also given by

$$f \bigg| \phi = 90° = \frac{c_d \ N_R \ \nu}{16 \ X_{sp} b_s^2} \ . \tag{45}$$

The amplitude response of LJARS is flat well beyond the 90-degree phase shift point. This is sho   figure 32 where excellent agreement between experimental   d theory was obtained with a sensor designed for a gun stabilization system.

Further examination of the equation for frequency response indicates that devices of the same size operating at the same Reynolds number have the same bandwidth, regardless of

fluid medium, provided that the kinematic viscosity remains the same. For example, at a temperature of approximately 30C, the kinematic vicosities of MIL-H-5606 hydraulic fluid and air are the same. Therefore, a rate sensor operating on either MIL-H-5606 or air will have the same response, provided that the supply pressure is adjusted to result in the same Reynolds number. This is the same result as was noted for the LPA.

6.3.3 Shock and Vibration

From a theoretical standpoint, shock and vibration constitute accelerations in axes perpendicular and parallel to the laminar jet. They act equally on all fluid particles in the region. As long as density gradients do not exist, the body forces produced act equally on all particles; thus, no net forces act on the jet. In addition, those accelerations along the jet axis and those perpendicular to the bounding planes produce body forces that are in the common mode to the outputs. They would not contribute any differential signal if the common mode rejection ratio (CMRR) were infinite. They may add some signal in the real case; however, since these forces do not move the jet, the CMRR for such a phenomenon is extremely high. In the cross axis, there exists the possibility of jet movement; however, since the structure, the field, and the jet move together, again no differential signals should appear. Rotational accelerations that are within the bandwidth of the device will be detected. Since it is assumed that the overall system has been designed to stabilize or respond within the sensor bandwidth, normal operation is expected. At higher frequencies, the signal will be attenuated. Similar reasoning applies to step inputs due to rotational shock loads. Under a sustained shock load of this type, system saturation will occur; however, this again will be within design limits.

As far as mechanical integrity of the sensor is concerned, normal design and test procedures should be followed. In a previous section, mechanical adjustment to minimize offset was discussed. Obviously, this is a problem in mechanical design; however, as indicated, the adjustments are extremely small and, therefore, this approach should be avoided in sensors that will be subjected to high shock and vibration environments.

6.3.4   Cross-Axis Sensitivity

To avoid spurious signals due to rate inputs orthogonal to the axis wherein it is desired to sense angular rate, it is necessary to precisely align the sensor. Figure 38 presents experimental data obtained with a LJARS operated on air and shows the cross-axis sensitivity of the sensor.
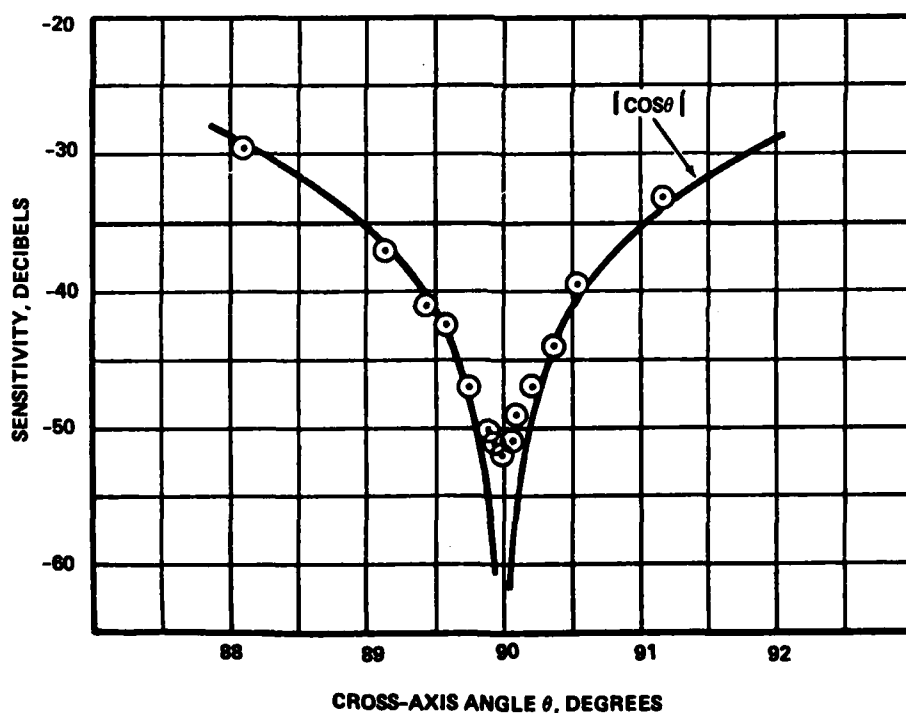
Figure 38.   Orthogonality and cross-axis sensitivity of the LJARS.

At a misalignment of ±1/2 degree, one one-hundredth of the orthogonal signal input will be perceived by the sensor. Obviously, alignment accuracy is dictated by the required accuracy of the sensor or accuracy of the controlled axis of the system.

6.3.5 Operating Fluids

In section 6.2 on sensor design, the importance of Reynolds number was indicated. In general, if the proper range of Reynolds number is maintained, operation of the LJARS will be independent of the fluid used. This implies that, over the required operating temperature range, a change in state of the fluid does not occur. It is also desirable that viscosity variations over this range also be minimal, or that compensation for Reynolds number change can be readily accomplished. The most commonly used fluids to date have been either hydraulic oil or air. Properties of these two fluids are given in Appendix B.

For many applications, precise Reynolds number control will be required, irrespective of the fluid used. For sensors operating on liquids, and even for most sensors operating on gas, closed cycle systems will be required to achieve Reynolds number compensation. Symmetrical output flow passages and close cross-coupling of vent regions must be ensured in the sensor design to prevent pressure gradients from deflecting the jet and affecting the output differential pressure. In general, all flow passages meeting at some junction for return to sump should be symmetrical to preclude the pressure gradients described above.

7. TYPICAL CIRCUIT ARRANGEMENTS

The previous sections presented information on LPA design, performance, and manufacturing, and introduced a standard format for integrated fluidic circuit assemblies. Design guidelines for staging LPA's were also presented. In many applications of LPA's a simple gain block to amplify low level signals is all that is required. More complex control systems need additional functions such as signal scaling and summing, dynamic compensation, and gain changing. This section reviews these additional features.

7.1 Signal Summing and Scaling

In analog fluidic control systems, it is often required to algebraically add or subtract two or more signals (usually differential signals) and obtain an output signal proportional to the sum or difference. The most frequently used method is to use a pair of restrictors connected to the control ports of an LPA as shown in figure 39. The restrictors should have linear pressure-flow characteristics so that their resistance remains constant over the required range of pressures and flow rates. This can be achieved with either circular or rectangular cross section capillary channels whose length is very much longer than the diameter (or depth for rectangular cross sections).
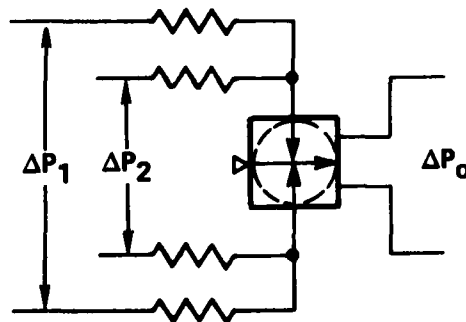
Figure 39.   Input resistance signal summing.

102

The resistance for a rectangular cross section capillary is given by

$$R = \frac{12\mu L}{A \, D_h^{\,2}},\tag{46}$$

where

R = resistance, $k_g/m^4 s$,

μ = absolute viscosity, $k_g/m\text{-}s$,

L = length, m,

A = cross-sectional area, m^2,

D_h = hydraulic diameter, m,

$$= \frac{4A}{\text{perimeter}}.$$

If the capillary has a square cross section, the equation becomes

$$R = \frac{32\mu L}{AD_h^{\,2}}.\tag{47}$$

The resistance of the summing restrictors must be equal to or higher than the input resistance of the LPA to achieve desirable summing characteristics. The input resistors attenuate the input signals and therefore have a gain which is less than one. If the LPA has a gain, G, and the input resistors have gains K_1 and K_2, then

$$\Delta P_o = (K_1 \Delta P_1 \pm K_2 \Delta P_2)G.\tag{48}$$

If the two summing restrictors have the same resistance, then they have the same gain, K, and

$$\Delta P_o = (\Delta P_1 \pm \Delta P_2)KG.\tag{49}$$

103

Since the output signal is proportional to the product KG, the input signals can be scaled by selecting the appropriate values of K. Variations in amplifier gain, G, due to changes in loading also affect the scaling of the input signals. This can be minimized by using an operational amplifier (op-amp) configuration.

An op-amp scaler, shown schematically in figure 40, uses feedback around a high-gain gain block. If the open loop forward gain, G, is sufficiently high, then it can be shown[2] that

$$\frac{\Delta P_o}{\Delta P_i} = \frac{R_f}{R_i} \left[\frac{GH}{1 + GH} \right] \sim \frac{R_f}{R_i},$$ (50)

where

$$H = \frac{1}{1 + R_f/R_i + R_f/R_c}.$$

Figure 40. The op-amp scaler.

[2]G. Mon, "Flueric Laminar Gain Blocks and an Operational Amplifier Scaler," Harry Diamond Laboratories HDL-TR-1730 (December 1975).

For large values of GH, the steady-state gain is only a function of the resistance ratio, R_f/R_i.

Multiple input signals can be summed by using additional input restrictors connected to the first stage in the same way they are shown in figure 39. If the input resistances have values R_{i1} and R_{i2} with corresponding input signals ΔP_1 and ΔP_2, then

$$\Delta P_o = \frac{R_f}{R_{i1}} \Delta P_1 \pm \frac{R_f}{R_{i2}} \Delta P_2 . \tag{51}$$

One problem associated with the design of an op-amp scaler is that of achieving stable operation. Because of the transport delay dynamic characteristic of the gain block, the open-loop phase lag can exceed 180 degrees, while the open-loop gain remains greater than one. If these conditions exist when the feedback path is connected, the op-amp will be unstable. Stability can be achieved in one of three ways:[2,25,26] (1) select a high value of R_f/R_i, (2) use a pressure divider circuit to attenuate the signal applied to the feedback resistance, or (3) use a resistor-capacitor (volume) network in the feedback path to create a first-order lag to attenuate the amplitude response.
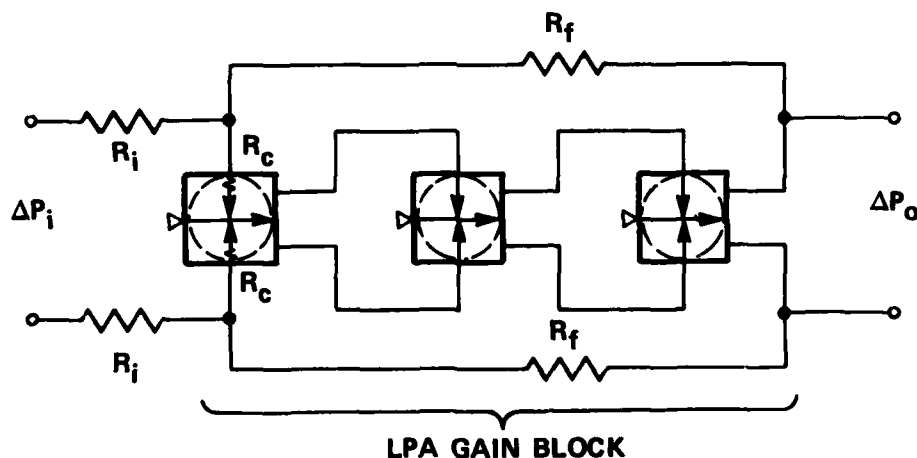
[2]G. Mon, "Flueric Laminar Gain Blocks and an Operational Amplifier Scaler," Harry Diamond Laboratories HDL-TR-1730 (December 1975).

[25]D. Lee, D. N. Wormley, "Multistage Hydraulic Summing and Signal Processing Amplifiers and Fluidic Input Servovalve Development," HDL-CR-76-223-1 (October 1976).

[26]T. F. Urbanosky, "Fluidic Operational Amplifier Summary," SAE Paper 670707 (1967).

Methods 1 and 2 are useful only for low ratios of
open/closed loop gain. Method 3 is usually necessary when using
open/closed loop gain ratios high enough to justify using op-amp
techniques. The resistor capacitor network lag must be somewhat
greater than the amplifier delay for stable operation, but must
not be great enough to cause a lead effect in closed-loop opera-
tion. By careful design, the op-amp can have flat response to
nearly the open-loop bandwidth.

In selecting input and feedback restrictors, it is
recommended that kinematically similar elements be used so that
they have the same temperature sensitivity. Parallel and series
combinations of these elements are then used to obtain the
required resistance values. Since the op-amp scaler depends on
resistance ratios, the actual resistance is less important and
each resistance element can be expressed as a ratio of its
resistance to some other resistance. The control port resist-
ance, R_c, is usually chosen for normalizing all resistance
values.

7.2 Dynamic Compensation

It is often required to use dynamic compensation in
feedback control systems to achieve a specific response charac-
teristic. The most common requirements include lag, lead-lag,
and integral response. Normally, these functions are required
at bandwidths well below the bandwidth of staged laminar propor-
tional amplifiers. The circuit characteristics are achieved
using various combinations of resistance and capacitance ele-
ments in configurations analogous to those used in electronic
circuits.

A fluid capacitor is any device that stores energy.
In gaseous fluidic systems, capacitance results from the gas
compressibility. Hence, a simple rigid volume is used to

generate capacitance. Even if volumes are connected in series, the transfer function always appears as a shunt capacitance to ground. If air is the working fluid, the capacitance is given by

$$C = \frac{V}{nP}, \tag{52}$$

where

C = capacitance, $m^4 s^2/kg$,

V = volume, m^3,

P = absolute pressure, $kg/m\text{-}s^2$,

n = 1.4 for rapid pressure changes (adiabatic), or

n = 1.0 for slow pressure changes (isothermal).

In liquid systems, compressibility of the fluid is usually negligible and either a bellows or spring-loaded diaphragm is required. The capacitance is then given by

$$C = \frac{A^2}{k}, \tag{53}$$

where

A = bellows (or diaphragm) effective area, m^2 and
k = effective spring rate, kg/s^2.

The bellows or spring-loaded diaphragm closely approximates a series capacitor when used with liquid fluidic systems if the fluid compressibility is negligible (small pressure differences). If this type of capacitance is used in a gaseous fluidic system, the gas compressibility cannot be neglected, and the total capacitance is the sum of equations 52 and 53, where the volume is the internal volume of the bellows or diaphragm. The capacitance due to compressibility (equation 52) always appears as a shunt capacitance to ground. The bellows device can provide a series capacitance depending on how it is connected in the circuit.

Dynamic compensation circuits are developed using combinations of resistance and capacitance as described below.

7.2.1 Lag Compensation

A simple first-order lag is generated using a linear resistance and capacitance as shown in figure 41. From the electrical analogy of this circuit, the transfer function is given by

$$\frac{\Delta P_2}{\Delta P_1} = \frac{K}{1 + \tau s},\tag{54}$$

where

$$K = \frac{R_C}{R_1 + R_C},$$

$$\tau = \frac{R_1 R_C}{R_1 + R_C} C, \text{ and}$$

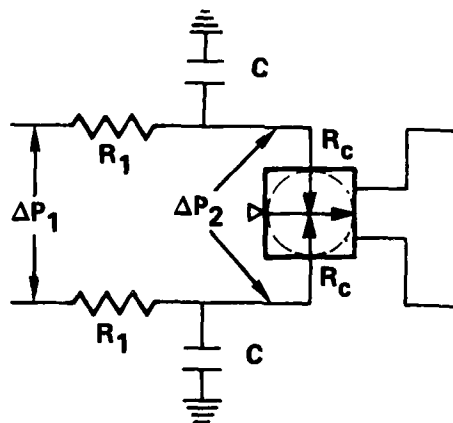$$s = \text{Laplace operator, } s^{-1}.$$

Figure 41. Simple first-order lag.

If the lag circuit is not connected to the inputs of an LPA (i.e., block loaded) or if it is connected to a relatively high input impedance op-amp, then the transfer function is given by

$$\frac{\Delta P_2}{\Delta P_1} = \frac{1}{1 + \tau s},\tag{55}$$

where

$$\tau = R_1 C.$$

Simple lags are usually constructed with the circuit shown in figure 41 connected to the inputs of the op-amp. Typical values of the lag time constant range from a few milliseconds up to several seconds. The higher the time constant, the larger the capacitor required in order to minimize the static gain attenuation associated with very high resistance values.

The performance of a capacitor depends on the manner in which it is physically connected in a fluidic circuit. Circuit diagrams are usually drawn to assist in making analytical models. The physical connection of the various elements, however, may be different from the way they are illustrated. In figure 41, for example, it appears that the capacitor (or volume) is connected to the circuit by means of a single port or "tee" connection. Actually, to obtain the desired function, the volume should be connected so that the signal is forced to flow through the volume. This requires a separate entrance and exit passage. If a single connection is made, as indicated in figure 41, the finite resistance associated with the connecting passage results in a lag-lead characteristic rather than in a simple lag.

7.2.2 Lead-Lag Compensation

Many high performance analog control systems require derivative action to compensate for the dynamics of the load or other control components. A lead-lag circuit, which

109

provides proportional-plus-derivative action, can be provided by using a capacitor in the feedback path of the op-amp circuit. The feedback resistance is usually divided into two series resistors with the capacitance (volume) placed between them as shown in figure 42. The transfer function is approximated by

$$\frac{\Delta P_o}{\Delta P_i} = K \frac{(1 + \tau_1 s)}{(1 + \tau_2 s)},$$ (56)

where

$$K \simeq 2 \frac{R_f}{R_i},$$

τ_1 = lead time constant,

τ_2 = lag time constant,

and $\tau_1 > \tau_2$.
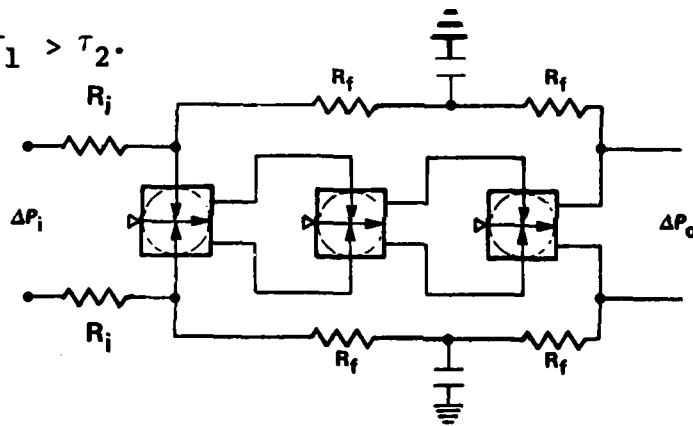
Figure 42. Lead-lag compensation using an op-amp.

The lead and lag time constants are related to the ratio of R_f/R_i and therefore the circuit gain is also a function of the lead-lag ratio. Stability of the op-amp circuit limits the value of the two break frequencies and their frequency separation. Typical performance on air would correspond to a lead time constant of up to 10 seconds and a lag time constant equal to 1/10 of the lead time constant.

The series capacitance characteristics of a bellows permit an alternative lead-lag circuit for use with liquid

fluidic control circuits. Figure 43 presents a typical arrange-ment[25] which uses a diaphragm capacitor, a shunt resistance (R_1), and a downstream resistance (R_2). If two of these cir-cuits are connected to the inputs of an LPA and operated push-pull, the transfer function is given by equation 56 with

$$K = \frac{R_2}{R_1 + R_2},$$ (57)

$$\tau_1 = R_1 C, \text{ and}$$ (58)

$$\tau_2 = \frac{R_1 R_2 C}{R_1 + R_2}.$$ (59)
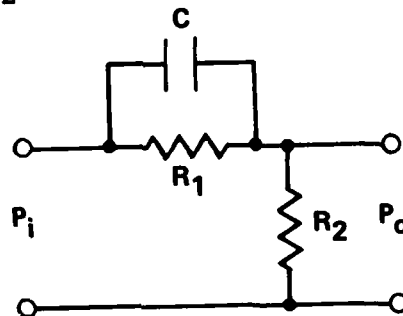
Figure 43.   Alternative lead-lag circuit
using a series capacitor.

The LPA control port resistance, R_c, could be used as the downstream resistance, R_2.

7.2.3 Integration

Integration is the most difficult frequency-dependent function to mechanize in fluidics. Pure integration cannot be achieved; however, a proportional-plus-integral action, which approximates integration, can be achieved in several ways. One method is to use an op-amp with positive and

---

[25]D. Lee, D. N. Wormley, "Multistage Hydraulic Summing and Signal Processing Amplifiers and Fluidic Input Servovalve Development," HDL-CR-76-223-1 (October 1976).

negative feedback. A capacitor to lag the positive-feedback path and an equal but unlagged negative-feedback path result in a lag-lead circuit having the following transfer function:

$$\frac{\Delta P_o}{\Delta P_i} = K \tau_2 \frac{(1 + \tau_1 S)}{(1 + \tau_2 S)}, \tag{60}$$

where

$$K = \text{integrating rate,}$$
$$\tau_1 = \text{lag or integrating constant, and}$$
$$\tau_2 = \text{lead-time constant.}$$

The lag-time constant can be made as high as 50 seconds or more so that

$$1 + \tau_2 S \simeq \tau_2 S, \tag{61}$$

and the transfer function becomes

$$\frac{\Delta P_o}{\Delta P_i} = \frac{K}{S} + K \tau_1. \tag{62}$$

Thus the lag-lead circuit gives proportional plus integral control.

Although simple in concept, this type of integrator can be quite temperature-sensitive, which causes changes in the integral and proportional gains (K and τ_1). Temperature compensation is difficult to achieve because of the differences in temperature sensitivity of the capacitance and feedback resistances. Tippetts[27] studied several concepts for mechanizing fluidic integration and concluded that a series capacitor approach could be more easily compensated for temperature effects.

---

[27] T. B. Tippetts, "Program for Analysis and Exploratory Development of a Fluidic Approach Power Compensator," Final Report NAVAIRSYSCOM Contract No. N0001974-C-0162 (March 1975).

The series-capacitor integrator is shown schematically in figure 44. The transfer function is also approximated by equation 61 with

$$K = \frac{1}{R_i C_1} , \tag{63}$$

and

$$K\tau_1 = R_f \frac{(C_1 + C_2)}{R_i C_1} , \tag{64}$$

where

$$C_1 = \text{series capacitance},$$

$$= A^2/k, \text{ and}$$

where

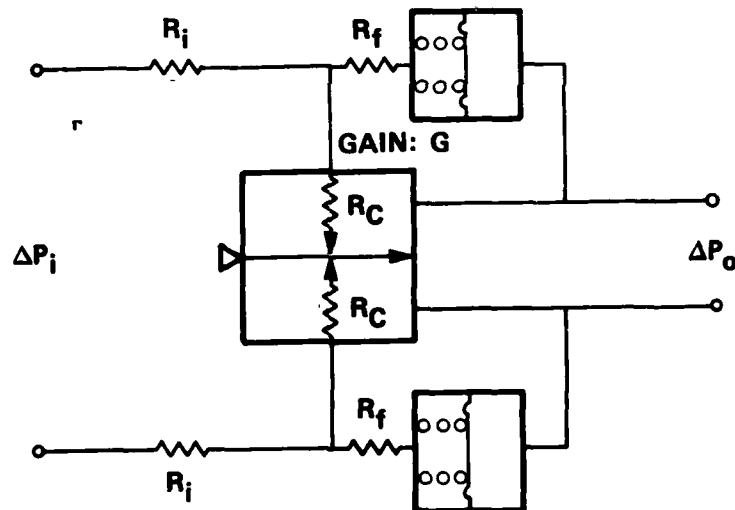$$C_2 = \text{ground capacitance},$$

$$= V/nP.$$

Figure 44. Series-capacitor integrator.

From equation 64 it would appear that if $R_f = 0$, then pure integration could be achieved. In practice, however, the gain block has transport delay and letting $R_f = 0$ would cause instability.

113

7.3 Gain Changing

It is often desirable to provide a variable gain feature in analog control circuits so that the gain can be adjusted for optimum performance. There are several methods by which this can be accomplished. One method, for example, utilizes the variation in LPA gain with changes in loading. If a pair of variable resistances are placed between two staged LPA's, then the gain across these amplifiers can be decreased by increasing the two resistances simultaneously. Likewise, if a single shunt resistance is placed across the outputs of the first LPA, the gain across the two LPA's can be decreased by decreasing the shunt resistance. Both methods can result in gain modulation from zero to 100 percent; however, to achieve this with the shunt resistance, it is necessary that the shunt be placed very close to the outputs of the first LPA so that the resistance of the connecting passage be kept sufficiently low.

The disadvantage of the shunt resistance is that it is not always possible to locate it close to the desired amplifier. The disadvantage of the paired series resistors is the design complexity of making two identical resistances with a common mechanical input. Any resistance mismatch will cause variations in the null offset at different gain settings.

LITERATURE CITED

(1)   F. M. Manion and T. M. Drzewiecki, "Analytical Design of Laminar Proportional Amplifiers," Proceedings of HDL Fluidic State-of-the-Art Symposium, $\underline{I}$, Harry Diamond Laboratories (October 1974).

(2)   G. Mon, "Flueric Laminar Gain Blocks and an Operational Amplifier Scaler," Harry Diamond Laboratories HDL-TR-1730 (December 1975).

(3)   F. M. Manion and G. Mon, "Fluerics 33: Design and Staging of Laminar Proportional Amplifiers," Harry Diamond Laboratories HDL-TR-1608 (September 1972).

(4)   C. L. Abbott, "Final Report: A Study of Fluidic Gun Stabilization Systems for Combat Vehicles," AiResearch Manufacturing Company of Arizona Report 41-2304 or HDL-CR-80-100-1 (April 1980).

(5)   T. M. Drzewiecki, F. M. Manion, "Fluerics 40: LJARS, The Laminar Jet Angular Rate Sensor," Harry Diamond Laboratories HDL-TM-79-7 (December 1979).

(6)   T. M. Drzewiecki, "Fluerics 37: A General Planar Nozzle Discharge Coefficient Representation," Harry Diamond Laboratories HDL-TM-74-5 (August 1974).

(7)   T. M. Drzewiecki, "A High-Order, Lumped-Parameter, Jet-Dynamic Model for the Frequency Response of Laminar Proportional Amplifiers," 20th Anniversary of Fluidics Symposium," ASME WAM (October 1980).

(8)   T. M. Drzewiecki, "Fluerics 38: A Computer-Aided Design Analysis for the Static and Dynamic Port Characteristics of Laminar Proportional Amplifiers," Harry Diamond Laboratories HDL-TR-1758 (June 1976).

(9)   J. S. Roundy, "Computer Programs for Laminar Proportional Amplifiers," AiResearch Manufacturing Company of Arizona, Phoenix, AZ, Report 42-0017 (June 1977).

(10)   T. M. Drzewiecki, D. N. Wormley, F. M. Manion, "Computer-Aided Design Procedure for Laminar Fluidic Systems," J. Dyn. Syst. Meas. Control, $\underline{97}$, Series G (December 1975).

(11)   Fluerics Testing Procedures, Department of Defense MIL-STD-1361 (1971).

(12)   R. M. Phillippi and T. M. Drzewiecki, "Fluerics 41: Single-Sided Port Characteristics of Laminar Proportional Amplifiers for Arbitrary Input Loading," Harry Diamond Laboratories HDL-TR-1901 (February 1980).

(13)   C. E. Spyropoulos, "Fluerics 36: Large Scale Modeling of Laminar Fluidic Devices," Harry Diamond Laboratories HDL-TM-73-28 (February 1978).

(14)   T. M. Drzewiecki, "A Fluidic Voice Communication System and Data Link," D. Eng. Thesis, Naval Post Graduate School, Monterey, CA (March 1980).

(15)   T. G. Sutton, W. J. Anderson, "Aerospace Fluidic Applications and Circuit Manufacture," AGARD-AG-215 (January 1976).

(16)   K. M. Lee, D. N. Wormley, "Fluidic Integrated Component Servovalve Description and Characteristic Performance," Department of Mechanical Engineering, Massachusetts Institute of Technology, Quarterly Report to HDL Contract No. ᴰAAK21-79-C-0158 (May 1981).

(17)   L. E. Scheer, J. S. Roundy, J. Joyce, "Manufacturing Techniques for Producing High Quality Fluidic Laminates in Production Quantities," 20th Anniversary of Fluidics Symposium, ASME WAM (November 1980).

(18)   J. S. Roundy, "Manufacturing Techniques for Producing High Quality Fluidic Laminates at Low Cost," AiResearch Manufacturing Company of Arizona Report 41-2697 (September 1980).

(19)   R. W. Van Tilburg, "Area Experience in Moderate Volume Fabrication of Pure Fluid Devices," Proceedings of the Fluid Amplification Symposium, VOL III, pp335-349 (October 1965).

(20)   L. S. Cox, "Fabrication Requirements in Fluidics Technology," AGARD-AG-215 (January 1976).

(21)   D. C. Cheffy, "Development of a Fluidic Pressure Ratio Control Unit For Vertical Take-off Aircraft Lift Engine," Proceedings of the Fourth Cranfield Fluidics Conference, VOL. 2, Paper L5 (March 1970).

(22)   W. Posingies, "Production Suitability of an Electro-formed Conductive Wax Process for the Manufacture of Fluidic Systems, Phase II," USSAAMRDL-TR-76-42 (January 1977).

(23)   A. E. Schmidlin and J. M. Kirshner, "Fluidic Sensors - A Survey," AGARD-AG-215 (January 1976).

(24)   H. Ziebolz, "Characteristics of Hydraulic and Pneumatic
         Relays as Energy-Converting Devices," Instruments, 15
         (September 1942).

(25)   D. Lee, D. N. Wormley, "Multistage Hydraulic Summing and
         Signal Processing Amplifiers and Fluidic Input Servo-
         valve Development," HDL-CR-76-223-1 (October 1976).

(26)   T. F. Urbanosky,   "Fluidic   Operational   Amplifier
         Summary," SAE Paper 670707 (1967).

(27)   T. B. Tippetts, "Program for Analysis and Exploratory
         Development of a Fluidic Approach Power Compensator,"
         Final Report NAVAIRSYSCOM Contract No. N0001974-C-0162
         (March 1975).

SELECTED BIBLIOGRAPHY

C. L. Abbott, T. B. Tippetts, "Development of an Electrofluidic Rate Sensor Using a Laminar Jet to Sense Rate," 20th Anniversary of Fluidics Symposium, ASME WAM (November 1980).

D. W. Chapin, "Application of Fluidics to Backup Flight Controls for V/STOL Aircraft," AiResearch Manufacturing Company of Arizona Report 41-2330A (September 1979).

K. C. S. Chen, V. F. Neradka, "Development of Critical Fluidic Components," HDL-CR-78-173-1 (March 1979).

R. A. Comparin, H. L. Moses, E. F. Rowell, "Contamination Effects in a Laminar Proportional Amplifier," HDL Fluidics State-of-the-Art Symposium, Volume 4 (September 1974).

T. M. Drzewiecki, "A Fluidic Audio Intercom," 20th Anniversary of Fluidics Symposium, ASME WAM (November 1980).

T. M. Drzewiecki, "A Fluid Amplifier Reynolds Number," HDL Fluidics State-of-the-Art Symposium, Volume 2 (September 1974).

T. M. Drzewiecki, F. M. Manion, "The Laminar Flip-Flop," HDL Fluidics State-of-the-Art Symposium, Volume 2 (September 1974).

R. N. Gottron, L. S. Cox, "Military Applications in Fluidics," AGARD-AG-215 (January 1976).

R. F. Hellbaum, "Experimental Design of Laminar Proportional Amplifiers," AGARD-AG-215 (January 1976).

R. F. Hellbaum, J. N. McDermum, "Experimental Design Studies and Flow Visualization of Proportional Laminar-Flow Amplifiers," NASA TN-D-8433 (August 1977).

L. R. Kelley, W. A. Boothe, "Hydraulic Fluidics," Transactions ASME, Journal of Dyn. Syst. Measurement and Control, Vol.95, No. 2, pp 161-166 (June 1973).

G. Mon, "The Power Supply Characteristics of Laminar Fluidic Components and Systems," 20th Anniversary of Fluidics Symposium, ASME WAM (November 1980).

G. Mon, "Laminar Proportional Amplifier," Proceedings, Sixth Cranfield Fluidics Conference (March 1974).

G. Mon, "Basic Design Concepts of Laminar Fluidic Digital Logic Using Laminar Proportional Amplifiers With Positive Feedback," Transactions ASME, Journal of Dyn. Sys., Measurement and Control, Vol. 101, No. 1, pp 77-80 (March 1979).

G. Mon, "The Design of a Fluidic Complimentary Gain Changer," Harry Diamond Laboratories HDL-TM-81-5 (February 1981).

R. M. Phillippi, "A Study of Fineblanking for the Manufacture of Flueric Laminar Proportional Amplifiers," Harry Diamond Laboratories HDL-TM-77-8 (May 1977).

L. E. Scheer, "Development Program for Analog Speed Sensors," Final Report DAAK70-78-0093 (April 1980).

T. G. Sutton, "Considerations and Applications for the Use of Fluidics in Aerospace Controls," 20th Anniversary of Fluidics Symposium, ASME WAM (November 1980).

T. B. Tippetts, "Fluidic Gun Stabilization System," 20th Anniversary of Fluidics Symposium, ASME WAM (November 1980).

T. B. Tippetts, "Temperature Compensated Operational Amplifier," AiResearch Manufacturing Company of Arizona Report 73-410261 (August 1973).

R. P. Trask II, "Fluidic Standardization Efforts," AGARD-AG-215 (January 1976).

R. Young, "Development of a Laminar Angular Rate Sensor," HDL Fluidics State-of-the-Art Symposium, Volume 2 (September 1974).

APPENDIX A.--COMMON TECHNICAL ABBREVIATIONS

Parameter, Units	Abbreviation
Area, m^2	A
Width, m	b
Width normalized by b_s, dimensionless	B
Capacitance, m^4s^2/kg	C
Discharge coefficient, dimensionless	c_d
Momentum flux discharge coefficient, dimensionless	c_θ
Frequency, Hz	f
Bandwidth, Hz	f_{bw}
Normalized frequency, dimensionless	F
Pressure gain, dimensionless	G_p
Blocked load pressure gain, dimensionless	G_{po}
Supply nozzle depth, m	h
Spring rate, kg/s^2	k
Fluid inertance (inductance), kg/m^4	L
Reynolds number, dimensionless	N_R
Modified Reynolds number, dimensionless	N_R'
Polytropic constant, dimensionless	n
Pressure, Pa	P
Volumetric flow rate, m^3/s	Q
Resistance, kg/m^4s	R
Sensitivity, Pa/deg/s	S
Transport delay, s	T_d
Velocity, m/s	U
Volume, m^3	V
Length, m	x
Length normalized by b_s, dimensionless	X
Complex impedance, kg/m^4s	Z

APPENDIX A.--COMMON TECHNICAL ABBREVIATIONS CONTINUED

Parameter, Units	Abbreviation
Angular rate, deg/s	$\dot{\theta}$
Absolute viscosity, kg/m-s	μ
Kinematic viscosity, m^2/s	ν
Density, kg/m^3	ρ
Aspect ratio ($\sigma = h/b_s$), dimensionless	σ
Phase shift, deg	ϕ
Frequency, rad/s	ω

Subscripts

Average	avg
Bias	B
Control	c
Exit	e
Feedback	f
Input	i
Output	o
Recovered	rec
Supply	s
Splitter	sp
Supply-to-vent	sv
Downstream control edge	t
Nozzle straight section	th

Superscripts

"prime" indicates dimensionless variable	'
"bar" indicates average value	─

APPENDIX B

FLUID PROPERTIES

Density

Figures B-1, B-2, and B-3 present graphical data on the density, ρ, as a function of temperature for air, hydraulic oil, and water.

Viscosity

The absolute viscosity of a fluid, μ, is a measure of the resistance of the fluid to shear when the fluid is in motion. Data on absolute viscosity are shown in figures B-4, B-5, and B-6 for air, hydraulic oil and water. As shown in these figures, the absolute viscosity of liquids decreases with temperature, while the absolute viscosity of gases increases with temperature. For most liquids, viscosity is a lesser function of the pressure; for air, the viscosity is almost independent of pressure between 1 and 30 atmospheres. The units of absolute viscosity are kg/m-s.

Kinematic Viscosity

The kinematic viscosity, ν, is the ratio of absolute viscosity and density,

$$\nu = \mu/\rho, \quad m^2/s. \tag{B-1}$$

Data on kinematic viscosity is given in figures B-7, B-8, and B-9.
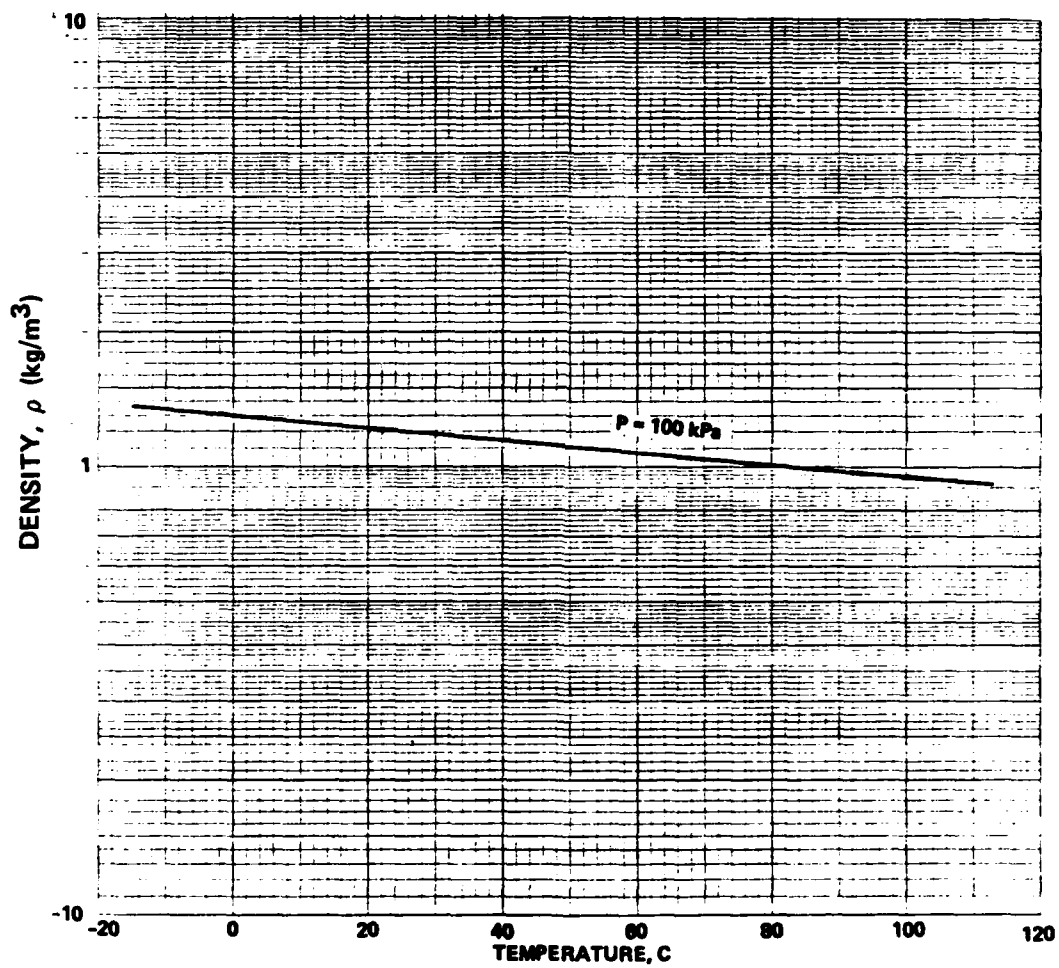
Figure B-1. Density of air versus temperature.
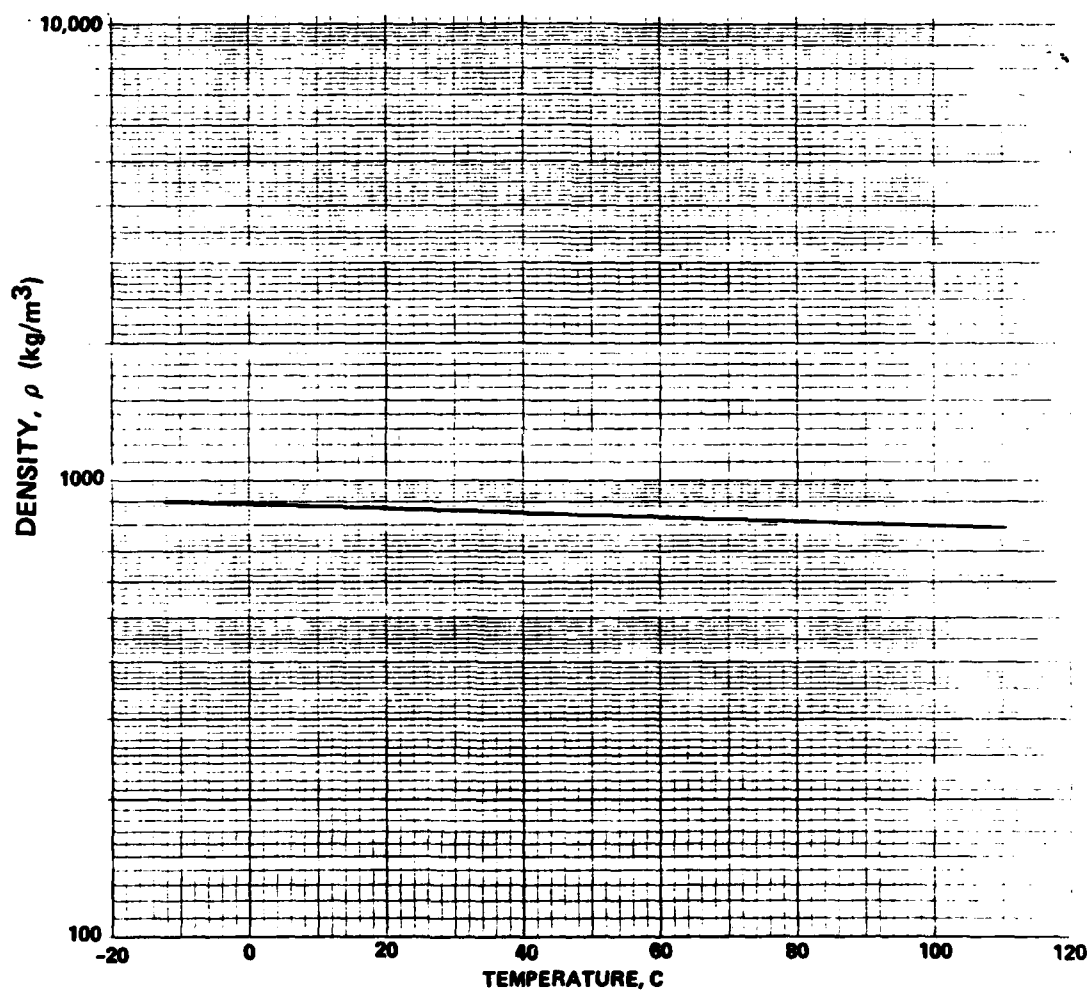
Figure B-2. Density of hydraulic oil (MIL-H-5606) versus temperature.

125
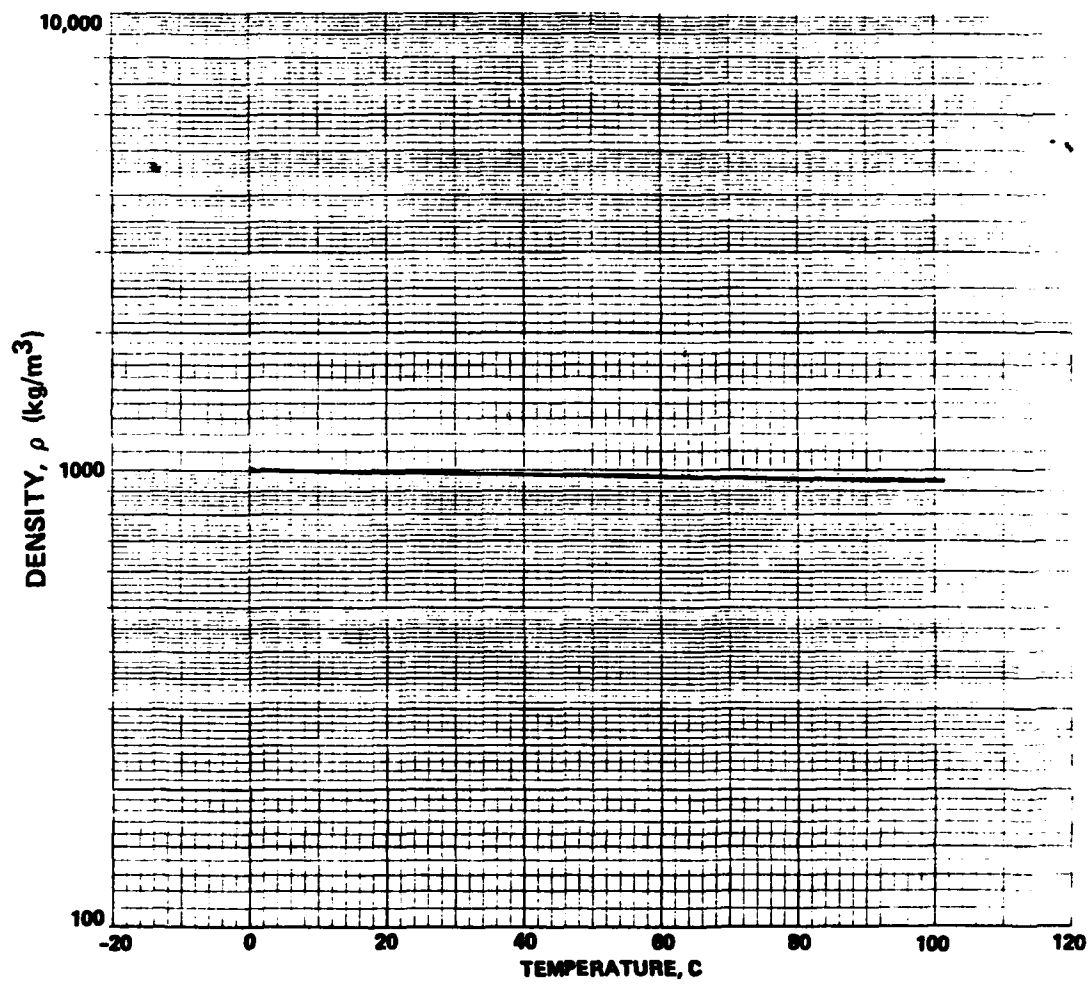
Figure B-3. Density of water versus temperature.

Figure B-4. Absolute of viscosity of air versus temperature.

Figure B-5.   Absolute viscosity of hydraulic oil
             (MIL-H-5606) versus temperature

Figure B-6.   Absolute viscosity of water versus temperature.
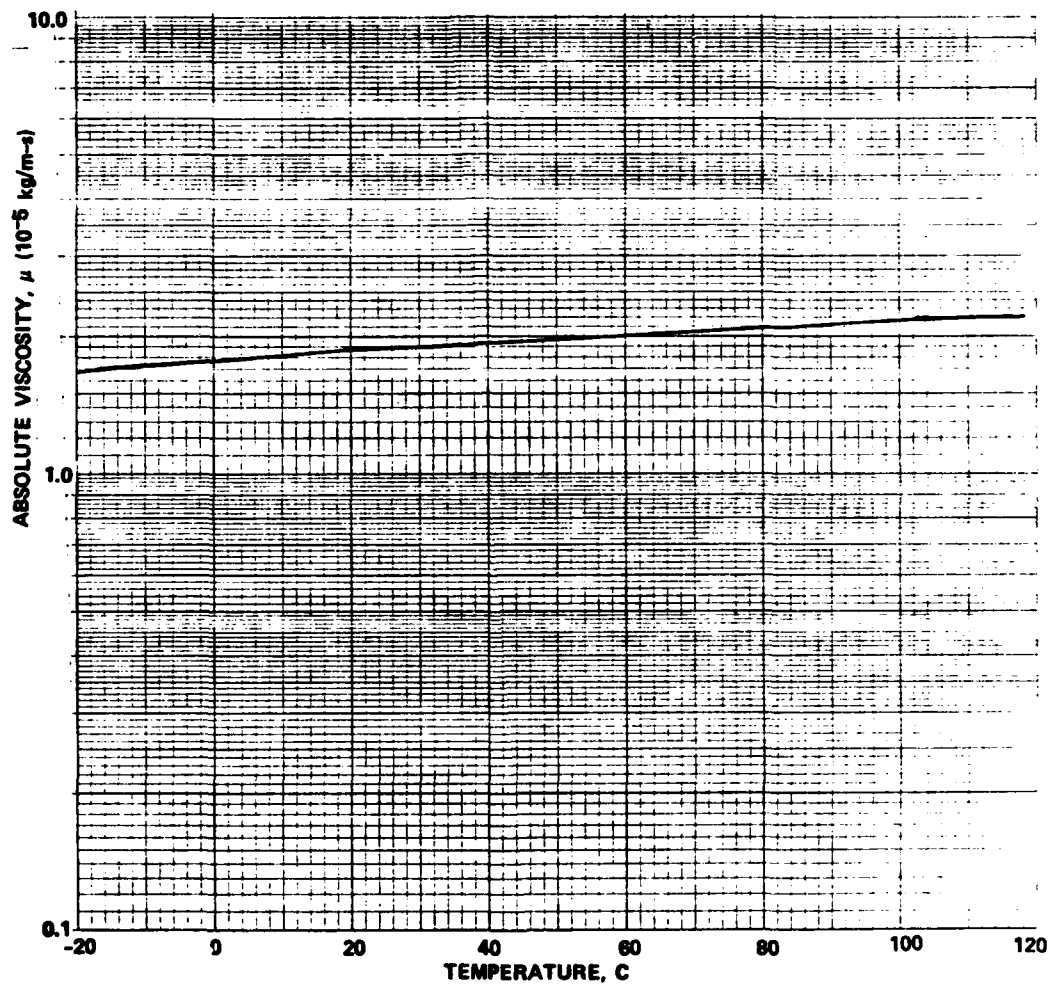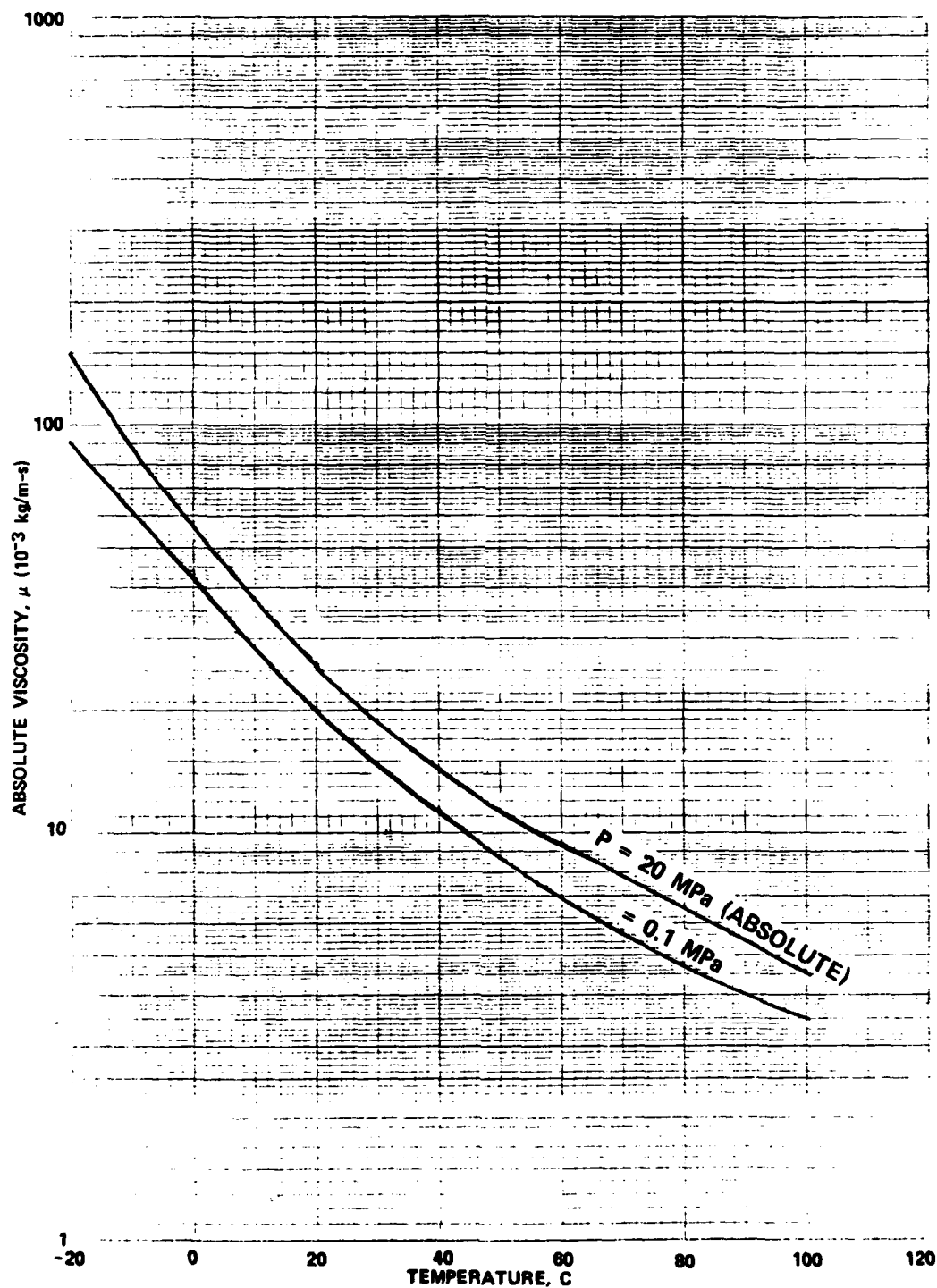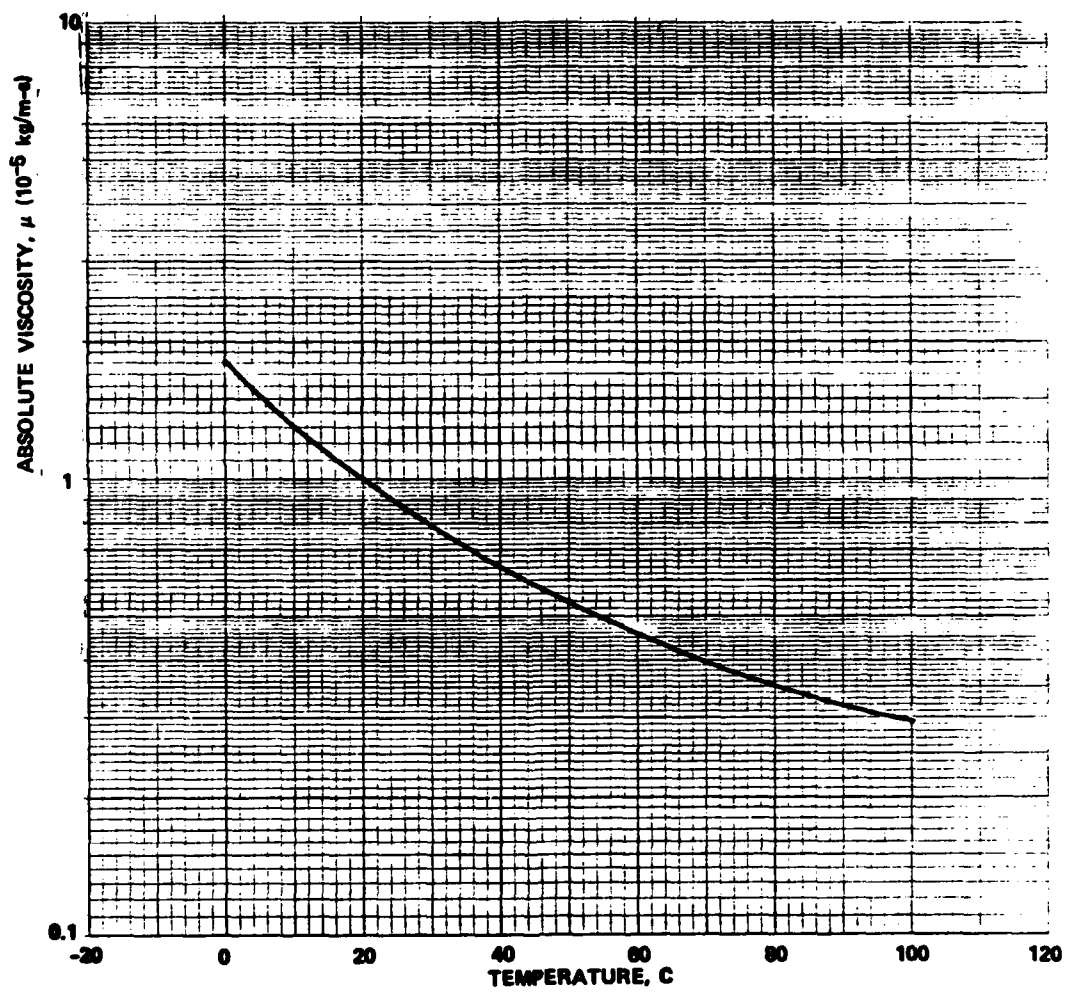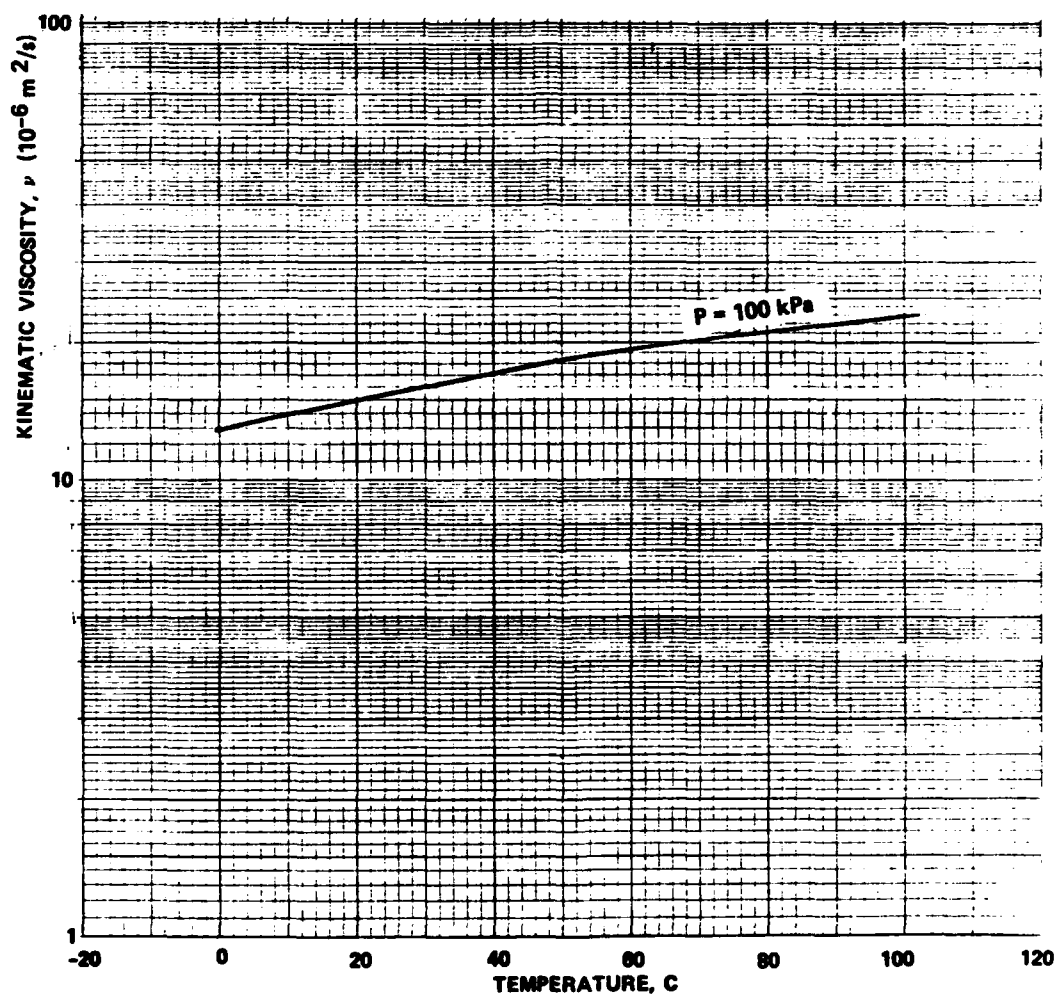
Figure B-7. Kinematic viscosity of air
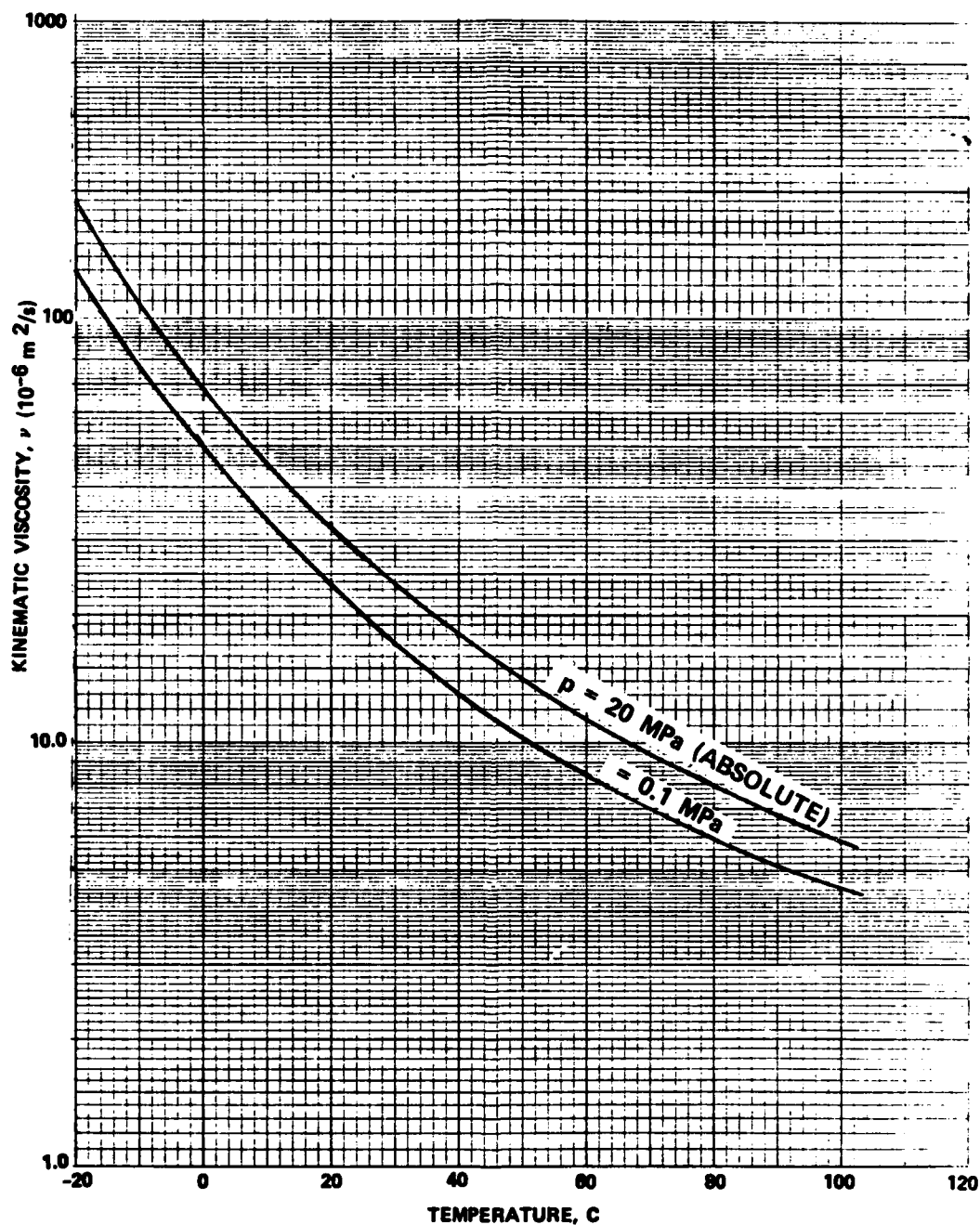versus temperature.

Figure B-8.   Kinematic viscosity of hydraulic oil
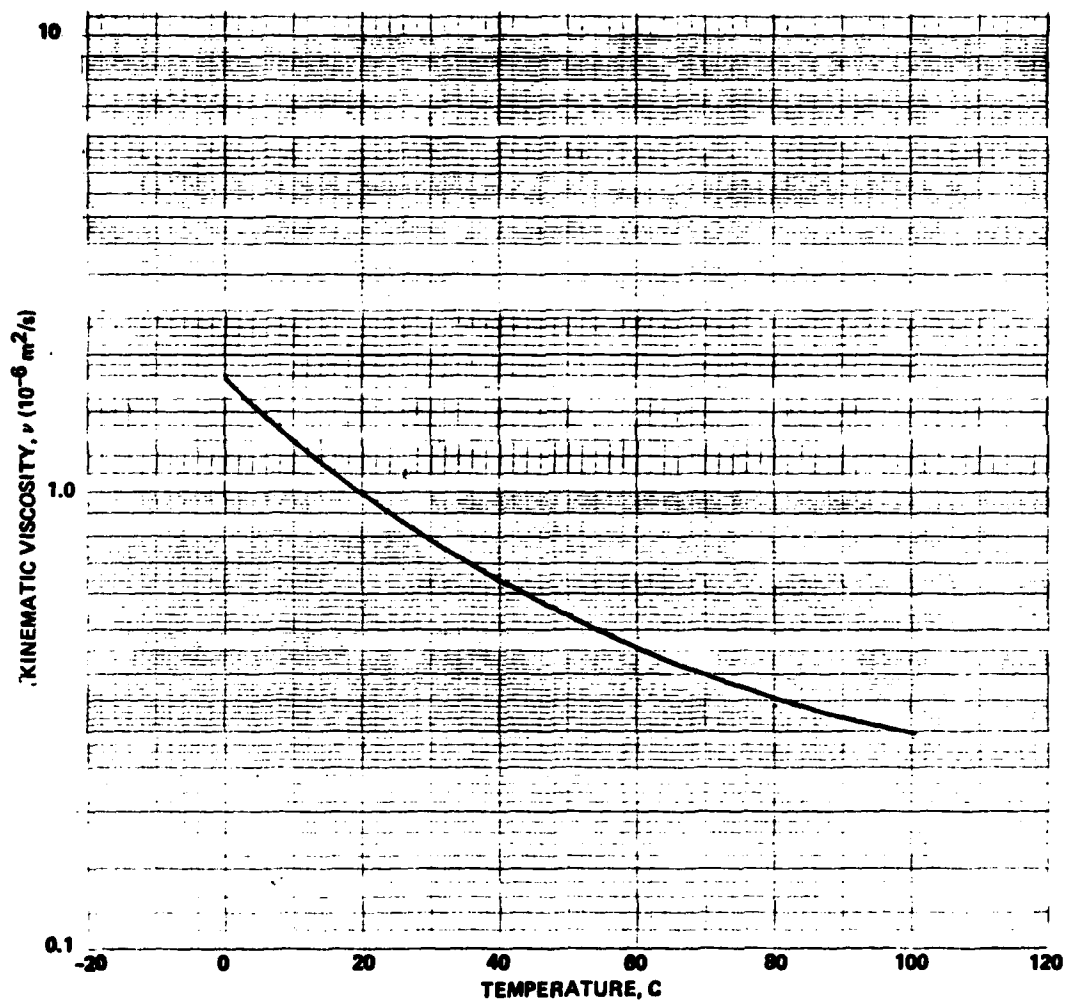(MIL-H-5606) versus temperature.

131

Figure B-9. Kinematic viscosity of water versus temperature.

APPENDIX C.--COMPUTER PROGRAMS FOR LPA ANALYSIS

One of the advantages of using laminar proportional
amplifiers (LPA's) and sensors is that accurate analytical models
exist which make it possible to predict component performance
for a variety of operating conditions. The analytical models
were developed at HDL and have been published by Manion and
Drzewiecki.[1] A complete description of the static and dynamic
port characteristics requires the solution of more than 70 equa-
tions. Because of this complexity, a computer-aided procedure
was soon developed to assist in the design and evaluation of
laminar proportional amplifiers and gain blocks.[2,3] These com-
puter programs, which were written in BASIC, provided output data
in both tabular and graphical form. Tabulated data represented
the input characteristics, the output characteristics, self-
staged operating conditions and gain, and the blocked gain.
Graphical outputs include the input and output characteristics
and Bode diagrams (gain and phase) for self-staged, self-loaded,
or block-loaded conditions. Typical calculations and a complete
listing of the program is given in reference 2, which also pre-
sents experimental data which shows that the computer analysis
is within ±10 percent of the measured values.

---

[1] F. M. Manion and T. M. Drzewiecki, "Analytical Design of
Laminar Proportional Amplifiers," Proceedings of HDL Fluidic
State-of-the-Art Symposium, I, Harry Diamond Laboratories
(October 1974).

[2] T. M. Drzewiecki, "Fluerics 38: A Computer-Aided Design
Analysis for the Static and Dynamic Port Characteristics of
Laminar Proportional Amplifiers," Harry Diamond Laboratories
HDL-TR-1758 (June 1976).

[3] T. M. Drzewiecki, D. N. Wormley, F. M. Manion, "Computer-
Aided Design Procedure for Laminar Fluidic Systems," J. Dyn.
Syst. Meas. Control, 97, Series G (December 1975).

Using the information in references 1 and 2, Roundy[4] developed a simplified computer program in FORTRAN to obtain the LPA static port characteristics. This program allows rapid evaluation of various LPA designs by calculating static input and output characteristics for the geometry of any amplifier. The only constraint is that the flow out of the supply nozzle remains laminar and that the modified Reynolds number is greater than 20. The computer program calculates: (1) supply resistance, (2) control channel impedance, (3) resistance at the boundary of the power and control jets, (4) output channel impedance, (5) output impedance, (6) deflected jet impedance, and (7) pressure gain.

The computer program is used to predict LPA performance as a function of geometry and operating conditions. This is particularly useful for evaluating various designs prior to actual fabrication. With practice, amplifier geometry can be optimized after two or three iterations.

[1]F. M. Manion and T. M. Drzewiecki, "Analytical Design of Laminar Proportional Amplifiers," Proceedings of HDL Fluidic State-of-the-Art Symposium, I, Harry Diamond Laboratories (October 1974).

[2]T. M. Drzewiecki, "A Computer-Aided Design Analysis for the Static and Dynamic Port Characteristics of Laminar Proportional Amplifiers," Harry Diamond Laboratories HDL-TR-1758 (June 1976).

[4]J. S. Roundy, "Computer Programs for Laminar Proportional Amplifiers," AiResearch Manufacturing Company of Arizona, Phoenix, AZ, Report 42-0017 (June 1977).

Using the design guidelines presented in section 3, in the body of the report, Drzewiecki has developed an even more simplified computer program for staging LPA's. Table C-1 gives the complete program in BASIC. Table C-2 gives a sample print-out for two different cases. The only inputs required are the number of stages, the nozzle width, and aspect ratio of each stage. The program calculates the supply pressure for $^\sigma N_R = 1000$, the supply flow, the supply resistance, the gain of each stage (which is corrected for bias pressure effects), the input resistance, the last stage output resistance, the staged gain, and the gain block bandwidth at 90 degrees of phase shift.

TABLE C-1. COMPUTER PROGRAM FOR LPA STAGING

```
10 DIM P(10),Q(10),K(10),A(10),B(10),G(10)
20 G0=10
30 PRINT "*****************************************************
*******"
40 PRINT "THIS PROGRAM GIVES DESIGN APPROXIMATIONS FOR MULTISTAG
E LPAS"
50 PRINT "BASED ON THE STANDARD HDL LPA, ASSUMING A ZERO-BIAS,BL
OCKED"
60 PRINT "SINGLE STAGE GAIN OF 10 OPERATING AT SIGMA*NR=1000 IN
AIR."
70 PRINT "FOR MAXIMUM DYNAMIC RANGE THE PRODUCT OF ASPECT RATIO
AND       NOZZLE WIDTH OF EACH SUCEEDING STAGE SHOULD BE 1/3RD O
F THE     PREVIOUS, E.G.FOR BS1=BS2,AR(1)=3 AND AR(2)=1."
80 PRINT "*****************************************************
*******"
90 PRINT
100 INPUT "IS YOUR LPA GAIN 10 ",Y$:IF STR(Y$,1,1)="Y"THEN 120
110 INPUT "WHAT IS YOUR GAIN",G0
120 INPUT "NUMBER OF STAGES",N
130 FOR M=1TO N
140 PRINT "STAGE ";M;" ASPECT RATIO";:INPUT A(M+1)
150 PRINT "NO. OF PARALLEL ELEMENTS IN STAGE ";M;:INPUT K(M+1)
160 PRINT "STAGE ";M;" NOZZLE WIDTH IN MM";:INPUT B(M+1)
170 P(M+1)=1/(A(M+1)*B(M+1))↑2
180 PRINT "STAGE ";M;" SUPPLY PRESSURE = ";P(M+1);" TORR"
190 Q(M+1)=2.5*SQR(P(M+1))*B(M+1)↑2/(1+1/A(M+1))↑2*K(M+1)
200 PRINT "STAGE ";M;" SUPPLY FLOW =";Q(M+1);"LPM"
210 PRINT "STAGE ";M;" SUPPLY RESISTANCE =";P(M+1)/Q(M+1);"TORR/
LPM"
220 NEXT M
230 INPUT "FIRST STAGE BIAS PRESSURE IN TORR",P0
240 P(1)=P0*3
250 PRINT "ENTER OUTPUT LOAD IN TERMS OF AN EQUIVALENT LPA"
260 PRINT "A BLOCKED LOAD IS PUT IN AS AN AR=1 AND BS=0"
270 INPUT "LOAD NO. OF PARALLEL STAGES",K(N+2)
280 INPUT "LOAD ASPECT RATIO",A(N+2)
290 INPUT "LOAD NOZZLE WIDTH(MM)",B(N+2)
300 IF B(N+2)=0 THEN 310:P(N+2)=1/(A(N+2)*B(N+2))↑2:Q(N+2)=2.5*S
QR(P(N+2))*K(N+2)*B(N+2)↑2/(1+1/A(N+2))↑2:GOTO 320
310 P(N+2)=1:Q(N+2)=0
320 L=0
330 FOR J=1 TO N
340 G(J)=G0*(1/(1+.20*P(J)/P(J+1)))*(1/(1+.667*P(J+1)*Q(J+2)/P(J
+2)/Q(J+1)))
350 PRINT "STAGE ";J;" PRESSURE GAIN = ";G(J)
360 L=L+B(J+1)/SQR(P(J+1))
370 IF J=1THEN 400
380 G=G(J)*G
390 GOTO 410
400 G=G(J)
410 NEXT J
420 PRINT "PRESSURE GAIN OF THE ";N;" STAGE GAINBLOCK =";G
430 PRINT "GAINBLOCK INPUT RESISTANCE = ";.75*P(2)/Q(2);"TORR/LP
M"
440 PRINT "GAINBLOCK OUTPUT RESISTANCE = ";.5*P(N+1)/Q(N+1);"TOR
R/LPM"
450 PRINT "GAINBLOCK BANDWIDTH AT 90DEG PHASE SHIFT = ";157.5/L;
"HERTZ"
460 INPUT "DO YOU WANT TO MAKE ANOTHER CALCULATION",I$:IF STR(I$
,1,1)="Y" THEN 470:GOTO 480
470 PRINT :PRINT :PRINT :PRINT :GOTO 120
480 STOP :END
```

TABLE C-2. SAMPLE COMPUTER PRINTOUT

```
****************************************************************
THIS PROGRAM GIVES DESIGN APPROXIMATIONS FOR MULTISTAGE LPA'
BASED ON THE STANDARD HDL LPA, ASSUMING A ZERO-BIAS,BLOCKED
SINGLE STAGE GAIN OF 10 OPERATING AT SIGMA*NR=1000 IN AIR.

FOR MAXIMUM DYNAMIC RANGE THE PRODUCT OF ASPECT RATIO AND
NOZZLE WIDTH OF EACH SUCEEDING STAGE SHOULD BE 1/3RD OF THE
PREVIOUS, E.G.FOR BS1=BS2,AR(1)=3 AND AR(2)=1.
****************************************************************
```
```
IS YOUR LPA GAIN 10 ? Y
NUMBER OF STAGES? 3
STAGE   1   ASPECT RATIO? .667
NO. OF PARALLEL ELEMENTS IN STAGE   1 ? 1
STAGE   1   NOZZLE WIDTH IN MM? .5
STAGE   1   SUPPLY PRESSURE = 8.991006745503   TORR
STAGE   1   SUPPLY FLOW = .3000299760059 LPM
STAGE   1   SUPPLY RESISTANCE = 29.96702817897 TORR/LPM
STAGE   2   ASPECT RATIO? .667
NO. OF PARALLEL ELEMENTS IN STAGE   2 ? 1
STAGE   2   NOZZLE WIDTH IN MM? .5
STAGE   2   SUPPLY PRESSURE = 8.991006745503   TORR
STAGE   2   SUPPLY FLOW = .3000299760059 LPM
STAGE   2   SUPPLY RESISTANCE = 29.96702817897 TORR/LPM
STAGE   3   ASPECT RATIO? .667
NO. OF PARALLEL ELEMENTS IN STAGE   3 ? 1
STAGE   3   NOZZLE WIDTH IN MM? .5
STAGE   3   SUPPLY PRESSURE = 8.991006745503   TORR
STAGE   3   SUPPLY FLOW = .3000299760059 LPM
STAGE   3   SUPPLY RESISTANCE = 29.96702817897 TORR/LPM
FIRST STAGE BIAS PRESSURE IN TORR? 0
ENTER OUTPUT LOAD IN TERMS OF AN EQUIVALENT LPA
A BLOCKED LOAD IS PUT IN AS AN AR=1 AND BS=0
LOAD NO. OF PARALLEL STAGES? 1
LOAD ASPECT RATIO? 1
LOAD NOZZLE WIDTH(MM)? 0
STAGE   1   PRESSURE GAIN = 5.998800239952
STAGE   2   PRESSURE GAIN = 4.99900019996
STAGE   3   PRESSURE GAIN = 8.333333333333
PRESSURE GAIN OF THE   3   STAGE GAINBLOCK = 249.900029992
GAINBLOCK INPUT RESISTANCE = 22.47527113422 TORR/LPM
GAINBLOCK OUTPUT RESISTANCE = .14.98351408948 TORR/LPM
GAINBLOCK BANDWIDTH AT 90DEG PHASE SHIFT = 314.842578708 HEF
DO YOU WANT TO MAKE ANOTHER CALCULATION? N
```

TABLE C-2.   SAMPLE COMPUTER PRINTOUT

```
IS YOUR LPA GAIN 10 ? NO
WHAT IS YOUR GAIN? 8
NUMBER OF STAGES? 3
STAGE   1   ASPECT RATIO? .667
NO. OF PARALLEL ELEMENTS IN STAGE   1 ? 2
STAGE   1   NOZZLE WIDTH IN MM? .75
STAGE   1   SUPPLY PRESSURE =  3.996002998001   TORR
STAGE   1   SUPPLY FLOW = .9000899280478 LPM
STAGE   1   SUPPLY RESISTANCE = 4.439559730068 TORR/LPM
STAGE   2   ASPECT RATIO? .5
NO. OF PARALLEL ELEMENTS IN STAGE   2 ? 3
STAGE   2   NOZZLE WIDTH IN MM? .508
STAGE   2   SUPPLY PRESSURE =  15.50003100006   TORR
STAGE   2   SUPPLY FLOW = .8466666666633 LPM
STAGE   2   SUPPLY RESISTANCE = 18.30712322849 TORR/LPM
STAGE   3   ASPECT RATIO? .333
NO. OF PARALLEL ELEMENTS IN STAGE   3 ? 6
STAGE   3   NOZZLE WIDTH IN MM? .375
STAGE   3   SUPPLY PRESSURE =  64.12819225632   TORR
STAGE   3   SUPPLY FLOW = 1.054159826531 LPM
STAGE   3   SUPPLY RESISTANCE = 60.83346248107 TORR/LPM
FIRST STAGE BIAS PRESSURE IN TORR? 1
ENTER OUTPUT LOAD IN TERMS OF AN EQUIVALENT LPA
A BLOCKED LOAD IS PUT IN AS AN AR=1 AND BS=0
LOAD NO. OF PARALLEL STAGES? 1
LOAD ASPECT RATIO? 1
LOAD NOZZLE WIDTH(MM)? 0
STAGE   1   PRESSURE GAIN =  5.987184216334
STAGE   2   PRESSURE GAIN =  6.335947153133
STAGE   3   PRESSURE GAIN =  7.63110643793
PRESSURE GAIN OF THE  3   STAGE GAINBLOCK = 289.4820758441
GAINBLOCK INPUT RESISTANCE =  3.329669797551 TORR/LPM
GAINBLOCK OUTPUT RESISTANCE =  30.41673124053 TORR/LPM
GAINBLOCK BANDWIDTH AT 90DEG PHASE SHIFT =  285.8192157212 HERTZ
DO YOU WANT TO MAKE ANOTHER CALCULATION? N

  STOP
```

APPENDIX D.--METHODS OF CONTROLLING REYNOLDS NUMBER

As indicated in section 1.2, in the body of the report, the gain of an LPA is sensitive to the Reynolds number at which the amplifier is operated. Variations in the fluid temperature produce changes in the density and viscosity of the fluid and these changes cause a variation in the Reynolds number. From the definition of Reynolds number (equation 7, section 1.2.1), amplifier supply pressure must be adjusted to offset changes in Reynolds number produced by changes in fluid properties. This is illustrated in figures D-1 and D-2 which show the supply pressure as a function of temperature for a typical LPA (b_s = 0.5 mm) at different aspect ratios operating on air and hydraulic oil (MIL-H-5606). These plots are scaled using the parameter $(\sigma N_R)^2$; thus, the pressure required for any Reynolds number can be quickly calculated. Likewise, if the pressure is held constant, the change in Reynolds number corresponding to a specified change in temperature can also be determined.

For LPA's operating on air and other gases, constant Reynolds number operation over a wide range of temperatures is possible by using a temperature-compensated pressure regulator to schedule supply pressure as a function of temperature. For example, using the data in figure D-1, the Reynolds number of an LPA operating on air can be held constant if the supply pressure is varied by a factor of 3 to 1 over the temperature range of minus 20C to plus 120C, If the viscosity varies substantially with temperature, however, it is impractical to achieve constant Reynolds number operation by scheduling the supply pressure as a function of temperature. Consider, for example, operation on MIL-H-5606 hydraulic oil. From figure D-2, over the temperature range of minus 20C to plus 120C, it would be necessary to change the supply pressure by a factor of more than 600 to 1 to maintain a constant Reynolds number. If a 2 to 1 change in Reynolds
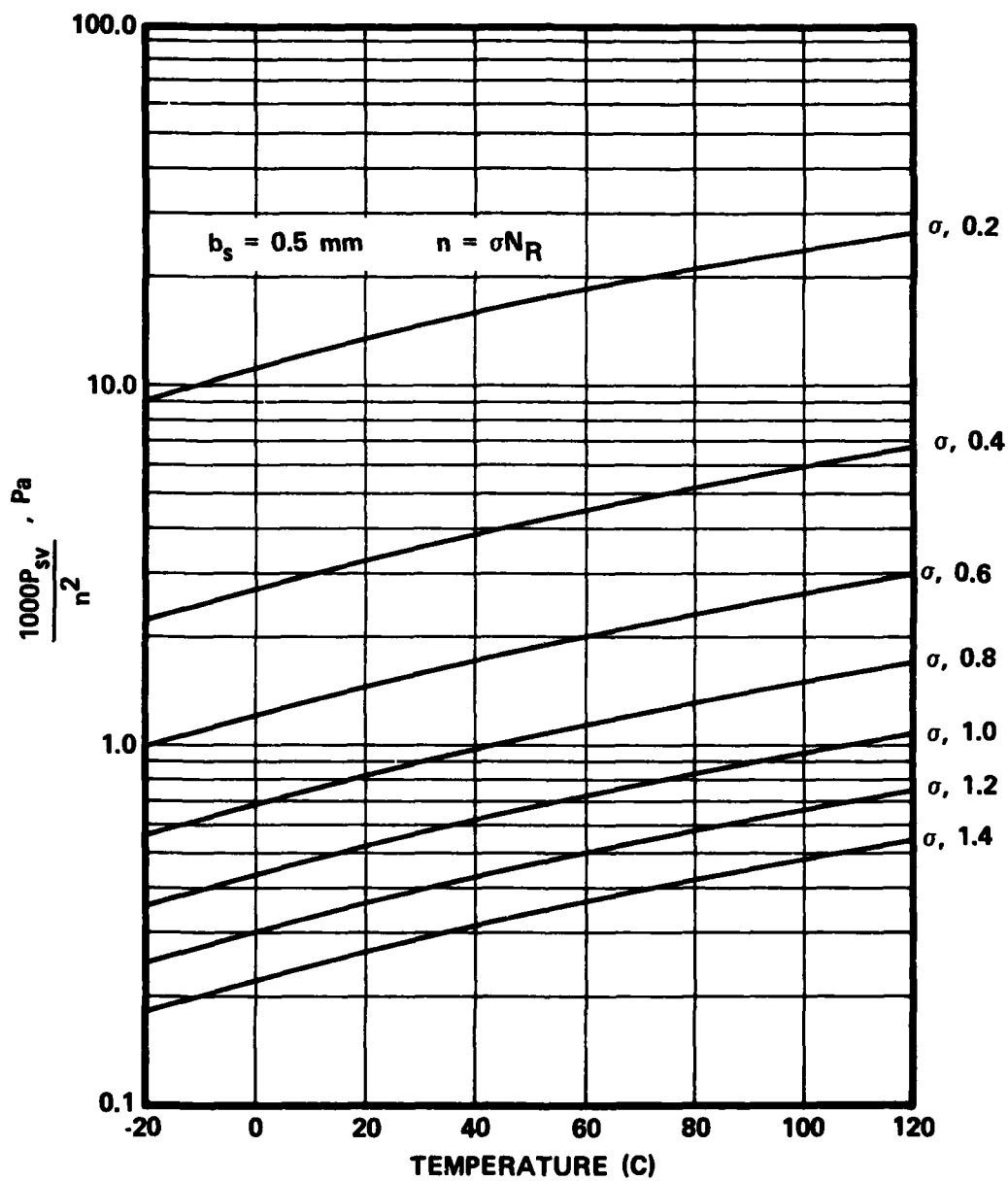
Figure D-1. LPA supply pressure as a function of
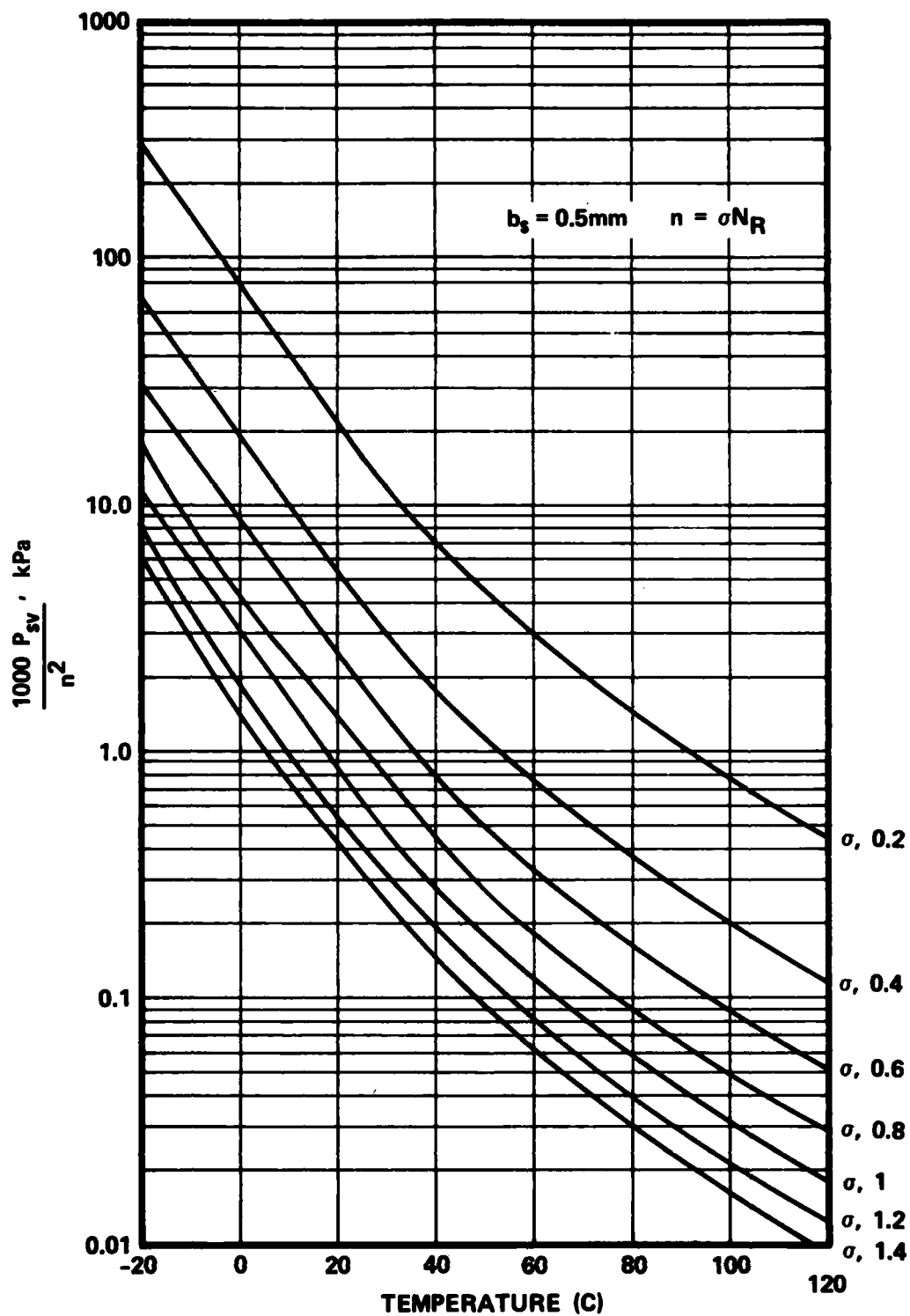temperature (operation on air).

Figure D-2. LPA supply pressure as a function of
temperature (operation on MIL-H-5606).

141

number can be tolerated, the required pressure change is reduced to approximately 150 to 1 over the same temperature range.

Another factor which reduces the temperature compensation requirements in hydraulic-fluidic circuits is heat generation and the constant flow through the fluidic amplifiers. In many applications, these factors can result in hydraulic fluid temperatures that stabilize over a much smaller range of temperatures, perhaps plus 50C to plus 120C or less. Over this range, the supply pressure must be varied only by a factor of 10 to 1 to maintain a constant Reynolds number or about 2.5 to 1 if a 2 to 1 change in Reynolds number is acceptable.[1,2]

The power supply for a typical fluidic circuit usually includes a preset pressure regulator and passive pressure dropping restrictions to obtain the desired pressure (or flow rate) through the various fluidic amplifier stages. Temperature compensation can be approached in two ways: (1) the regulated supply pressure (or flow) can be varied as a function of temperature, or (2) the passive pressure dropping restrictions can be made temperature-sensitive in a manner as to vary the supply pressure (or flow) to the individual stages.

[1]J. B. Leonard, T. A. Sorenson, and W. F. Stratford, "Fluidic Flight Control Technology Evaluation: Problem Areas and Proposed Solutions," Grumman Aerospace Corp., Report MD-FC-07-79-02, (December 1979).

[2]W. M. Posingies, "Advanced Fluidic Temperature Studies," USARTL-TR-78-33 (October 1978).

In order to temperature compensate fluidic components and systems, the pressure-flow (P-Q) characteristics must be known over the temperature range of interest. Mon[3] has shown that, in general, the P-Q characteristics of a fluidic system can be expressed as

$$P = R\mu Q + K\rho Q^2,$$ (D-1)

where R and K are constants which are only functions of the geometry and are independent of fluid temperature. These constants can be determined by a least-squares fitting of the experimental P-Q curves. Since most of the flow measuring instrumentation is calibrated at standard conditions, it is more convenient to modify equation D-1 so that the flow rate is determined at standard conditions. From the law of conservation of mass

$$\rho Q = \rho_o Q_o = \text{constant}$$ (D-2)

or

$$Q = \frac{\rho_o}{\rho} Q_o,$$ (D-3)

where Q_o and ρ_o are the flow rate and density, respectively, at standard conditions. Substituting this into equation D-1 gives

$$P = R\mu \frac{\rho_o}{\rho} Q_o + K \frac{\rho_o^2}{\rho} Q_o^2.$$ (D-4)

In using equation D-4, the density (ρ) and viscosity (μ) are calculated at the actual operating conditions.

---

[3]G. Mon, "The Power Supply Characteristics of Laminar Fluidic Components and Systems," 20th Anniversary of Fluidics Symposium, ASME WAM (November 1980).

Equation D-4 defines the P-Q characteristics of the fluidic
system or any of the components in the system. Once the con-
stants R and K are established, the temperature-compensation
components must then be designed. If the system supply pressure
or flow is to be varied, an active power supply system might
consist of a servo-controlled pump or pressure regulator which
uses pressure and temperature sensors with an electronic control
unit to schedule pressure (or flow) as a function of fluid tem-
perature. This method is attractive for self-contained hybrid
fluidic systems or sensors which are required to interface with
other electronic controls. If temperature compensation is
desired without using electronic components, a passive power
supply conditioner can be made using a temperature sensitive
flow restriction placed either in series or in parallel with the
fluidic system. One such device, reported by Mon,[4] uses a pair
of concentric cylinders made of materials with dissimilar coef-
ficients of expansion. By proper selection of the material
restrictor geometry, a passive temperature sensitive flow
restriction can be designed for either liquid or gaseous fluidic
systems.

The temperature-sensitive restrictor approach can also be
used on selected critical components when the total supply flow
to the component is held constant. One method is to use a linear
(capillary) restriction in parallel with the LPA supply nozzle
that has an orifice characteristic to bypass some of the flow as
a function of temperature. This method may be only slightly

---

[4]G. Mon, "Temperature Compensation of Laminar Fluidic Com-
ponents and Systems," 20th Anniversary of Fluidics Symposium,
ASME WAM (November 1980).

effective as a Reynolds number regulator if the LPA supply nozzle has a large linear component as in a long-nozzle LJARS.[5] Even if the supply nozzle can be made without a linear component (i.e., almost a pure orifice), the bypass method requires a large change in system flow rate if the kinematic viscosity varies substantially over the operating temperature range. For example, operating on hydraulic oil, the bypass method could yield a reduction of approximately 30 percent in the Reynolds number variation of a typical LPA over the temperature range of 15C to 55C. Therefore, a compromise is required between the amount of compensation and the total supply flow to the system.

A very effective method of compensation for Reynolds number effects is through the use of an op-amp scaler that utilizes feedback and input resistors that are dependent on viscosity and density (capillaries and orifices), respectively. The gain function can be made to either increase or decrease (as desired) with temperature, thus offsetting opposite changes in gain. Drzewiecki and Manion[5] discuss this approach in connection with the LJARS.

---

[5] T. M. Drzewiecki, F. M. Manion, "Fluerics 40: The Laminar Jet Angular Rate Sensor," Harry Diamond Laboratories HDL-TM-79-7 (December 1979).

DISTRIBUTION LIST

Administrator
Defense Technical Informaton Center
Attn: DTIC-DCA (12 copies)
Cameron Station, Building 5
Alexandria, Va 22314

Harry Diamond Laboratories

Attn: CO/TD/TSO/Division Directors

Attn: Record Copy, 81200

Attn: HDL Library, 81100 (2 copies)

Attn: HDL Library, 81100 (Woodbridge)

Attn: Technical Reports Branch, 81300

Attn: Chairman, Editorial Committee

Attn: Legal Office, 9700

Attn: J. Joyce, 13400 (150 copies)

2800 Powder Mill Road
Adelphi, Md 20783

Naval Air Systems Command
Attn: Dean Houck, AIR-5143J (20 copies)
Washington, D.C. 20361